

A SAMPLE RESEARCH PAPER/DIRECTED WORK/DISSERTATION ON
ASPECTS OF MATERIALS AND CONSTRUCTION

By

Wilver David Castillo Parra

B.S., Escuela Colombiana de Ingeniería, 2021

A Research Paper/Thesis/Dissertation

Submitted in Partial Fulfillment of the Requirements for the
Bachelor of Civil Engineering

Civil Engineering Department
Escuela Colombiana de Ingeniería
Bogotá, Colombia

2021

RESEARCH PAPER/THESIS/DISSERTATION APPROVAL

INDIVIDUAL COMPARISON AND JOINT EVALUATION OF FIBER
REINFORCED POLYMERS (FRP) AND ULTRA-HIGH-PERFORMANCE
FIBER REINFORCED CONCRETE USED TO RETROFIT
STRUCTURES.

By

Wilver David Castillo Parra

A Directed Work/ Dissertation Submitted in Partial

Fulfillment of the Requirements

For the Degree of

Bachelor

In the field of Civil Engineering

Director:

Nancy Torres Castellanos. Civil Engineering Ph.D.

Graduate School
Escuela Colombiana de Ingeniería
August 18 of 2021

AN ABSTRACT OF THE DISSERTATION OF

Wilver David Castillo Parra, for the Civil Engineering Bachelor, presented in December 2021, at Escuela Colombiana de Ingeniería Julio Garavito.

INDIVIDUAL COMPARISON AND JOINT EVALUATION OF FIBER REINFORCED POLYMERS (FRP) AND ULTRA HIGH PERFORMANCE FIBER REINFORCED CONCRETE USING AS REINFORCEMENT AND FOR STRUCTURES REHABILITATION.

ADVISOR: Nancy Torres Castellanos Ph. D.

This dissertation is a rigorous investigation that studies two important essential materials in construction: Polymer Fiber Reinforced (FRP) and Ultra-High-Performance Fiber Reinforced Concrete (UHPFRC), and their applications for strengthening and rehabilitation. Hence, this study exposes and describes the history, characteristics, types, laboratory tests, and applications of these materials by collecting data from previously published works. Then, a deep comparison of the features of these materials and especially an evaluation of the possibility to use these together to reinforce structures and for structures rehabilitation are assessed.

On the other hand, these materials have been studied in the last years because they fulfilled in the last years because they fulfill the high quality and performance demanded in construction. Therefore, it's clear that one of the most important aspects of FRP and UHPFRC is their high strength and ductility (in the UHPFRC case), so it is interesting to compare them and even more evaluate them if it's possible to use them together. However, there are some minima negative aspects like the high cost. Hence, there are multiple studies focused on finding materials that could partially replace UHPFRC high-cost components, such as cement, silica fume, and superplasticizer. To this end, these investigations evaluate economical materials even better if there are recycled. Sequent, knowing the importance of sustainability and economy in constructions, it will be important to review that.

DEDICATION

I want to dedicate this work to my grandmother who passed the way this year. She always courage me to be better person and student and she taught me to give all myself to achieve good results, to be successful, to never give up and to love God and my family.

ACKNOWLEDGMENTS

I am so glad with God first for give me the opportunity of study this bachelor degree, with my family, specially mom and dad, with all my teachers who taught me a lot on this stage, and even more in the structures, materials and construction area my materials teacher Ricardo Matallana, my structural analysis teacher Sandra Jerez, my statics and materials resistant teacher Daniel Leon, my design of concrete structures teacher Maria Carolina, Nancy engineering teacher who directed this research and specially the engineer Joaquin Abellan who guided me and helped me through the development of this work.

Content Table

AN ABSTRACT OF THE DISSERTATION OF	3
DEDICATION	4
ACKNOWLEDGMENTS	5
LIST OF TABLES	7
LIST OF FIGURES	8
INTRODUCTION	10
FIBER REINFORCED POLYMER (FRP).....	11
POLYMERS:	12
HISTORICAL DEVELOPMENT:	13
TYPES:	14
CHARACTERISTICS:.....	15
ADVANTAGES & DISADVANTAGES:	18
LABORATORY TESTS:	19
APPLICATION:	20
ULTRA HIGH-PERFORMANCE FIBER REINFORCED CONCRETE (UHPFRC)	22
HISTORICAL DEVELOPMENT:	25
FIBER TYPES:.....	26
CHARACTERISTICS:	29
LABORATORY TESTS:	33
ADVANTAGES & DISADVANTAGES:	34
APPLICATION:	34
FRP AND UHPFRC COMPARISON.....	36
FRP:	36
UHPFRC:.....	51
EVALUATION OF FRP AND UHPFRC WORKING TOGETHER	71
CONCLUSIONS	78
REFERENCES	80

LIST OF TABLES

Table 1. FRP's density. Source: ACI.	15
Table 2. FRP's Coefficient of Thermal Expansion. Source: ACI.....	15
Table 3. FRP's Tensile Characteristics. Source: ACI.	17
Table 4. FRP's advantages and disadvantages. Own Source.	18
Table 5. UHPFRC's advantages & disadvantages. Own Source.	34
Table 6. FRP's strips summary. Source: Own.	37
Table 7. Column's description, displacement of sharp and failure load of rounded & edged columns. By: Esraa.	37
Table 8. Increase in loading capacity. By: Esraa.....	38
Table 9. Specimen details. By: Kumar.	39
Table 10. Initial crack load & ultimate failure load. By: Kumar.....	39
Table 11. Service load. By: Kumar.	40
Table 12. Beam specimen reinforcement details. By: Zhao.....	40
Table 13. Test results. By: Zhao.....	41
Table 14. Specimens' characteristics. By: Ilki.	44
Table 15. Strength & deformation characteristics of specimens. By: Ilki.....	45
Table 16. Specimens and reinforce details. By: Kashyap.	46
Table 17. Test results. By: Kashyap.	47
Table 18. Test Characteristics. By: Galal.....	49
Table 19. Test Results. By: Galal.	50
Table 20. Specimens' properties. Source: Own.	51
Table 21. Table 21. Test results. Source: Own.....	51
Table 22. Specimens' properties. By: Own.....	52
Table 23. Group 1 specimens results. By: Aghani.	52
Table 24. Group 2. Specimens' results. By: Aghani.	53
Table 25. Specimens' details. By: Yeong Koo.....	55
Table 26. Test result. By: Yeong Koo.....	56
Table 27. Description of specimens. By: Devaux.	57
Table 28. Specimens details.	63
Table 29. Program test.....	64
Table 30. Test results.....	67
Table 31. Beams Comparison. Source: Own.....	69
Table 32. Columns Comparison. Source: Own.	69
Table 33. Masonry walls comparison. Source: Own.....	69
Table 34. Bridges Comparison. Source: Own.	70
Table 35. Test specimens' characteristics. By: Wang.....	71
Table 36. Strength specimens' results. By: Wang.....	72
Table 37. Deformation specimens' results. By: Wang.....	72
Table 38. Specimens' conditions. By: Cheng. Source: ASCE.	76
Table 39. Specimens test results. By: Cheng. Source: ASCE.....	76

LIST OF FIGURES

Figure 1. Representation of FRP material. Source: Researchgate.net.....	11
Figure 2. What are Polymers? Graphic. Source: jagranjosh.com.....	12
Figure 3. FRO historical development. Source: Own.	13
Figure 4. FRP Stress-Strain curve. Source: ACI 440R96.	16
Figure 5. FRP reinforcing systems on bridges. Source: DocPlayer.	20
Figure 6. FRP reinforcing beams and columns. Source: Basalto.	21
Figure 7. FRP's multiple reinforcing uses. Source: Interempresas.net.....	21
Figure 8. Real image of UHPFRC. Source: IStructe Victoria Branch.	23
Figure 9. UHPFRC historical development timeline. Source: Own.	25
Figure 10. Hybrid fiber concrete (mix of fibers). Source: concrete.org.....	27
Figure 11. Synthetic and steel fibers used in concrete structures. Source: Abellan [62].	28
Figure 12. Characteristic tensile behavior of UHPFRC. Source: Abellan [62].....	32
Figure 13. Stress-strain relationship of different UHPFRC's in compression. Source: Researchgate.net.	32
Figure 14. Geometries of "UHPFRC-concrete " elements for bridge deck slabs. Source: core.ac.uk.....	35
Figure 15. Before a) and after repair and protection b) of a canal bridge by a UHPFRC slab. Source: Researchgate.net.....	36
Figure 16. Effective confinement areas in circular, square, and rectangular columns. By: Esraa.	38
Figure 17. Load vs deflection curve. By: Kumar.	39
Figure 18. Load vs deflection behavior of bonded FRP reinforcing RC beams. By: Zhao.	41
Figure 19. Peeling failure of concrete cover for specimen B2. By: Zhao.	42
Figure 20. Debonding failure between FRP fabric and concrete, specimen B3. By: Zhao..	42
Figure 21. Load-slip relationship at the composite interface. By: Zhao.	43
Figure 22. Principal stress distribution under the rebar and at the concrete-epoxy interface. By: Zhao.	43
Figure 23. Reference (type A) plastered (type B) & retrofitted (type C) specimens. By: Ilki.	44
Figure 24. Load vs average vertical deformation relationships for all specimens. By: Ilki.	45
Figure 25. Geometric specimens' details - Walls 5-15. By: Kashyap.....	47
Figure 26. Load vs deflection, showing effect of FRP strip spacing. By: Kashyap.....	48
Figure 27. Influence of Pre-compression. By: Kashyap.....	48
Figure 28. Influence of reinforcement ratio. By: Kashyap.....	48
Figure 29. Anchorage system for retrofit steel beams with FRP. By: Galal.	50
Figure 30. Reinforcement scheme & location of prefabricated UHPFRC sheets. By: Aghani.	52
Figure 31. Load vs deflection relationship for group 1 specimens. By: Aghani.....	53
Figure 32. Crack pattern: (a) control series, (b) reinforced series. By: Aghani.	53
Figure 33. Load vs deflection relationship for group 1 specimens. By: Aghani.....	54
Figure 34. Crack pattern: (a) control series, (b) reinforced series. By: Aghani.	54
Figure 35. Load vs displacement curves. By: Yeong Koo.	55

Figure 36. Load-displacement envelop. By: Yeong Koo.	56
Figure 37. hysteresis loop (left) and cracking pattern at the end of the test (right) for WUR wall. By: Devaux.	57
Figure 38. Hysteresis loop recorded during testing the WRU specimen (left); cracking pattern at the end of the WRU specimen testing (right). Legend: hatched areas show falling parts of masonry and cracks are reported with dashes whose thickness represents the cracks opening. By: Devaux.	58
Figure 39. Hysteresis loop recorded during testing the WRL specimen (left); cracking pattern at the end of the WRL specimen testing (right). Legend: see Figure 38. By: Devaux.	58
Figure 40. hysteresis loop recorded during testing the WRS specimen. By: Devaux.	58
Figure 41. Specimens envelop curve. By: Devaux.	59
Figure 42. Specimens Dimensions. By: Azizinamini.	60
Figure 43. a) Damaged part before and after repair using UHPFRC shell (Unit 1 and 2), b) Damaged part with no repair (Unit 3).	60
Figure 44. Force vs displacement hysteretic responses of a) Unit 1, b) Unit 2, c) Unit 3; Moment vs displacement hysteretic responses of d) Unit 1, e) Unit 2, f) Unit 3.	61
Figure 45. Stiffness curves (left), Stiffness degradation curves (right).	62
Figure 46. The energy dissipated vs. drift ratio (left). Energy dissipated energy vs. number of cycles (right).	62
Figure 47. Test Scheme.	63
Figure 48. Horizontal load vs horizontal displacement response.	65
Figure 49. crack pattern of the specimen, before the strengthening (left) and after the strengthening (right)	65
Figure 50. Average crack spacing.	66
Figure 51. Average crack width.	66
Figure 52. Horizontal load vs Horizontal displacement.	67
Figure 53. Axial stress-strain behaviors of specimens. By: Wang.	73
Figure 54. Axial stress-strain behaviors of specimens. By: Wang.	73
Figure 55. Axial stress-strain behaviors of specimens. By: Wang.	74
Figure 56. Axial stress-strain behaviors of specimens. By: Wang.	74
Figure 57. Axial stress-strain behaviors of specimens. By: Wang.	74
Figure 58. Specimens' mode of failure. By: Wang.	75
Figure 59. Load-deflection curves. By: Cheng. Source: ASCE.	77

INTRODUCTION

Technology developments in the last years have been included advances in the construction and materials area. Especially prominent has been the development of new materials with superlative characteristics of strength, stiffness, durability, and ductility compared to conventional concrete [1–3]. Among them, two materials could be highlighted: FRP (Fiber Reinforced Polymers) and UHPFRC (Ultra-High-Performance Fiber Reinforced Concrete) [4–6].

Polymers Fiber Reinforced, composed of Carbon Fiber, Glass Fiber, and Aramids, are known for having high tensile strength, high elasticity module, high corrosion resistance y and lightweight [7]. These characteristics make FRP be an interesting material to be studied in the construction area and commonly used to reinforce structures with high tensile stresses. However, this material has some disadvantages: low ductility, limited use outdoors, and high price [8].

Alternatively, ultra-high performance fiber reinforced concrete has emerged as the response to the multiple types of research of a material that satisfies the high quality demanded by constructions around the world lately [9–12]. These concretes are based on an elevated particle packing density, whereby its durability and strength characteristics are higher than conventional concrete [13–15]. Its more remarkable properties are its high tensile, compression, flexion strength, and low permeability because of its low porosity, which protects it from harmful agents [10,16–18]. Like FRP, this kind of concrete is costly and is not friendly to the environment because of its high cement content [5,19,20]. However, some researchers and studies are looking to make it cheaper and more sustainable, keeping its remarkable properties.

In the same way, multiple types of research are based on the incorporation of different types of reinforcing fibers that are cheaper [21–23]. Another one is to analyze the possibility of the cement or silica fume partial substitution with some coproducts like glass powder recycled, fly ash, blast furnace slag, and rice husk ash [10,11,19,24–29]. All of these are looking to reduce costs and contribute to sustainability. Consequently, some studies are looking for use recycling concrete aggregates that some studies are looking for use using recycling concrete aggregates that although decreased the compression strength, strength losses could be limited [30].

Besides, one of the most important applications of FRP and UHPFRC is the reinforcement of the structures [6,22,23,31]. In this sense, some studies have compared the performance of each of them. Then, there are some reinforcement techniques, such as replacing the damaged concrete with UHPFRC or conventional concrete covered with an FRP “jacket” [6]. Both technologies have proved their excellent results. However, UHPFRC presents advantages in cost and time concerning FRP jackets. It is important to mention that the repaired structures show better service performance than in original conditions in some of these studies [6]. Furthermore, has been studied the possibility of using FRP and UHPFRC together through

the concrete confinement in two kinds of FRP, CFRP Carbon Fiber Reinforced Polymers and GFRP Glass Fiber Reinforced Polymers. These studies have shown some different outcomes, which let us analyze what is expected in the future with these materials [32].

FIBER REINFORCED POLYMER (FRP)

Fiber-reinforced polymer (FRP) is a long unidirectional fiber of carbon, glass, or aramid, although other fibers like paper, timber, or asbestos have been sometimes used, embedded in a polymer matrix [7]. Then, the polymer is usually an epoxy, vinyl ester, or polyester thermosetting plastic, and phenol-formaldehyde resins are still in use [7]. In the same way, FRP is a category of composite plastics that specifically use fiber materials (not mixed with polymer) to improve the mechanical properties of plastics. The matrix is the original polymer material without fibers, which is a relatively weak plastic, but when fibers or filaments are incorporated, it gets stronger [3,4]. In that sense, FRP's mechanical properties depend on both components, the fiber and the matrix, their volume relative to one another, and the fiber length and orientation within the matrix [33].

Additionally, FRP composites have been included in new constructions and for retrofitting concrete structures, bridge decks, beams or piers, modular structures, formwork, and external reinforcements in general, with the principal purpose of strength elements and for the seismic upgrade. In the same way, this inclusion in new constructions is due to different FRP characteristics as lightweight, no-corrosive, very high tensile strength, high stiffness, easily constructed, and because FRP can be tailored to satisfy performance requirements [7]. Furthermore, the fiber reinforced polymer composites (FRPs) are increasingly being considered as an enhancement to be a substitute for infrastructure components or systems that are used traditionally in civil engineering, namely concrete and steel [33]. Figure 1 gives a better idea of FRP composition:

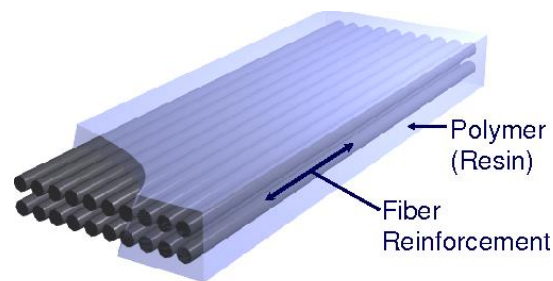


Figure 1. Representation of FRP material. Source: Researchgate.net.

Consequently, as presented in Figure 1, it is necessary for the polymeric matrix to keep the fibers together. Although fibers lose some strength by being embedded in the matrix, the matrix is necessary because a loose bundle of fibers doesn't work because they need to be linker. Furthermore, fibers are strong, but they have a brittle failure, and the matrix helps add toughness to the composite and absorbs energy by deforming under stress. Finally, it is worth mentioning that fibers are not strong in compression [3]. Hence, they buckle when they are

subjected to compression stresses. However, the matrix gives compressional strength to the composite [33].

Typically, there are two main goals in FRP composites. The first one is to enhance strength, toughness, stiffness, or dimensional stability through embedding fibers in a matrix. And the second one is to employ readily available and inexpensive filler to extend a more expensive or scarce resin [4,33]. This goal is important because petroleum materials have become less reliable and more expensive. Therefore, fillers are used for reducing permeability too or enhancing processability (glass spheres).

POLYMERS:

Polymers are the joining of monomers (small molecules) with the objective of making larger molecules. Thus, that linking process is called polymerization. Each of these small molecules needs to have functional groups or at least two reaction points. There are two principal types of polymerization processes. The first one is condensation polymerization, in which the chain growth is accompanied by the elimination of small molecules such as H_2O or CH_3OH . In the second one, addition polymerization, the polymer is formed without the loss of other materials [33]. Figure 2 shows how polymerization works:

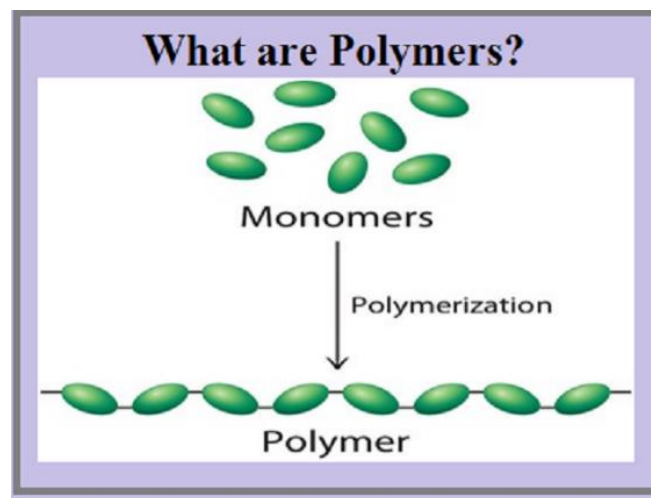


Figure 2. What are Polymers? Graphic. Source: jagranjosh.com.

HISTORICAL DEVELOPMENT:

The next timeline is a summary of FRP's historical development:

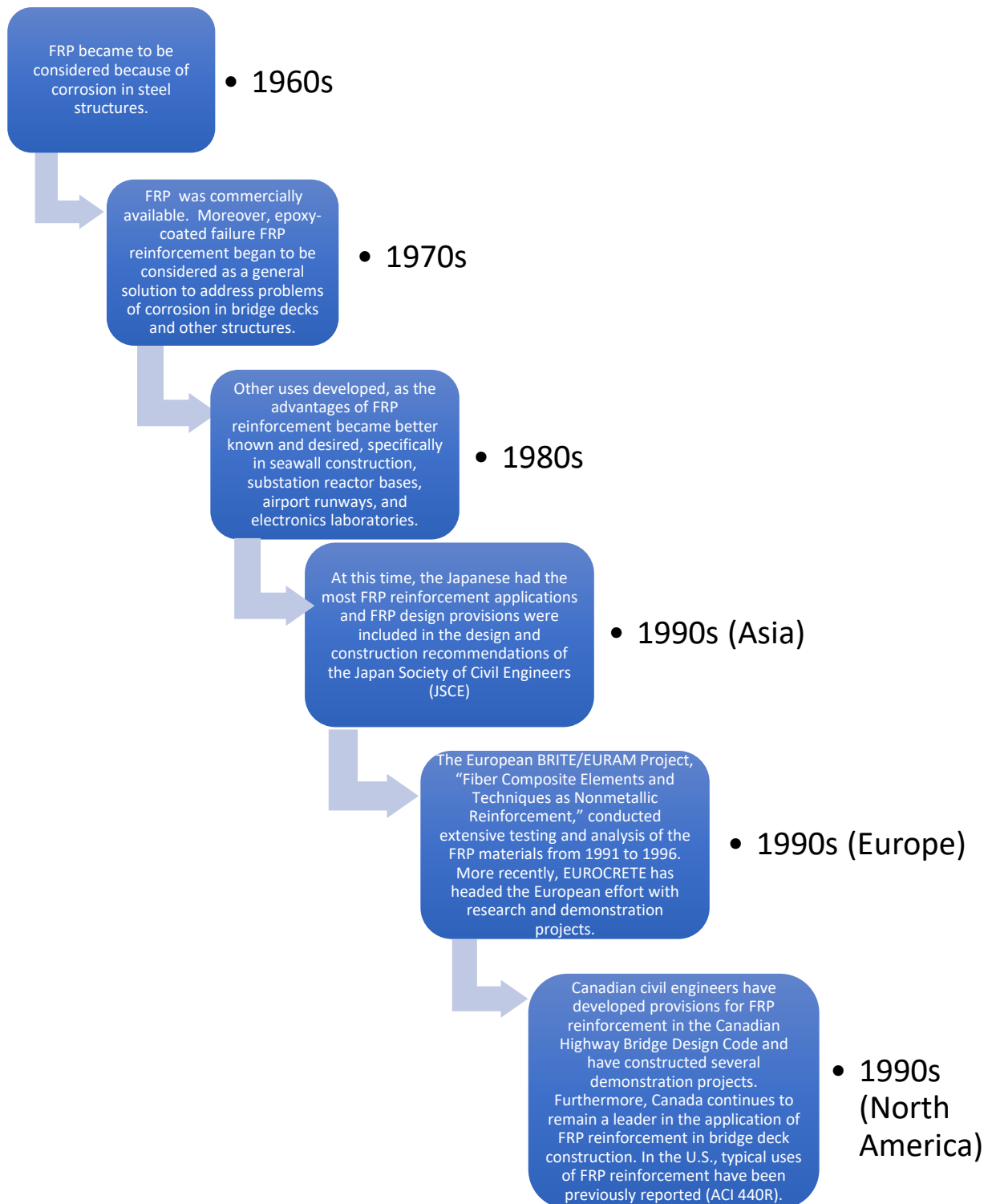


Figure 3. FRO historical development. Source: Own.

In addition to the timeline exposed before, it's remarkable that, within the last ten years, in Asia, some institutes have been publicized multiple documents about the use of FRP composites in concrete structures. Among these are the Railway Technical Research Institute (RTRI), the Japan Society of Civil Engineers (JSCE), and the Japan Concrete Institute (JCI). In Europe, Task Group 9.3 of the International Federation for Structural Concrete (FIB) produced a report on design guidelines for reinforcing concrete structures with FRP bonded externally. And finally, in North America, The Canadian Standards Association (CSA) and ISIS have been working on developing guidelines for FRP systems. In that sense, in 2006 was completed the Section 16, "Fiber Reinforced Structures," of the Canadian Highway Bridge D, and CSA approved CSA S806-00. In the United States, there are some criteria in the construction industry for evaluating FRP systems [7].

TYPES:

There are three kinds of FRP:

CFRP (Carbon Fiber Reinforced Polymer):

In 1879, Edison brought out a patent for manufacturing carbon filaments used in electric lamps. This was the first experience worldwide working with carbon fibers. Carbon-fiber-reinforced polymer is a very strong and light fiber-reinforced polymer that contains carbon fibers. In the same way, when polyacrylonitrile fibers (PAN) are carbonized (by thermal pyrolysis and oxidation) at elevated temperatures. Therefore, graphitizing and stretching fibers can improve strength and elasticity, respectively. Finally, it is worth mentioning that there are multiple types of CFRP. These are classified based on their properties (modulus, strength, or final heat treatment temperature) or based on their precursor materials [7,33,34].

GFRP (Glass Fiber Reinforced Polymer):

Today GFRP is a common material used in different areas. In the same way, Glass fibers are formed from melts and manufactured in various compositions by changing the number of raw materials as clay for alumina, sand for silica, colemanite for boron oxide, and calcite for calcium oxide. Therefore, varying amounts of silica or other sources in different kinds of glass fibers exhibit different performances like higher mechanical properties or alkali resistance. According to their geometry, glass fibers can be divided into two principal groups: continuous fibers commonly used in yarns and textiles, and the discontinuous (short) fibers used as batts, blankets, or boards for filtration and insulation [33,35].

Aramid

Aliphatic polyamides are macromolecules whose structural units are generally interconnected by the amide linkage (NH-CO). A basis for polyamides classification is the nature of the structural units. Hence, aromatic polyamides in which at least 85% of the amide linkages are directly adjacent to aromatic structures are known as aramids. At the same time, aliphatic polyamides with structural units derived mainly from aliphatic monomers are members of the generic class of nylons. Aromatic polyamides are the result of the search for material characterized by good thermal properties [7,33].

CHARACTERISTICS:

Physical:

- Density:

Table 1. FRP's density. Source: ACI.

lb/ft³ (g/cm³)			
Steel	GFRP	CFRP	AFRP
493.00 (7.90)	77.8 to 131.00 (1.25 to 2.10)	93.3 to 100.00 (1.50 to 1.60)	77.80 to 88.10 (1.25 to 1.40)

It's shown in the last table that FRP density is approximately five times less than steel density.

- Coefficient of Thermal Expansion:

The coefficients of thermal expansion of FRP vary in the transverse and longitudinal direction, depending on the fiber's kind, resin, and volume fraction of fiber. Vary in the longitudinal and transverse directions depending on the types of fiber, resin, and volume fraction of fiber. Therefore, fibers dominate the longitudinal coefficient of thermal expansion, whereas the resin dominates the transverse coefficient [36].

Table 2. FRP's Coefficient of Thermal Expansion. Source: ACI.

Direction	CTE, $\times 10^{-6}/^{\circ}\text{F}$ ($\times 10^{-6}/^{\circ}\text{C}$)			
	Steel	GFRP	CFRP	AFRP
Longitudinal, α_L	6.5 (11.7)	3.3 to 5.6 (6.0 to 10.0)	-4.0 to 0.0 (-9.0 to 0.0)	-3.3 to -1.1 (-6 to -2)
Transverse, α_T	6.5 (11.7)	11.7 to 12.8 (21.0 to 23.0)	41 to 58 (74.0 to 104.0)	33.3 to 44.4 (60.0 to 80.0)

*Typical values for fiber volume fraction ranging from 0.5 to 0.7.

Observation: a negative coefficient of thermal expansion indicates that the material contracts with increased temperature and expands with decreased temperature.

Mechanical:

Certainly, to talk about FRP mechanical properties and understand some important facts, it is important to show the Stress-Strain curve. Figure 5 shows this curve:

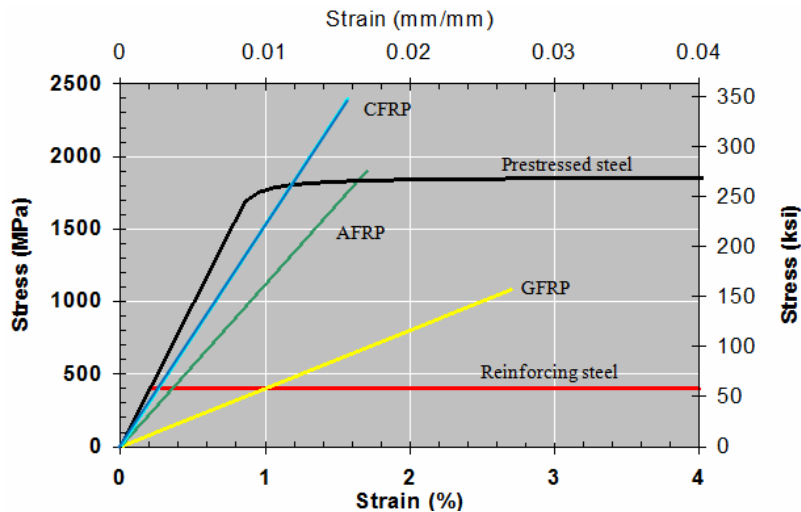


Figure 4. FRP Stress-Strain curve. Source: ACI 440R96.

From this figure, it's easy to analyze that FRP materials (CFRP, AFRP, and GFRP) are brittle, which means that they fail suddenly and consequently don't have ductility. Also, it is clear that these materials have a stress-strain better behavior than Reinforcing steel and, in some cases, than prestressed steel [7].

- **Effects of High Temperatures:**

Though FRP reinforcement embedded in concrete cannot be on fire thanks to an oxygen absence, polymers get soft at high temperatures. Hence, the temperature at which a polymer will soften is known as the glass-transition temperature T_g . Then, temperatures above T_g will decrease the elastic modulus of the polymer because of changes in its molecular structure. T_g values are typically between 150 to 250 °F (65 to 120 °C), and depend on the type of resin [7].

Therefore, it's noteworthy that fibers present better thermal properties than the matrix. So, the experimental campaign has pointed out that temperatures of 480 °F (250 °C), higher by far than the T_g , will lessen the tensile strength of GFRP and CFRP by more than 20%. Therefore, at temperatures beyond T_g , other characteristics as shear and bending strength are decreased notably. In the same way, at temperatures close to T_g , the polymer is not able to transfer stresses from concrete to fibers, and still, mechanical properties are reduced notably. Hence, for design purposes, some researchers recommended that materials have a T_g at least 54 °F (30 °C) above the maximum expected temperature [7].

Then, it is worth mentioning that structural failure can occur if anchorage is lost due to softening of the polymer and when the temperature rises above the temperature threshold of fibers: 2900 °F (1600 °C) for carbon fibers, 1600 °F (880 °C) for glass fibers and 360 °F (180 °C) for aramid fibers. In the case of carbon fibers, elevated temperatures originate higher oxidizing rates when oxygen is in the atmosphere [7].

- **Tensile Behavior:**

FRP composites, as is shown in table 3, do not show any yielding (plastic behavior) in advance of rupture, whereby its failure mode is brittle. Hence, the tensile behavior of FRP materials is distinguished by a linearly elastic stress-strain relationship up to the failure. Typical tensile strength values of some frequently used FRP composites are summarized in the next table [7]:

Table 3. FRP's Tensile Characteristics. Source: ACI.

	Steel	GFRP	CFRP	AFRP
Nominal yield stress, ksi (MPa)	40 to 75 (276 to 517)	N/A	N/A	N/A
Tensile strength, ksi (MPa)	70 to 100 (483 to 690)	70 to 230 (483 to 1600)	87 to 535 (600 to 3690)	250 to 368 (1720 to 2540)
Elastic modulus, $\times 10^3$ ksi (GPa)	29.0 (200.0)	5.1 to 7.4 (35.0 to 51.0)	15.9 to 84.0 (120.0 to 580.0)	6.0 to 18.2 (41.0 to 125.0)
Yield strain, %	0.14 to 0.25	N/A	N/A	N/A
Rupture strain, %	6.0 to 12.0	1.2 to 3.1	0.5 to 1.7	1.9 to 4.4

*Typical values for fiber volume fractions ranging from 0.5 to 0.7.

Thus, as is shown in table 3, GFRP could have a tensile strength more than two times higher than steel. In the case of CFRP, tensile strength could be five times higher than steel. Finally, AFRP could have three times the higher tensile strength [7].

- **Compressive Behavior:**

Compressive strength in FRP is much lower than tensile, and there is a relation between them. Thus, compressive strengths are higher for FRP composites with higher tensile strengths, except AFRP, where the fibers present nonlinear behavior in compression at a relatively low level of stress. In the same way, the tensile modulus of elasticity of FRP reinforcing appears to be bigger than its compressive modulus of elasticity. According to reviews, the compressive modulus of elasticity is approximately 100% for AFRP, 80% for GFRP, and 85% for CFRP of the tensile modulus of elasticity for the same product [7].

- **Shear Behavior:**

Most FRP usually doesn't have reinforcement (fibers) across layers. Thus, the interlaminar shear strength is driven by the relatively weak polymer matrix. Hence, FRP composites are relatively weak in interlaminar shear, where sheets of unreinforced resin lie between sheets of fibers. However, orientating the fibers in an off-axis direction across the layers of fiber will enhance the shear resistance, depending upon the degree of offset [7].

- **Creep rupture:**

Generally, glass fibers are the most susceptible to creep rupture, while aramids are reasonably susceptible and carbon fibers are the least susceptible. In that sense, FRP reinforcing subjected to a constant load over time can suddenly fail after a time called

the endurance time. This phenomenon is known as static fatigue (or creep rupture). Thus, while endurance time decreases, the ratio of the sustained tensile stress to the short-term strength of the FRP increase s[7].

- **Modes of Failure:**

Structural failure can happen in FRP composites in some ways [7]:

- The material fails at shear in the interface between fibers and matrix because tensile forces stretch the matrix more than the fibers.
- Fibers are separated from the matrix because tensile forces close to the end of the fibers exceed the tolerances of the matrix.
- The material fails because tensile forces exceed the fiber's tolerances causing the fibers to fracture and consequently leading to material failure.

ADVANTAGES & DISADVANTAGES:

There are several benefits and drawbacks of this material for structural strengthening. This is presented in table 4:

Table 4.FRP's advantages and disadvantages. Own Source.

ADVANTAGES	DISADVANTAGES
<ul style="list-style-type: none"> • Corrosion Resistant. • Lightweight. • Ease of handling. • Non-magnetic Properties. • High tensile strength. • Low coefficient of thermal expansion. • Thermal and Electric Insulator. • Future improvements are expected. • Decreasing the unit cost of FRP reinforcements are expected with the increased market share and demand. 	<ul style="list-style-type: none"> • Brittle Failure: Linear response in tension up to failure. • Poor transverse or shear resistance. • Poor resistance to high temperatures and fire. • Lack of plastic behavior (no ductility). • Sensitive to stress-rupture effects. • Lose significant strength upon bending. • High per unit weight or based on force carrying capacity. • Differences in the thermal and mechanical properties with the concrete

It is worth denoting that some of the disadvantages, as the high cost, will get better in the future because compared with steel or concrete, this is relatively new material. Thus, it has a long range of improvement [7,37,38].

In the same way, In the strength viewpoint, there is an interesting analysis that will be explained:

In FRP composites, the loading capacity is better when the force is applied parallel to the fiber's orientation and consequently weakest when the fibers are perpendicular to the force. In that sense, fibers' orientation directly affects the mechanical properties of the FRP reinforcement. Thus, this ability is at once both a limitation and a benefit depending on the context of use. Weak spots of perpendicular fibers can be used for natural hinges and connections but. However, conduce to material failure too, when production processes fail to correctly orient the fibers parallel to forces awaited. Therefore, when forces are applied perpendicular to the orientation of fibers mechanical properties of the polymer are less than the matrix resin alone. In the same way, in cast resin components made of GFRP like UP and EP, the fibers can be oriented in two-dimensional and three-dimensional weaves. This means that when forces are perpendicular to one orientation, they are parallel to another orientation. Thus, the potential for weak spots in the polymer is eliminated [33].

LABORATORY TESTS:

Mechanical properties measurements

Strength

To measure the tensile strength of a polymer specimen, it is usually be stretched by a machine. The machine has clamps on each end of the specimen, with the objective of stretching the sample. While it is stretching the sample, it measures the force (F) that is being applied. Then, the applied force is divided by the cross area of the sample. The answer is the stress that the sample is experiencing. Then, the amount of force is increased on the specimen until it breaks or fails. The stress used to break the sample is the tensile strength of the FRP composite [7,33,35,36].

Elongation

When a tensile stress is exerted, the sample becomes longer, it's called elongation, and usually, it is calculated as a percentage, then, elongation is just the length of the polymer specimen after it is stretched (L), divided by the specimen original length (L_0), and finally multiplied by 100 [7,33].

Modulus

After calculating the tensile strength, applying stresses, and measuring the elongation for each stress level until the sample breaks, it is possible to make a graphic with some different points (deflection, stress). This plot is called a stress-strain curve. Then, the tensile modulus is the slope of this plot. In general, fibers have the highest tensile modulus, and elastomers have the lowest, and plastics have tensile modulus somewhere in between elastomers and fibers. Modulus is measured by calculating stress and dividing by elongation and is expressed in the same units as strength (N/mm^2) [33].

Toughness

That plot of stress versus strain exhibits another valuable piece of information [35]. Measuring the area underneath the stress-strain curve, the number you get is something called

toughness. Then, Toughness is really a measure of the energy a sample can absorb before it breaks. In the same way, from a physics point of view, toughness is how much energy is needed to break a sample [7,35].

APPLICATION:

FRP can be applied to strengthening beams, columns, and slabs in buildings or beams and piers in bridges [7,39,40]. It is possible to enhance the strength of these structural members even after these have been gravely damaged because of bearing conditions. For strengthening beams, two techniques are adopted. The first one is to paste FRP plates at the general tension face of the beam (the bottom). This enhances the strength of the beam, deflection capacity of the beam, and stiffness (load required to make unit deflection) [41]. Alternatively, FRP strips can be pasted in a 'U' shape around the sides and bottom of a beam, resulting in higher shear resistance. On the other hand, Columns in a building can be wrapped with FRP for achieving higher strength. The technique works by restraining the lateral expansion of the column. Finally, slabs can be strengthened by pasting FRP strips at their tension face (the bottom). This will result in better performance since the tensile resistance of slabs is supplemented by the tensile strength of FRP. In the case of beams and slabs, the effectiveness of FRP strengthening depends on the performance of the resin chosen for bonding [7,33,38,40,41].

According to the explanation exposed in the last paragraph, Figure 5 shows how FRP can be used as reinforcing for bridge's beams:



Figure 5. FRP reinforcing systems on bridges. Source: DocPlayer.

In addition, Figure 6 shows how FRP can be implemented in beams and columns reinforce:



Figure 6. FRP reinforcing beams and columns. Source: Basalto.

In the same way, the next figure is a summary of different uses of FRP reinforcing structures:

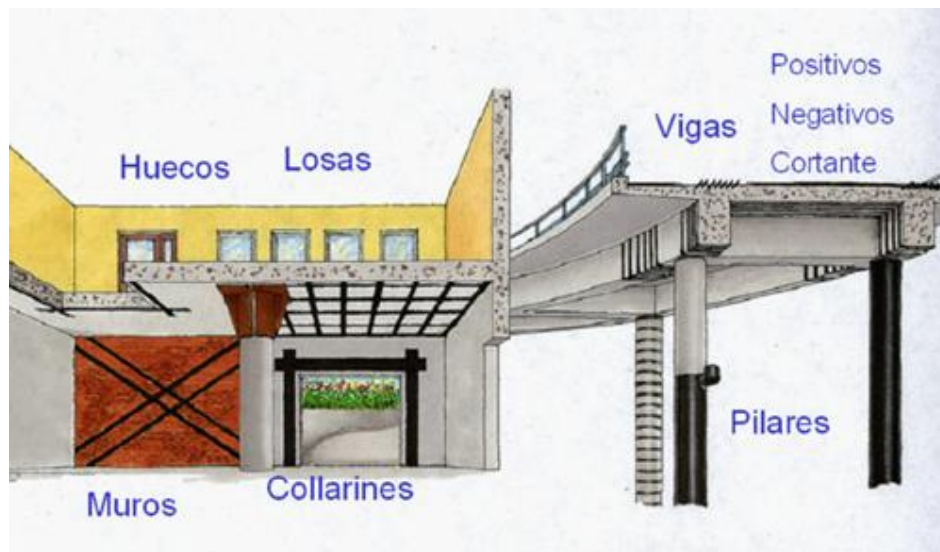


Figure 7. FRP's multiple reinforcing uses. Source: Interempresas.net.

Design Philosophy:

These design recommendations are based on limit-states design principles. This approach sets acceptable levels of safety for the occurrence of both ultimate limit states (failure, stress rupture, and fatigue) and serviceability limit states (excessive deflections and cracks). Evaluating the nominal strength of a structural member, the possible failure modes, and subsequently, strains and stresses in each material should be assessed. Thus, engineering principles, such as modular ratios and transformed sections, may be implemented for evaluating the serviceability of a member. FRP strengthening systems should be designed in

accordance with ACI 318-14 [42] strength and serviceability requirements using the strength and load factors stated in ACI 318-14. Therefore, there are some reduction factors that are typically above 3.5, though in some cases, these factors are between 3.0 to 3.5. These cases are when high ratios of FRP are combined with low ratios of steel reinforcement. In that sense, these reduction factors were recommended on this guide to reflect incertitude inherent to FRP systems in comparison with prestressed concrete and steel reinforced. It is worth mentioning that these reduction factors were determined based on statistical evaluation of variability in mechanical properties, predicted versus test results in full scale, and field applications. In general, lower reliability is expected in retrofitted and repaired structures than in new structures [7,36,43].

ULTRA HIGH-PERFORMANCE FIBER REINFORCED CONCRETE (UHPFRC)

Concrete is a material that is the result of mixed water, sand, gravel, and cement, and when it forges gets more strength [44]. It also may be considered as an artificial rock made by the human, which takes advantage of its strength and durability in construction. Generally, the cementing material is hydraulic cement, which develops its properties in water presence, and its principal purpose is to join the aggregates and pozzolans (in case this be present in the mixture). In the same way, aggregates are composed of a thin part (sand) and a thick part (gravel), and their principal purpose is to work as filling [42,45].

Consequently, there are multiple aspects that define the type of concrete. Thus, the type of cement or aggregate used, the specific attributes it manifests, or the methods used to fabricate it, all these facts let characterized the concrete. Therefore, it is known that in normal structural concrete, the concrete performance is closely related to the water/cement ratio. The lower the water content, all else being equal, the stronger the concrete. Hence, to ensure each aggregate particle is covered by the cement paste, that the concrete mixture is liquid enough to be spread and poured correctly and that the holes between the aggregates are filled, the mixture must have enough water. Another durability factor is the amount of cement in relation to the aggregate (expressed as a three-part ratio-cement to fine and coarse aggregate). There may be relatively less aggregate where stronger concrete is needed [46,47].

Therefore, it is known that concrete is naturally brittle [48]. Typical stresses like impact, fatigue, and loading, lead to cracking and eventual failure. Adding reinforcement to the concrete helps to absorb these stresses and to limit the formation of cracks, increasing the load-bearing capacity and ductility of the concrete structure [45]. There are several ways of reinforcing concrete. Since its introduction over 40 years ago, steel fiber reinforcement has proven its merits in the most demanding structures and applications [45]. In the same way, the core difference between steel fiber and other reinforcement solutions is that fibers turn the concrete in a composite material instead of supplying strength in different positions, thus steel fibers form a reinforcing network throughout the entire concrete structure, increasing its overall ductility. Particularly, the inclusion of fibers significantly enhances the tensile

capacity, leading to high deformability, beyond 1%, with a multi-cracking phase (pseudo-plastic) and an improvement in the tensile capacity before crack localization and strength depletion [45].

As explained in the introduction section, UHPFRC is one of the latest developments in recent years regarding concrete technology. When UHPFRC is subjected to loading, compressive flexural or tension stresses start to work in the specimen, and small cracks will appear in places where the stress reaches a critical point [49–52]. Hence, steel fiber interacts within the concrete matrix, absorbing tensile stresses at any point and in any direction. As a result, steel fiber picks up small cracks much faster than traditional reinforcement. When a crack occurs, the hooked ends of the fibers remain solidly anchored on each side of the crack, acting as a stress transfer media. Once the maximum bond strength with the concrete is reached, the pull-out takes full effect [53–55].

Certainly, after talking about concrete and fibers, it is important to talk about Ultra-High-Performance Concrete (UHPC), which is a cementitious composite characterized by very small aggregates size (lower than 6mm), a significant cement quantity (higher than 600 kg), small size binders (pozzolana, fly ash, silica fume, reactive powder) and a low water/cement ratio ($w/c < 0.2$) [9,51,56]. This mix composition produces an interconnected and dense microstructure with a compressive strength higher than 150 MPa, high homogeneity, and a capillary porosity lower than 1.5%. Thanks to these properties, the concrete will have a better performance, higher durability, and increased loading capacity and toughness in comparison with normal and high-strength concrete [26,57,58]

Finally, combining UHPC characteristic and reinforcing it with fibers is possible to get UHPFRC. This combination gives UHPC more ductility and works through the entire composite. In the same way, its mechanical behavior and its unique characteristics are suitable for construct, more durable, lighter, more efficient, and innovative structural elements [26,59].

Figure 8 shows how fibers work in UHPFRC and how this kind of concrete looks:



Figure 8. Real image of UHPFRC. Source: IStructe Victoria Branch.

Basic principles for obtaining UHPFRC:

There are some basic principles to obtain an adequate UHPFRC mixture [16,17,60]:

1. Increase in homogeneity by eliminating coarse aggregate.
2. Increase density by optimizing grain size distribution in such a way as to achieve maximum packing of particles.
3. Improvement of placed concrete by heat treatment.
4. Water quantity in concrete is optimally reduced, and its quantity is insufficient for cement hydration, which can result in the formation of micro cracks because of desiccation; non-hydrated cement acts as a reactive micro aggregate of high modulus of elasticity that can hydrate subsequently.
5. Improvement in ductility by adding a higher quantity of fibers. By adhering to the first four principles, high compressive strengths can be achieved, while by adding fibers, tensile strength and ductility are improved, thereby ensuring deformation and redistribution of forces and prevention of brittle failure of the structure or the test element.

HISTORICAL DEVELOPMENT:

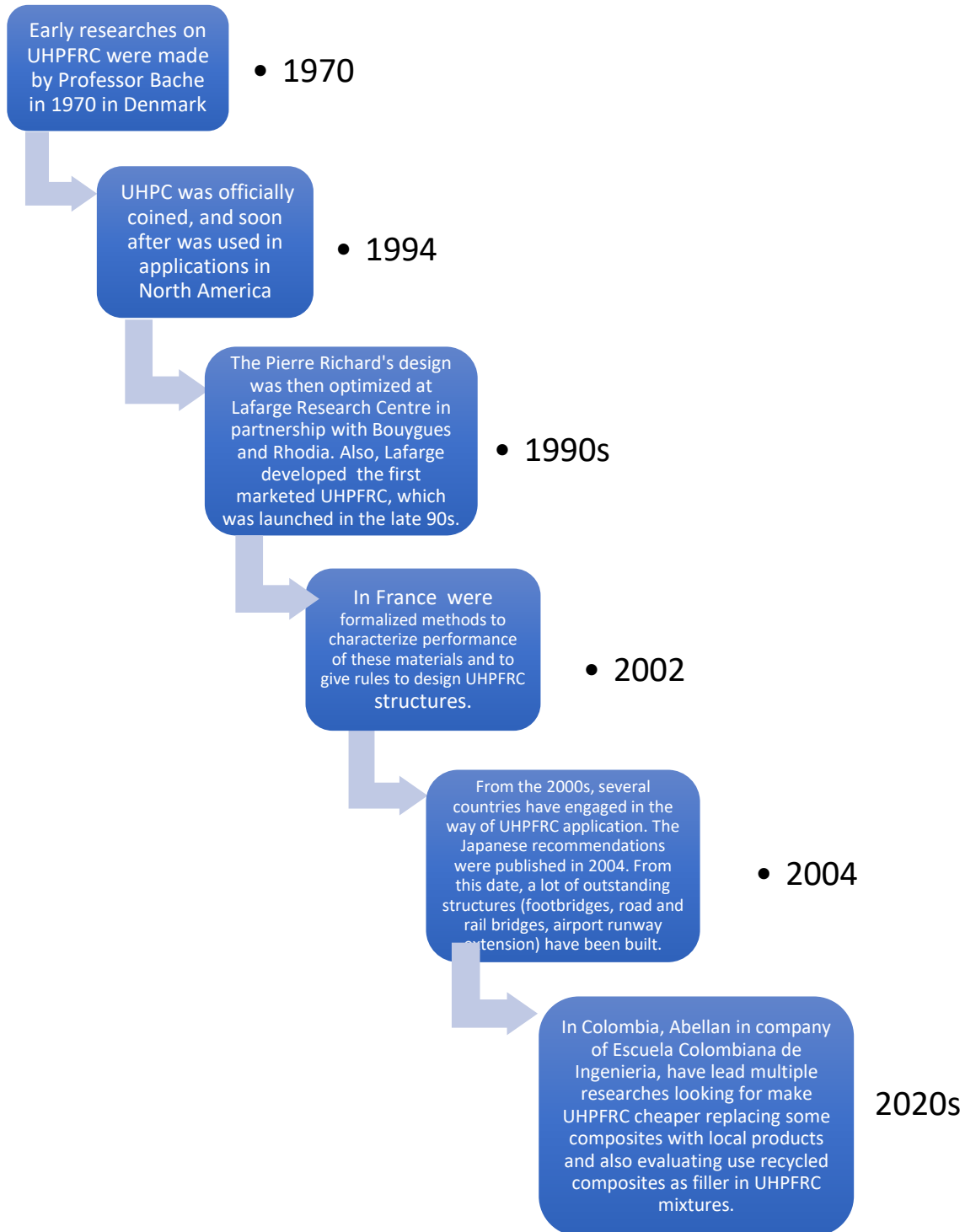


Figure 9. UHPFRC historical development timeline. Source: Own.

FIBER TYPES:

The addition of high-strength steel fibers is the key to making brittle material much more ductile. This is influenced by the following parameters: fiber content; fiber geometry (length, diameter in relation to maximum particle size UHPC); fiber orientation; the bond between fiber and matrix; and stiffness of the fibers.

The selection of fibers is very important for the design of the UHPC, as it has a strong influence on the composition, strength, ductility, and price of the concrete and the final product. Although there are many types of fibers – including carbon, basalt, and many synthetic fibers

There are multiple types of Fibers used in fiber reinforced concrete:

- **Cellulose Fibers:** These fibers are used in a similar way as micro-synthetic fibers for the control and mitigation of plastic shrinkage cracking. In addition, these fibers are fabricated from processed timber pulp products, cellulose fibers.
- **Glass Fibers:** Glass-fiber reinforced concrete (GFRC) has been mainly implemented to modify cement-based panel structures and in architectural applications.
- **Macro-Synthetic Fibers:** This relative type of fibers has been developed as a suitable alternative to steel fibers when dosed properly over the last 15 years. Typical materials include polypropylene and other polymer blends with identical physical properties to steel fibers (e.g., length, shape). Finally, it is worth mentioning that these fibers can be dosed from 3 to 20 lbs/yd (1.8 to 12 kg/m³).
- **Micro-Synthetic Fibers:** These fibers are usually used for protecting and mitigating the plastic shrinkage cracking in concrete. Then, most fiber kinds are fabricated from polypropylene, polyethylene, polyester, nylon, and other synthetic materials, such as carbon, aramid, and acrylics. These fiber types are generally dosed at low volumes ranging between 0.03 and 0.2% by volume of concrete from 0.3 to 0.9 kg/m³
- **Natural Fibers:** Materials as coconut, sisal, jute, and sugarcane are included in natural fibers and come in different lengths, geometries, and material properties. Therefore, these fibers are commonly implemented to reinforce cement-based products in non-commercial applications worldwide.
- **Poly-Vinyl Alcohol (PVA) Fibers:** PVA fibers are synthetic-made fibers, which at higher volumes can improve the compressive and flexural performance of concrete. Then, PVA fibers are mainly used for smaller elements and when very high flexural strengths are demanded.
- **Specialty Fibers:** This classification of fibers covers materials not described in this section and generally concerns recently manufactured or specified materials not common to these categories.

- **Steel Fibers:** These fibers are commonly implemented for providing concrete with better toughness and post-crack bearing capacity. Generally, loose or bundled, these fibers are made from carbon or stainless steel and are shaped into varying geometries such as crimped, hooked end, or with other mechanical deformations for anchorage in the concrete. This fiber is classified according to ACI 544 as Types I through V. Consequently, these fibers can be dosed at 6 to 67 kg/m³ and have maximum lengths between 1.5” and 3” (30 to 80 mm).
- **Steel & Micro/Macro Blends:** A recent development in the field of fiber-reinforced concrete has been the combination or mixing of steel and/or macro-synthetic fibers with different types of micro-synthetic fibers. These combinations help to control plastic shrinkage cracking (i.e., micro-synthetics) and improve the concrete post-crack bearing capacity and toughness compared with using only steel and macro-synthetic fibers.

It is important to mention that there could be some combinations and types not mentioned in this section.

(Fiber Reinforced Concrete Association)

- **Mix of fibers:** It is thus also possible to make a fiber blend/ cocktail. This can be a mix of different types of fibers, such as steel and polypropylene fibers to improve fire resistance and steel fibers of different lengths and diameters. Park et al. carried-out research with UHPC and combinations of steel fiber blends of short and long fibers [52]. While short fibers are very efficient to bridge micro-cracks, longer fibers are very efficient to bridge macro-cracks (Figure 10). This positively influences the strain hardening but also impacts the strength and toughness of the UHPC [52].

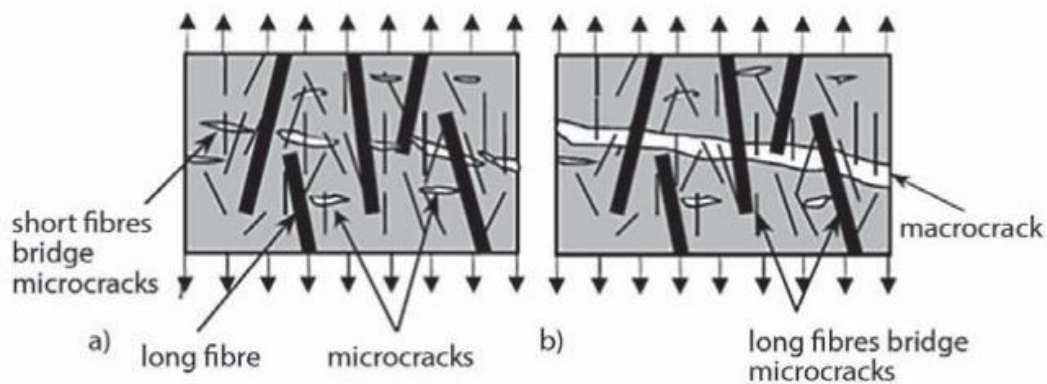


Figure 10. Hybrid fiber concrete (mix of fibers). Source: concrete.org.

- a) The influence of short thin fibers on the bridging of micro-cracks and the increase of tensile strength.
- b) the influence of long thick fibers on the bridging of macro-cracks and the increase of ductility [61]

Remarkably, the most common fibers used in UHPFRC are Steel and Synthetic fibers as shown in the following Figure:

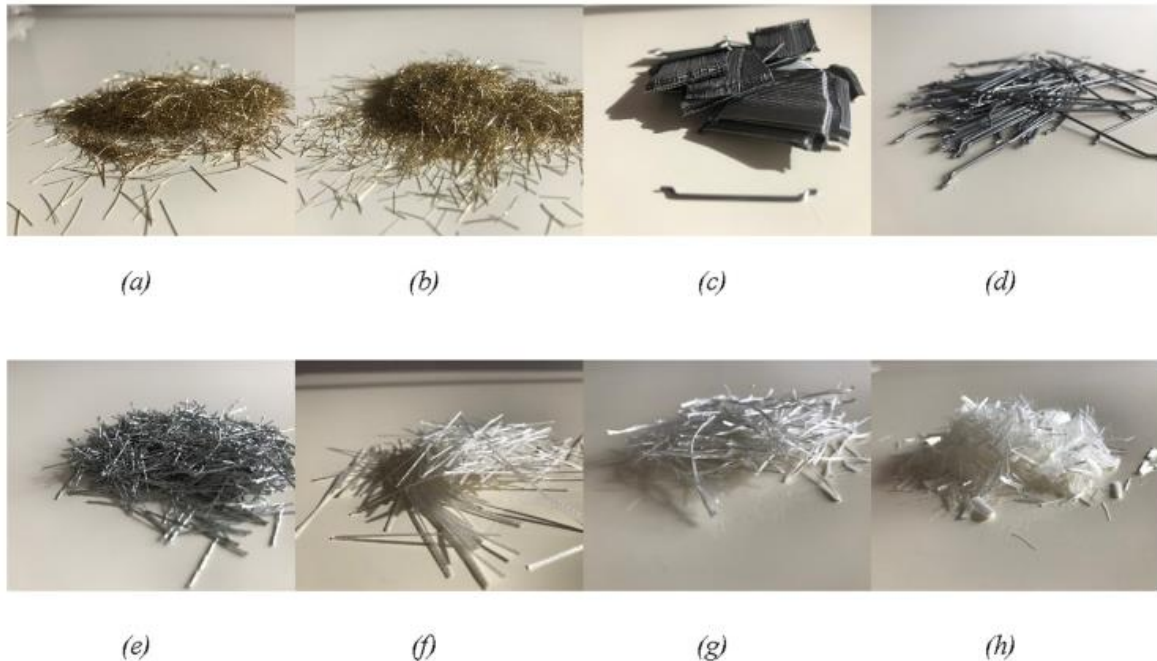


Figure 11. Synthetic and steel fibers used in concrete structures. Source: Abellan [62].

Finally, some important facts are that Fiber lengths for UHPC are 6–20mm, while fiber diameters are 0.009–0.5mm.

Fibers Role:

Incorporating relatively long fibers (If > 10 mm) increases the material's deformability. Immediately after cracking, fibers are progressively engaged, contributing to a pseudo-hardening phase (multi-cracking pattern) and a softening behavior (crack localization) [63].

On the other hand, incorporating short and microfibers with only a few mm lengths had a consequence at the material level, contributing to enhancing the tensile strength of the pseudo-elastic domain. Hence, after the concrete microcracking, the microfibers are activated immediately, leading to a concrete behavior distinguished by a longer elastic phase (elastic + pseudo-elastic) [21,63].

On the other hand, it is important to mention the effect of fibers alignment and distribution in the mixture. Fiber's alignment and distribution are affected by multiple factors like specimen size, boundary conditions, mixture workability, fiber volume, and compaction procedures [55]. Hence, experimental tests have exhibited that the best results in terms of strength capacity are presented when the concrete is pouring concrete from the center. Thus, the flow of concrete outwards from the center of the panel conducts to a preferential alignment of the fibers, perpendicular to the radius of the panel, enhancing the numbers of fibers bridging the cracks [64].

CHARACTERISTICS:

Workability & Mixing Procedure:

The prediction of UHPFRC workability cannot be based on slump tests because this test doesn't give too much information about the physical properties of the mixture. It only verifies the level of flowability. Hence, rheological measurements can be used to find the range of workability. Concrete workability is directly related to the w/c ratio. In UHPC, the w/c ratio is around 0.2. Thus, the control of water content is more critical than in conventional concrete. In this sense, a rise in water content can lead to a significant decrease in concrete strength. Then, to guarantee the mixture's workability, high levels of hyper and super plasticizers may be incorporated in the mixture [65,66].

In UHPFRC, a high flowability is required to guarantee uniform distribution and orientation of fibers during casting, and the flowability is directly related to the number of fibers. Besides, the incorporation of fibers decreases the level of fresh mix flowability because of changes in the skeleton structure, fiber friction, and cohesive forces. Tests carried on UHPFRC, considering different steel fibers content, demonstrated a reduction of the relative slump flow due to the increase of the number of fibers. Therefore, tests considering the same mix design, but with different quantities of filler, have exhibited that to achieve better workability, a solution can be replacing part of the cement with filler [67,68].

UHPFRC fresh mix also is characterized by a high viscosity and thixotropy (time-dependent change in viscosity), which demands high standard quality levels to ensure proper mixing and casting procedures (homogeneity and dispersion of particles) and the quality of the constituents (purity, RH, and gradation). Moreover, the formation of balls is favored by the low w/c ratio and the high amount of binder, also the mixture overheating (thermo-activated chemical reactions generating heat) and self-desiccation (because of water evaporation and hydration) during preparation and placement. Besides, the fiber orientation can be affected by the size and shape of test elements (wall and loose effect) [69,70].

Finally, to achieve good workability, the UHPFRC mixing procedure must guarantee fibers orientation and dispersion through the bulk concrete and ensure a good packing density, avoiding materials agglomeration (formation of cement balls). Hence is recommended, before the addition of water, to mix first the binder and sand (fine particles) due to the tendency of agglomeration. Later, after the addition of water and chemical admixtures (super and hyper plasticizers). Finally, the fibers are added in the last phase. The shear action of steel fibers helps to destroy the remaining agglomerates. The complete mixing procedure should take between 8 to 20 minutes [16,57].

Hydration:

UHPFRC hydration reaction is characterized by a long initial period of dormant (approximately 24 hours), followed by a fast reaction time, which leads to a rapid evolution of the mechanical properties. On the 7th day of hydration, the material reaches approximately 60% of the tensile strength and more than 80% of both the modulus of elasticity and the

compressive strength. After 90 days, the hydration process is relatively completed. It is important to mention that the high amount of binder associated with the low w/c ratio in the UHPFRC mix design changes the hydration kinetics and the mechanical properties of the material. (Buttignol, 2017)

In that sense, cementitious grains separate from the pore water due to the incorporation of hyper and super plasticizers. Thus, it's the cause of UHPFRC's long period of dormancy. Therefore, the first contact of anhydrous cementitious products with the moisture produces an amorphous layer of hydration product around the cement particles, which separates them from the pore solution (water that contains multiple ionic species), preventing faster reactions [16].

After the dormant period, the hydration process successfully begins, then the initial phase takes around 12 hours and is characterized by a thermal process (a significant amount of energy release). This process conducts to a non-negligible temperature rise in the inner concrete layers, even for relatively thin members, which could favor concrete microcracking. Therefore, as exhibited in a UHPFRC research, due to the hydration process, the temperature can increase on the core of the material from 20°C to 32°C. [16].

Permeability:

One of UHPFRC properties is a low w/c ratio, which is not enough to hydrate all cement components. Hence, portlandite and calcium silicates (The anhydrous grains) stay as an inert filler in the matrix, acting as a reserve of the process (healing capacity), which in the hydration process can be activated, after concrete cracking to close or reduce the crack appearance. Moreover, the anhydrate binder, thanks to its small size, helps to enhance the matrix compactness, filling out the small apertures between cement particles (densification process), conducting to very low permeability.

Thus, in comparison with normal and high strength concretes, in UHPFRC, the hydrated grains make a dense and interconnected microstructure with a higher fiber-matrix bond strength (interfacial transition zone with lower porosity). In the same way, due to its very low permeability, UHPFRC protects the structures from noxious agents, such as chloride ions that cause corrosion of steel bars and sulfate attack, which can conduct to concrete expansion, crack propagation, and loss of bond between the aggregates and the cement paste. It is worth noting that in UHPFRC, because of the hardening behavior, small microcracks are developed before crack localization, keeping the material permeability very low even at the post-cracking phase [16,71].

Behavior at high temperatures:

Concrete is susceptible to thermal expansion, cracking formation, and spalling activation, at a macroscopic level. These thermo-hygro-chemical phenomena are responsible for concrete damage and degradation. And are influenced by the previous fire exposure, the maximum temperature reached, and heating rate (temperature history). Therefore, high temperatures affect concrete creep behavior. In the same way, concrete behavior is strongly linked to the

stress level, relative humidity changes and CSH gel viscoelastic response. This is because creep is directly related to the long-term relaxation of self-equilibrated micro-stresses in the CSH nano-porous microstructure [16].

In the same way, the CSH gel is created by the expansion reaction of both cement constituent minerals belite (C2S) and alite (C3S) in contact with water (concrete hydration and short-term aging). This expansion produces a reduction in the capillary pore system and in the concrete permeability because the concrete volume doesn't change. Then, a continuous phase is created by the interconnected gel, isolating free water within its nanostructure interlayer. Therefore, CSH strong van der Waals force leads to high water adsorption on its surface. In that sense, concrete heating beyond 200°C, CSH is progressively decomposed into new calcium silicates (C2S and C3S), releasing the chemically bound water, and reducing concrete binding properties. In temperatures up to 250°C removes most of the CSH physically bound water (dehydrated CSH). And, beyond 750°C, there is a complete disintegration of the CSH gel [16].

Consequently, concrete thermochemical transformations during heating are directly related to dehydration due to the loss of physical and chemical water properties. These transformations can lead to concrete strength reduction, and ductility enhances, and matrix micro prestress relaxation (time-dependent deformation). Besides, the wetness diffusion due to free water evaporation at 100°C (vaporization process) helps increase the pore pressure that could conduct violent spalling. This phenomenon is remarkably important in UHPC because of its dense microstructure and low porosity, leading to the moisture clog. The latter is the vaporization and dilatation of moisture content, which obstructs the interconnected porous network, conducting pore-pressure build-up [32,72].

Tensile Strength & Ductility:

As illustrated in Figure 11, UHPFRC tensile behavior is characterized by three phases:

- First Phase: The material has an elastic behavior until the elastic limit stress, typical values for elastic limit stress are between 7 and 11MPa [49,73].
- Second Phase: This phase is called the strain hardening phase and is characterized by fiber activation accompanied by multiple fine micro-cracking of the matrix. Though, the material still has a continuum behavior [74].
- Third Phase: The third phase begins with the formation of a discrete macro-crack at ultimate resistance, and strain softening begins. Thus, there is no more tensile stress transferred on these crack openings [75].

It is worth mentioning that the tensile hardening and softening behavior of UHPFRC depend on the aspect ratio, content, bond, and orientation of fibers used for reinforcing [55].

Therefore, it is important to highlight that ductility is the most important aspect of UHPFRC for seismic retrofitting applications. And the UHPFRC ductility is commonly measured by direct tensile test. Similarly, the fibers' bridging effect significantly affects performance in the hardening and softening domain [21]. Figure 12 shows the tensile behavior of UHPFRC, and the graphic's shape exhibits the material's ductility:

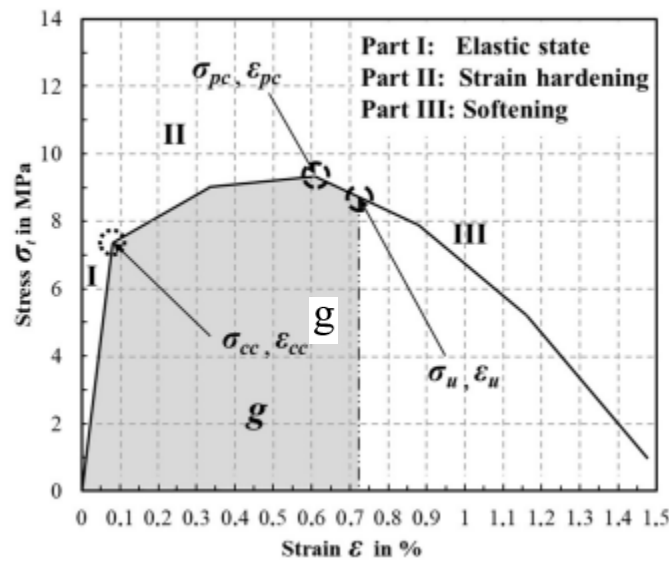


Figure 12. Characteristic tensile behavior of UHPFRC. Source: Abellan [62].

Subsequently, the ductility properties to be met in the multi-objective optimization algorithm for seismic retrofitting applications of UHPFRC will be $g \geq 50 \text{ kJ/m}^3$ and $\epsilon_{Utu} \geq 0.3\%$, thus, ensuring high ductility and the contribution of the UHPFRC above the steel yield of the concrete structure reinforcement to be retrofitted [62].

Compressive Strength:

UHPFRC in an initial phase behaves elastically under compression. In that sense, it is characterized by a linear stress-strain relationship up to the compressive strength, of typical between 130 and 180 MPa, is achieved. For design purposes, a slightly non-linear relationship may be used to describe the ascending branch of the stress-strain diagram. (Bruhwiler, 2016). Figure 13, shows a stress-strain diagram from a UHPFRC sample:

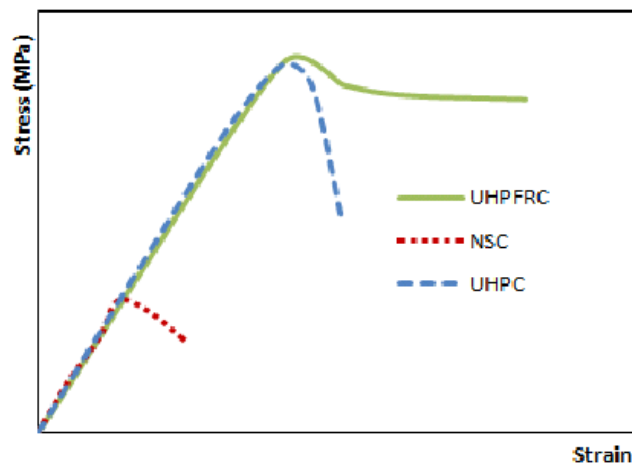


Figure 13. Stress-strain relationship of different UHPFRC's in compression. Source: Researchgate.net.

It's interesting to note that the specimen can reach a good percentage of its total maximum strength in a relatively few days. Then, the graphic also shows the stress-strain diagram typical for UHPFRC materials compared to normal strength concrete (NSC) and ultra-high-performance concrete (UHPC) diagrams. It's clear that UHPFRC & UHPC exhibit better strength than NSC and that UHPFRC is more ductile than UHPC because of the fiber's presence.

Stiffness and Elastic Modulus:

Typical values of UHPFRC modulus of elasticity, for both tension and compression, are between 45 and 50 GPa, which is a relatively low value in view of the stiffness of new structures built with UHPFRC. Although, for composite R-UHPFRC & RC members, a similar modulus of elasticity of UHPFRC and concrete is advantageous concerning deformation-induced stresses such as temperature and shrinkage effects. In the tensile strain hardening domain, UHPFRC exhibits an apparent reduction of the modulus of elasticity with increasing hardening strain [76].

Abrasion:

UHPFRC presents very high resistance against hydro abrasion and abrasion in comparison with other materials [76].

Sustainability:

The sustainability of UHPFRC application has been investigated. Since the UHPFRC cement content is about twice that of conventional concrete, it produces twice as much CO₂ and consumes two times more energy to be produced. However, the experience of UHPFRC achievements shows that when used appropriately, it can divide the quantities of material used in a structure by two or three, and savings can be expected for the structural execution. Compared to a conventional reference solution, if relevant, the UHPFRC alternative allows only a slight gain in terms of CO₂ and energy but offers a significant gain in terms of durability. The standard methods in life cycle analysis should be upgraded to better account for this advantage [27].

LABORATORY TESTS:

The French standard NF P18-470 P published in July 2016 a document about UHPFRC performance, specification conformity, and production. Thus, this document's appendices detailed standardized methods and test protocol adaptations, which were guided to determine UHPFRC important properties. These guidelines covered both structural and non-structural UHPFRC.

ADVANTAGES & DISADVANTAGES:

There are multiple advantages of using UHPFRC and some fewer disadvantages. Both will be described in the next table:

Table 5. UHPFRC's advantages & disadvantages. Own Source.

ADVANTAGES	DISADVANTAGES
<ul style="list-style-type: none"> • High compression strength. • Lightweight. • High Ductility, energy absorption and flexibility. • Low permeability. • Higher tension strength than NSC. • High chemical resistance. • Multiple researches have been developing. • Future improvements are expected. • Fibers make concrete hold together longer (toughness). • Reinforcing everywhere in the concrete. • Strength after cracking. • Reduces damage in fire. • Could be used with rebar (R-UHPFRC). • Multiple researches focus on become this cheaper and more sustainable. 	<ul style="list-style-type: none"> • Difficult to control fibers orientation, sometimes these are randomly oriented. • 2% of fiber content means 40% of UHPFRC final cost. • Must adjust mixture design. • Must be careful in mixture finishing, cause fibers sometimes stick up out of the surface. • Compared with conventional concrete, produces twice as much CO₂, and consumes two times more energy to be produced.

APPLICATION:

Retrofitting Structures:

The concept of the application of UHPFRC for the rehabilitation of structural members is schematically illustrated in Figure 14. Where a UHPFRC layer is applied on the bridge superstructure in zones of hard mechanical and environmental loads (exposure classes XD2, XD3). Hence, critical steps of the construction process like the application of waterproofing membranes or compaction by vibration can be prevented, and the associated sources of errors avoided. Thus, the waterproofing properties of the UHPFRC avoid the utilization of a waterproofing membrane. In that sense, the bituminous concrete can be applied after only 8 days of moist curing of the UHPFRC [77].

In the same way, this constitutes a very significant time saving with respect to the drying period of around 3 weeks necessary prior to the application of a waterproofing membrane on a usual mortar or concrete. Further, the thickness of the bituminous concrete layer can be limited to the absolute minimum necessary for the traffic loads. It is unnecessary to increase it to apply weight on the waterproofing membrane to prevent the formation of air pockets. When it is required, the combination of the protective properties and deformation capability of UHPFRC with the mechanical performance of reinforcement bars (normal or high grade) provides a simple and efficient manner of increasing the bearing capacity and stiffness with compact cross-sections. This new construction technique is especially well-suited for bridges but can also be implemented for galleries, tunnels, retaining walls, following the same approach [77].

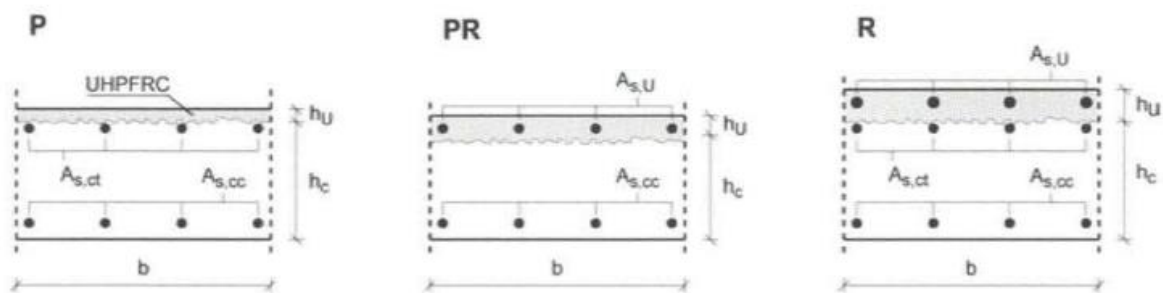


Figure 14. Geometries of "UHPFRC-concrete" elements for bridge deck slabs. Source: core.ac.uk.

Protective overlay, shells, and panels:

First developed within the framework of the European project SAMARIS, UHPFRC has been used in a thin overlay to repair reinforced or prestressed concrete bridge decks. It thus increases the rigidity of the structure, its mechanical strength, and its durability while dispensing with any waterproofing membrane and its further maintenance. Application is currently growing on Swiss infrastructures. Extension of this concept has been applied on steel bridge decks and on concrete slabs of buildings. For these applications, restrained shrinkage shall be controlled by sufficiently high fiber content, and control of early age desiccation is critical. Repair and protection of structures subject to torrential flows and abrasion have found very efficient solutions using UHPFRC. First reference cases concern Valabres pier protection, a canal bridge over the access road to the Fréjus tunnel, or repair of the River Tunnel.

Hosokawa in Japan. UHPFRC is used in thin and smooth elements which is favorable for the hydraulic constraints, while abrasion resistance proves excellent.

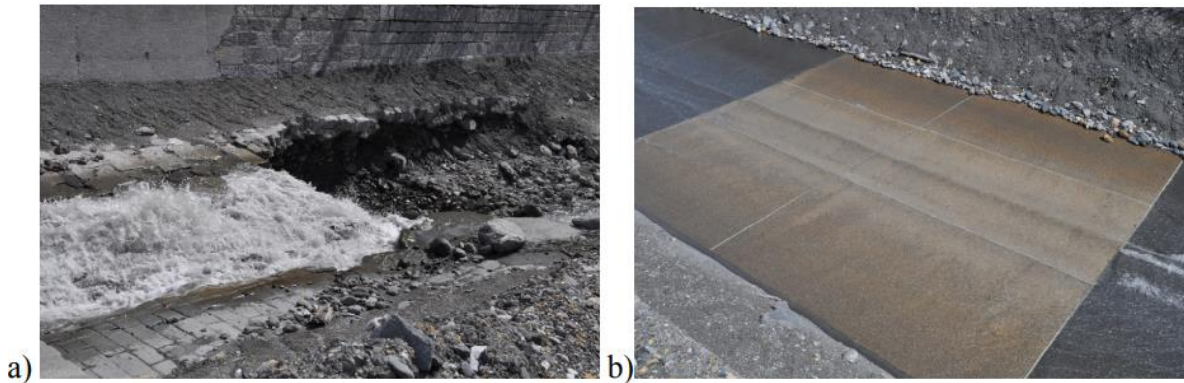


Figure 15. Before a) and after repair and protection b) of a canal bridge by a UHPFRC slab. Source: Researchgate.net.

Columns and highly compressed members:

Direct worthwhile application of UHPFRC capacity in compression has been found with strengthening or retrofitting works, which shall limit additional volumes of materials, e.g., to accommodate the larger interior volume, while additional bearing capacity is required. This may have led to pure UHPFRC (fire-resisting) columns for the retrofitting of Albi Museum or rue Volney building, UHPFRC jacketing of columns in the parking of the building in Perpignan, or steel tube columns filled with UHPFRC (rue Volney, Reina Sofia Museum). Similarly, the favorable ratio of design compressive stress to weight has been used first historically in the prestressed UHPFRC girders of the Cattenom power plant cooling tower, which constituted an additional thermal exchange bearing structure and should thus be light enough. It was also applied with retrofitting of the bridge over Huisne River in Le Mans, the beams of which had to be thickened and strengthened with additional prestressing. In such applications, high Young's modulus, low creep, and no necessity of passive rebars are decisive advantages.

FRP AND UHPFRC COMPARISON

To compare these two materials will be studied different researches of some case of study where these materials will be tested in different ways and conditions to evaluate its performance, and then it will be possible to make a comparison table:

FRP:

1. Strengthening of Reinforced Concrete columns using FRP-ESRAA Esmail Elsayed Esmail.

Objective: This research is focused on evaluating different FRP's strips used for strengthening columns

Test Conditions: Two different kinds of columns, which are differenced in its shape (one is a sharp-edged column and another one is a rounded-edged column), will be wrapped with three different FRP: CFRP, GFRP, and Basalt Fiber Reinforced Polymer (BFRP), and each one of this will have different width and space between them, next table is a summary of the FRP's strips that will be used on the test:

Table 6. FRP's strips summary. Source: Own.

Fiber Type	Width (mm)	Spacing (mm)
CFRP	83.33	125
	50	62.5
GFRP	83.33	125
	50	62.5
BFRP	83.33	125
	50	62.5

Then, the size of the column is 100mmx200mmx500mm. Hence, the idea is to load these columns wrapped with the different FRP strips, compare the axial strength and deformation, and compare the results with a conventional concrete column (conventional concrete column).

Results: Next tables show the results of the test:

Table 7. Column's description, displacement of sharp and failure load of rounded & edged columns. By: Esraa.

Description of Column	Failure load and Displacement of Sharp edged columns			Failure load and displacement of Rounded edged columns		
	Load (KN)	Displacement (mm)	Designation	Load (KN)	Displacement (mm)	Designation
Control column	419.1	6.8	CC	419.1	6.8	CC
Glass 83.33mm strip	506.1	7.7	SGR3.33	599.85	7.1	RGR3.33
Glass 50mm strip	625.25	8.1	SG50	684.53	9.7	RG50
Basalt 83.33mm strip	447.2	6.8	SB83.33	523.75	8.3	RB83.33
Basalt 50mm strip	475.2	7.7	SB50	588.2	7.9	RB50
Carbon 83.33mm strip	542.7	8	SC83.33	649.0	7.5	RC83.33
Carbon 50mm strip	691.7	7.4	SC50	701.0	7.5	RC50

Table 8. Increase in loading capacity. By: Esraa.

Column designation	%increase in load carrying capacity of Sharp edged columns (%)	%increase in load carrying capacity of Rounded edged columns (%)
Control column	0	0
Glass 83.33mm STRIP	20.7	43.1
Glass 50mm STRIP	49.1	63.33
Basalt 83.33mm strip	6.7	24.9
Basalt 50mm strip	13.3	40.3
Carbon 83.33mm strip	29.49	54.85
Carbon 50mm strip	65	67.26

Conclusions:

- In all cases, the FRP reinforce improves the strength in the column, even more in rounded edged because, as shown in Figure 16, effective confinement area in circular areas, so the rounded edged helps to improve this effective confinement area wrap with FRP strips.

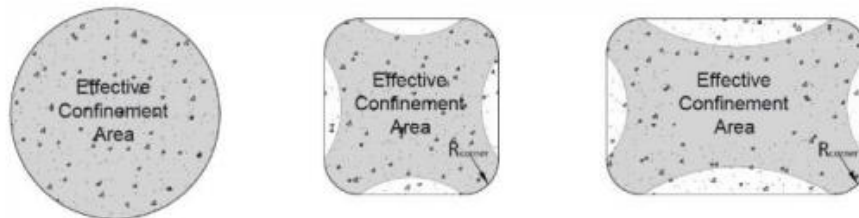


Figure 16. Effective confinement areas in circular, square, and rectangular columns. By: Esraa.

- All FRP's strips with 50mm width and 62,5mm spacing have better results than 83,33mm width and 125mm spacing, it means that thicker strips don't are related with better performance.
 - Carbon fibers have better performance than the other ones, because had the maximum percentage in load-carrying capacity in the test.
2. Study on flexural behavior of RC beam Strengthened with FRP- Dinesh Kumar J1, Sattainathan Sharma A2, Suganya Devi K3

Objective: Study flexural behavior of beams reinforced with FRP by different methods.

Test Conditions: Six specimens of armored cement beams will be tested by applying a two-point load which was started with several cycles of small loading and was applied until the failure happened afterward. Therefore, beam dimensions are 1000mm length, 150mm width, and 200mm depth. One of these specimens will be the control specimen, and the other five will be reinforced with GFRP. Table 9 shows reinforcement details:

Table 9. Specimen details. By: Kumar.

SPECIMEN ID	STRENGTHENING METHODS	THICKNESS
BCN	Control specimen	-
BB01	Bottom wrap	1mm thickness
BB02	Bottom wrap	2mm thickness
BL01	Loading surface	1mm thickness
BL02	Loading surface	1mm thickness
BF01	Full wrap	1mm thickness

Results: Next figure shows the load-deflection curves of each specimen:

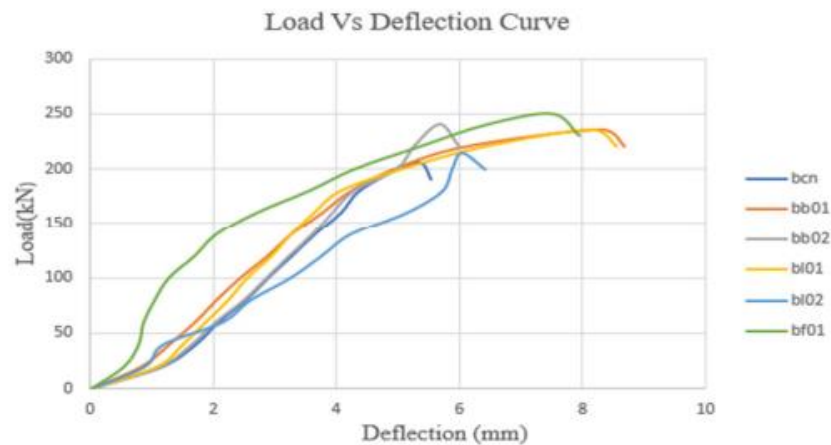


Figure 17. Load vs deflection curve. By: Kumar.

It's easy to observe that the best performance is for a full wrap beam because it could carry more load before failing, also is the possible view that this specimen and the specimens BB01 and BL01 show better ductility than the control beam and the other ones.

Table 10, shows the initial crack load and ultimate failure load for each specimen:

Table 10. Initial crack load & ultimate failure load. By: Kumar.

SPECIMEN ID	INITIAL CRACK LOAD (kN)	ULTIMATE FAILURE LOAD (kN)
BCN	90	205
BB01	70	230
BB02	80	240
BL01	105	225
BL02	60	215
BF01	110	250

Finally, the service load calculated for each specimen is given in table 11:

Table 11. Service load. By: Kumar.

SPECIMEN ID	SERVICE LOAD (kN)
BCN	136.67
BB01	153.33
BB02	160
BL01	166.67
BL02	156.67
BF01	167.33

Conclusions:

- The full wrap beam showed better load carrying capacity, ductility, and energy absorption results than the other specimens. Moreover, comparing the control specimen with the full wrap beam, full wrap reached 28% higher load-carrying capacity.
- All GFRP reinforced beams showed better performance than the control beam, demonstrating that FRP support is successful in beams.
- Bottom wrap beams showed better performance than the loading surface strengthening method. However, the bottom wrap 2mm thickness specimen didn't show much more improvement with respect to 1mm thickness, the main difference between this two was the deflection, 5,67mm & 8,23 mm respectively. Hence, that meant higher ductility for 1mm thickness specimen.

3. Monitoring of Bond in FRP Retrofitted Concrete Structures

Objective: Study of bond and interfacial transfer of stresses between FRP and concrete, and by the same way measured interface slip between FRP and concrete.

Note: Slip corresponds to the relative displacement between the FRP reinforcement and the concrete.

Test Conditions: Seven beam specimens were tested under displacement control. All the beam's length was 2,9m and was loaded symmetrically about its centerline at two points separated at 0,914m. Table 12 shows the specimen's reinforcement details:

Table 12. Beam specimen reinforcement details. By: Zhao.

Beam no. (1)	Number of \varnothing 16 mm steel rebars (2)	CFRP system		Distance from CFRP end to support (mm) (5)
		Thickness (mm) (3)	Length (m) (4)	
B0	2	NA	NA	NA
B1	2	2	2.134	381
B2	2	2	2.286	305
B3	2	2	2.744	76
B4	2	2	2.744	76
B5	2	4	2.134	381
B6	3	4	2.134	381

It is important to mention that, except B3, all the beams were pre-loaded until several cracks formed in the constant moment region and then repaired with CFRP. It was made with the purpose of simulating service load conditions.

Results: Table 13, shows test results for each specimen:

Table 13. Test results. By: Zhao.

Beam no. (1)	Load when FRP applied (kN) (2)	Ultimate load (kN) (3)	Midspan deflection (mm) (4)	Mode of failure (7)
B0	NA	104.44	70.17	Flexural
B1	28.18	157.28	31.86	Peeling
B2	23.29	164.76	24.31	Peeling
B3	0.00	183.79	34.17	Debonding
B4	25.83	198.46	34.70	Peeling
B5	24.07	183.26	20.40	Peeling
B6	26.23	181.42	20.97	Peeling

By the same way, Figure 18 shows Load-deflection curve for each beam:

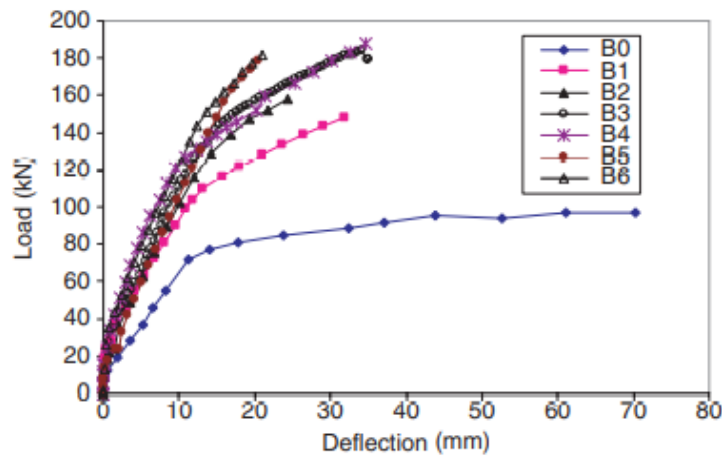


Figure 18. Load vs deflection behavior of bonded FRP reinforcing RC beams. By: Zhao.

Next, to figures show two types of failure for FRP retrofitted beams Peeling failure, in which the CFRP sheet looks like it was ripped off from concrete (Figure 19), and debonding failure where the CFRP sheets disjoin from concrete (Figure 20).

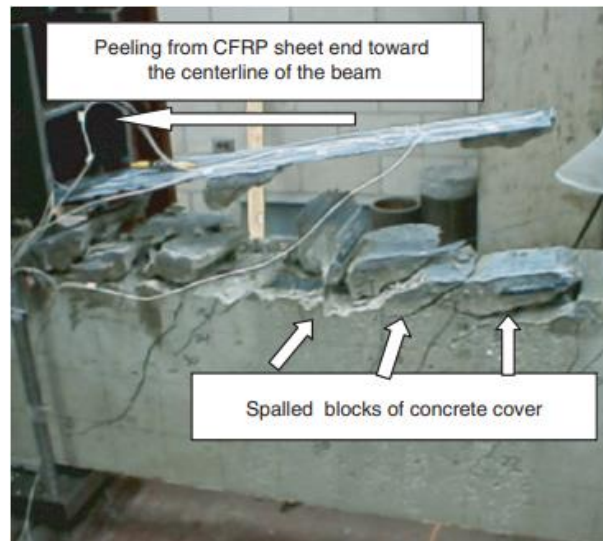


Figure 19. Peeling failure of concrete cover for specimen B2. By: Zhao.

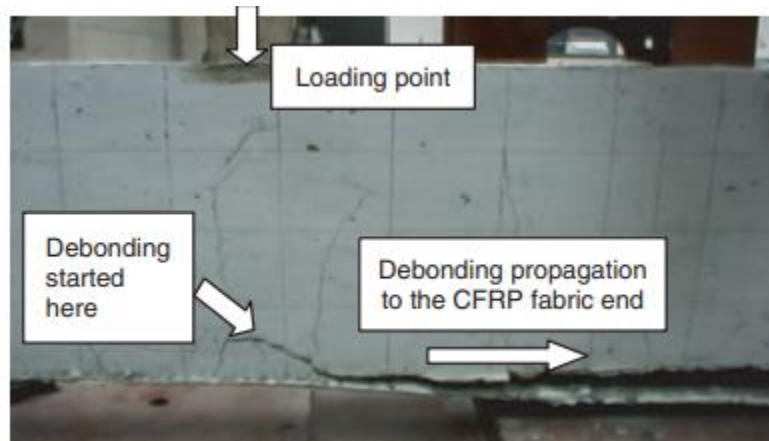


Figure 20. Debonding failure between FRP fabric and concrete, specimen B3. By: Zhao.

The next graph shows how slip between concrete and CFRP reinforce increase with loading increase until it reaches a maximum and later turns down to the specimen reach the failure.

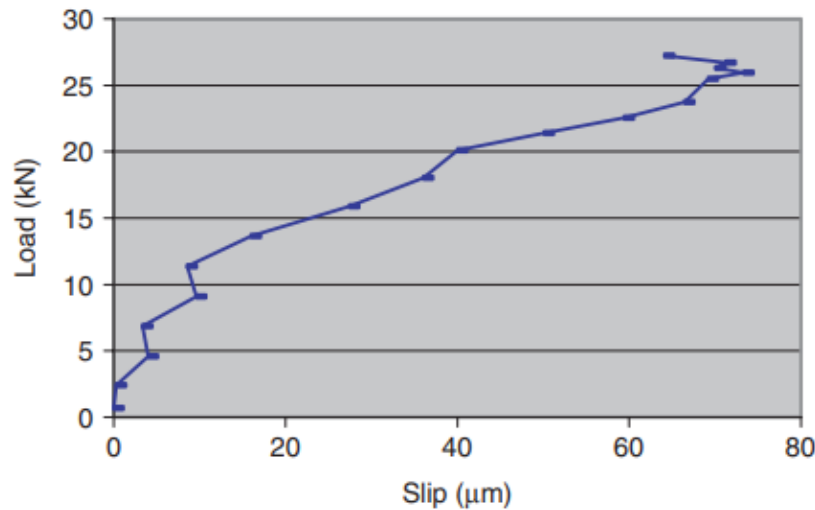


Figure 21. Load-slip relationship at the composite interface. By: Zhao.

Finally, Figure 22 principal stresses variation in the concrete cover along with the steel reinforcement and in the concrete/epoxy interface.

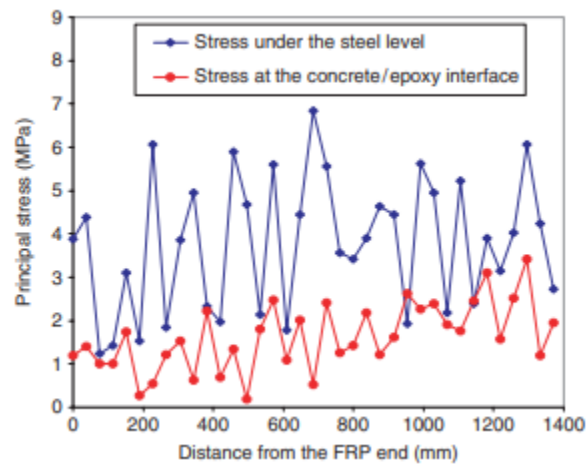


Figure 22. Principal stress distribution under the rebar and at the concrete-epoxy interface. By: Zhao.

Conclusions:

- The retrofitted beams reach a strength increase from 46-70% compared with the control beam. Therefore, comparing the control beam with retrofitted beams, retrofitted beams showed larger stiffness but reduced ductility.
- As exhibited in the results, the control beam failed by crushing the concrete long after the yielding of steel. However, all other beams (except B3 beam) failed by peeling the concrete cover. B3 beam failed by debonding the FRP from concrete and the adhesive layer.

- In general, the measured surface slip between concrete substrate and FRP at the ultimate load stage was $< 60 \mu\text{m}$.
- It was observed some important facts about reinforce performance. First, the longest CFRP reinforcement showed better performance than the other ones, including sheets with more thickness. In case of beam B3, which wasn't preloaded, is interesting that the performance difference with beam B4 (which reinforcement had the same thickness and length) wasn't big and moreover, B4 beam showed a better performance.
- Principal stresses variation in the concrete/epoxy interface is much less than concrete cover along the steel reinforcement, which demonstrated how FRP reinforcement strengthened the element.

4. FRP retrofit of walls constructed with historical bricks

Objective: Determine the effect of FRP used to retrofit walls made of old bricks taken from a historical building and compare it performance with specimens plastered with repair mortar.

Test Conditions: The dimensions of specimens were approximately $500 \times 500 \times 230 \text{ mm}^3$. For specimen construction, a special mortar mixture was used to represent the mechanical characteristics of the mortar used in this historic building. The thicknesses of horizontal and vertical joint mortar were 20 and 10 mm, respectively. Then, Figure 23, shows how specimen retrofitting will be carried out for testing:



Figure 23. Reference (type A) plastered (type B) & retrofitted (type C) specimens. By: Ilki.

By the same way, Table 14 shows general characteristics of specimens:

Table 14. Specimens' characteristics. By: Ilki.

Specimen	Plaster	FRP	FRP plies on both surfaces	FRP anchors
A	No	No	0	No
B	Yes	No	0	No
C-1	Yes	Yes	1	No
C-2	Yes	Yes	2	No
D	Yes	Yes	2	Yes

Results: The test results in terms of strength and deformation characteristics are summarized in Table 15. In this table, P_{cr} and P_{max} are the loads at the formation of vertical crack and maximum load, respectively, and ϵ_{cr} and ϵ_{max} are the average vertical axial strains corresponding to these loads.

Table 15. Strength & deformation characteristics of specimens. By: Ilki.

Specimen	P_{cr} (kN)	ϵ_{cr}	P_{max} (kN)	ϵ_{max}	Enhancement in strength (%)	Enhancement in vertical deformation corresponding to strength (%)
A	23.0	0.0002	24.5	0.0008	-	-
B	32.0	0.0011	32.0	0.0011	31	38
C-1	82.0	0.0029	82.0	0.0029	234	263
C-2	67.0	0.0039	67.0	0.0039	173	388
D	58.0	0.0018	63.0	0.0033	157	313

Figure 24, shows load vs average vertical deformation relationship curves for each specimen studied:

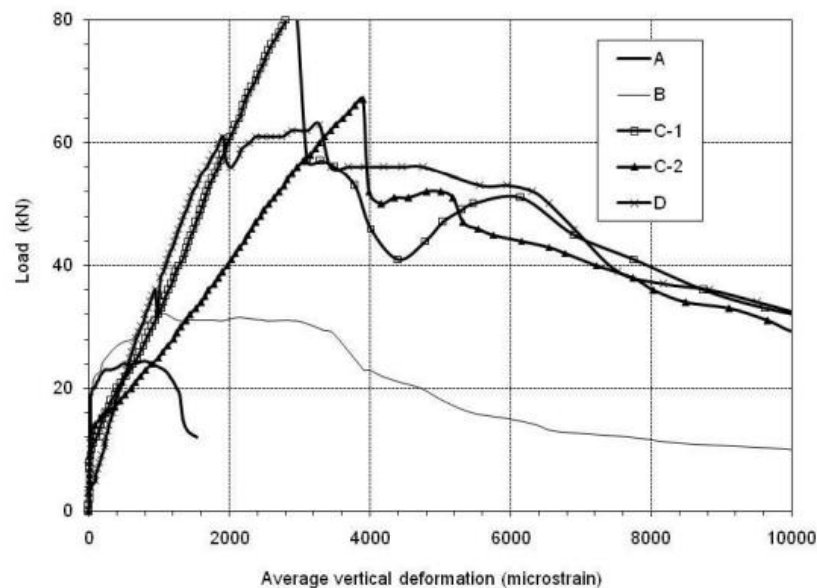


Figure 24. Load vs average vertical deformation relationships for all specimens. By: Ilki.

Conclusions:

- FRP retrofitting improved strength and vertical deformation from 157 to 234% & from 263 to 388%, respectively. It is interesting to highlight that specimen C-1 had the best performance, even better than specimen C-2, which was composed of two plies of FRP.
- The failure mode of FRP reinforcement was characterized by a separation of FRP sheets together with a thin layer of bricks from the core of the wall and the plaster. Hence, FRP sheets weren't efficiently utilized.
- It is important to mention that, though FRP significantly enhanced the tensile strength and the vertical deformation, the FRP retrofitted walls' capacity was governed by the tensile strength of bricks themselves rather than the quality of FRP sheets bonding adhesive or plaster.
- The anchors made from glass FRP rolls inserted into the brick wall to retard the separation of outer shell were successful in preventing sudden loss of strength,

as well as providing significantly better ductility in the case of FRP retrofitted specimens. However, its tensile strength performance wasn't as good as specimens C-1 and C-2.

5. Experimental study on flexural behavior of FRP retrofitted masonry walls

Objectives: Evaluate the behavior of NSM CFRP used to retrofit masonry walls in flexure.

Test Conditions: Table 16 shows the details of the walls tested in this research. In Table 1, W, H, and t refer to the wall's width, height, and thickness, respectively; b and d refer to the thickness and width of FRP strip, respectively. Further, S/C (Column 1) stands for static or cyclic loading; O/D (Column 7) refers to strips on one or double sides; ρ (Column 10) is reinforcement ratio, and strip spacing (Column 8) refers to the horizontal spacing between vertically oriented strips. Tests on walls 1-4 were conducted as pilot tests to refine the test techniques. After that, walls 5, 6 and 8 were used to investigate the influence of strip spacing on the flexural behavior of retrofitted walls. The effects of axial loading on the flexural response under static loading were considered by tests on walls 6, 10 and 14 while cyclic loading was investigated with walls 11, 12, and 15.

Table 16. Specimens and reinforce details. By: Kashyap.

Wall S/C (1)	Wall Dimensions			Strip Size		# of Strips O/D (7)	Strip spacing (mm) (8)	Pre-compression (MPa) (9)	$\rho =$ A_{FRP}/A_{Wall} (%) (10)
	W (mm) (2)	H (mm) (3)	t (mm) (4)	b (mm) (5)	d (mm) (6)				
1S	355	1710	110	3.6	10	1D	355	0	9.2
2S	355	1710	110	3.6	10	1D	355	0	9.2
3C	355	1710	110	3.6	10	1D	355	0	9.2
4S	230	1710	110	3.6	10	1D	230	0	14.2
5S	1070	2310	110	7.2	10	1O	1070	0	6.1
6S	1070	2310	110	4.8	7.5	2O	535	0	6.1
7S	1070	2310	110	3.6	10	3O	357	0	9.2
8S	1070	2310	110	4.8	5	3O	357	0	6.1
9S	1070	2310	110	3.6	10	1O	1070	0	3.1
10S	1070	2310	110	4.2	10	2O	535	0.1	7.1
11C	1070	2310	110	4.2	10	2D	535	0	7.1
12C	1070	2310	110	4.2	10	2D	535	0.1	7.1
13C	1070	2310	110	4.2	10	2O	535	0	7.1
14S	1070	2310	110	4.2	10	2O	535	0.2	7.1
15C	1070	2310	110	4.2	10	2D	535	0.2	7.1

In that sense, Figure 25 shows schemes of cross section & elevation test measurements for walls 5-10, 13, 14 (a) and cross section for walls 11, 12 & 15:

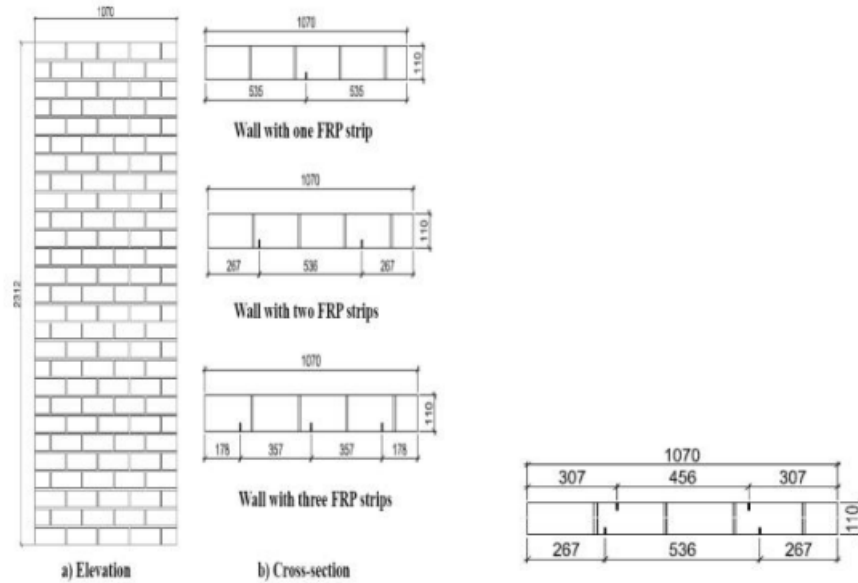


Figure 25. Geometric specimens' details - Walls 5-15. By: Kashyap.

Results: Table 17 is a summary of the results for each wall specimen tested:

Table 17. Test results. By: Kashyap.

Wall S/C (1)	Strip size (mm) (2)	ϵ_{max} ($\mu\epsilon$) (3)	F_{max} (kN) (4)	Δ at F_{max} (mm) (5)	Δ_{ult} (mm) (6)	P_{exp} (kN) (7)	$\epsilon_{max}/\epsilon_{rupt}$ (%) (8)	a_{exp}/a_{URM} (9)
1S	3.6x10	0.00983	18.6	43.7	44.3	58.4	70.3	14.3
2S	3.6x11	0.00998	18.4	34.9	36.6	59.3	71.3	14.2
3C	3.6x12	0.00829	15.6	30.7	30.3	49.3	59.3	12.0
4S	3.6x13	0.00818	15.6	26.5	27.6	48.6	58.5	18.6
5S	3.6x14	0.00699	17.1	44.0	58.0	83.1	50.0	7.5
6S	4.8x7.5	0.01098	27.0	61.0	70.0	65.3	78.5	11.9
7S	3.6x10	0.01188	41.0	70.3	75.7	70.6	84.9	18.1
8S	4.8x5	0.01245	36.6	75.0	78.9	49.3	89.0	18.2
9S	3.6x10	0.00947	12.4	51.8	61.2	56.3	67.7	6.2
10S	4.2x10	0.01109	30.8	66.2	69.3	76.9	79.2	12.7
11C	4.2x10	0.00995	+27.3/-27.6	+48.7/-48.8	+53.7/-64.5	69.0	71.1	13.6
12C	4.2x10	0.00953	+28.9/-29.1	+48.4/-48.2	+56.8/-53.0	66.0	68.1	11.9
13C	4.2x10	0.01117	+30.2/-1.4	+54.3/-9.2	+69.4/-57.0	77.4	79.8	15.0
14S	4.2x10	0.01055	29.7	48.1	52.0	73.1	75.4	10.4
15C	4.2x10	0.00821	+27.8/-26.6	+36.3/-40.0	+60.0/-55.0	56.9	58.7	9.5

In that sense, Figure 26 is useful to analyze FRP strips spacing effect on load capacity performance of walls retrofitted with FRP:

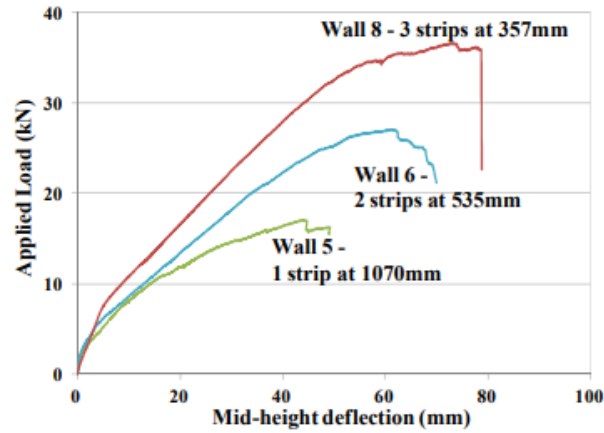


Figure 26. Load vs deflection, showing effect of FRP strip spacing. By: Kashyap.

Figure 27, shows the pre-compression effect on walls retrofit in two study cases (monotonically loaded and cyclic loading)

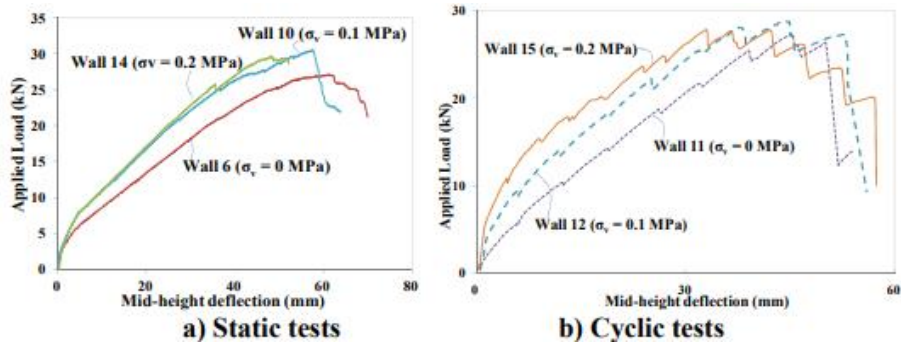


Figure 27. Influence of Pre-compression. By: Kashyap.

Finally, the effect of reinforcement ratio was studied on this research, and the results are shown in Figure 28:

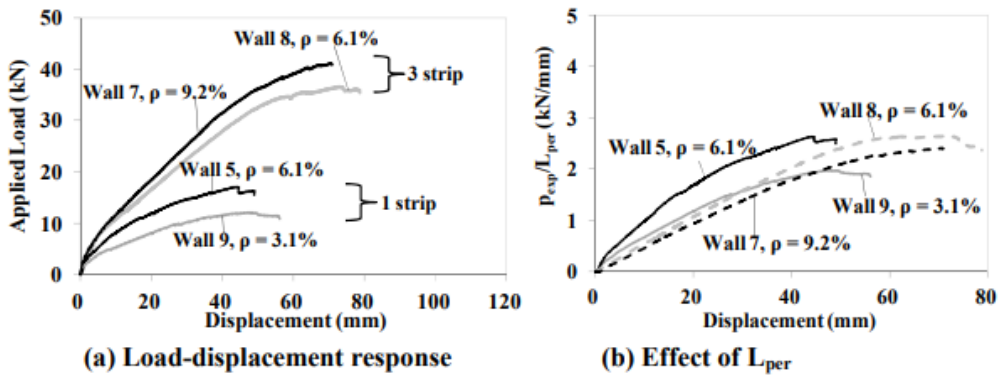


Figure 28. Influence of reinforcement ratio. By: Kashyap.

Conclusions:

- NSM FRP system retrofitting is an effective technique. As exhibited in this research, walls strength and especially vertical bending capacity could increase up to twenty times compared with unreinforced walls.
- Strength and displacement capacity increased significantly, 114% and 60%, respectively, when the same FRP reinforcement was distributed more evenly. Hence, the same total amount of FRP reinforcement was used covering three different effective strip spacings, and the results of the strips distributed more evenly, as shown in Figure 26, were the best.
- An increase in the reinforcement ratio results in an increase in strength but the reduction in displacement capacity and hence could have a negative effect on the overall flexural behavior of masonry walls. Thus, for efficient use of FRP, it is recommended that optimal FRP strip spacing be used rather than increasing the reinforcement ratio as it provides better results for the overall behavior of the wall.

6. Steel Beams Strengthened in Flexure:

Objectives: Evaluate FRP reinforcement effectiveness for retrofit deteriorated steel beams (principally affected for corrosion), and study performance and functionality of a recently developed new anchorage system in debonding prevention.

Test Conditions: thirteen steel beams (W150x30) were tested in four-point bending. Therefore, some damages of 33-50% area reduction were made in the specimen to simulate deterioration principally caused by corrosion. Hence, Table 18 shows specimen characteristics for testing:

Table 18. Test Characteristics. By: Galal.

Group	Beams	ID	Area losses mm ²	Retrofit material CFRP	Epoxy material	Retrofit method
G1	B1	BFO	None	—	—	—
	B2	BF-H0.33	8 – 6.35 mm dia. holes	—	—	—
	B3	BF-N0.33	2 – (25.4 × 450) mm ² Notch	—	—	—
	B4	BF-N0.50	2 – (38.1 × 450) mm ² Notch	—	—	—
G2	B5	BF-H0.33-F1(5)-B1	8 – 6.35 mm dia. holes	SCH-11UP (5 layers)	Tyfo S	Fully bonded
	B6	BF-N0.50-F1(5)-B1	2 – (38.1 × 450) mm ² Notch	SCH-11UP (5 layers)	Tyfo S	Fully bonded
	B7	BF-H0.33-F1(5)-B2	8 – 6.35 mm dia. holes	SCH-11UP (5 layers)	MB-3	Fully bonded
	B8	BF-N0.50-F1(5)-B2	2 – (38.1 × 450) mm ² Notch	SCH-11UP (5 layers)	MB-3	Fully bonded
G3	B9	BF-H0.33-F2(1)-B2	8 – 6.35 mm dia. holes	UC strip (1strip 1.4 mm)	MB-3	Fully bonded
	B10	BF-H0.33-F2(1)-B2w	8 – 6.35 mm dia. holes	UC strip (1strip 1.4 mm)	MB-3	Fully bonded
G4	B11	BF-H0.33-F1(1)-A1D1	8 – 6.35 mm dia. holes	SCH-11UP (1 layers)	—	Ductile anchorage
	B12	BF-H0.33-F1(1)-A2D1	8 – 6.35 mm dia. holes	SCH-11UP (1 layers)	—	Ductile anchorage
	B13	BF-H0.33-F1(5)-A1D2	8 – 6.35 mm dia. holes	SCH-11UP (5 layers)	—	Ductile anchorage

There are four groups, G1 corresponds to control beams, G2 are all the beams retrofitted using FRP sheets bonded in a wet-layup system, G3 beams were bonded too but, in this case, the FRP reinforce were plated. Finally, G4 is that beams used to evaluate using the innovative system with anchorage, which pretends to delay debonding of FRP. To have a better idea of the anchored system, it is shown in Figure 29:

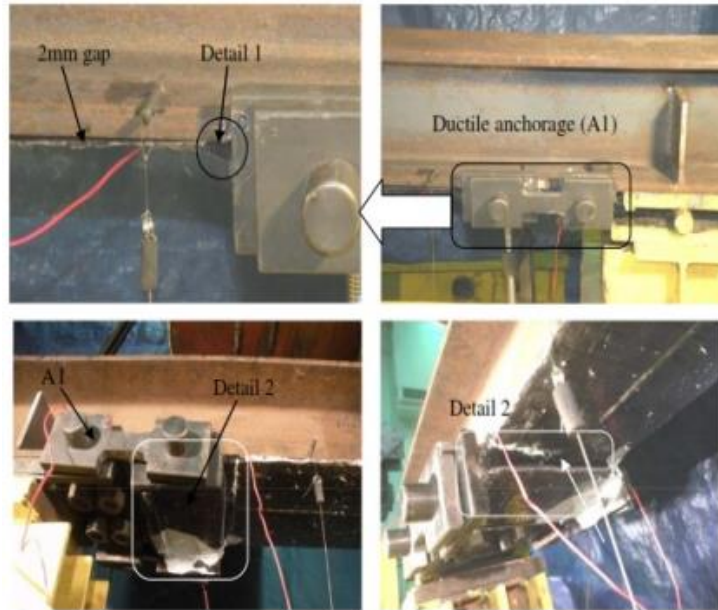


Figure 29. Anchorage system for retrofit steel beams with FRP. By: Galal.

Results: Table 19 is a summary of the results gotten from this test:

Table 19. Test Results. By: Galal.

Group	Beam ID	At yield		At failure		Mode of failure
		Load P_y (kN)	Defl. Δ_y (mm)	Load P_u (kN)	Defl. Δ_u (mm)	
G1	BFO	245	7.7	331	73.6	Steel-buckling
	BF-H0.33	242	8.0	330	69.8	Steel-buckling
	BF-N0.33	190	6.4	311	74.3	Steel-buckling
	BF-N0.50	155	5.8	290	95.4	Steel-buckling
G2	BF-H0.33-F1(5)-B1	245	7.9	307	18.1	CFRP peeling
	BF-N0.50-F1(5)-B1	181	5.7	262	12.1	CFRP peeling
	BF-H0.33-F1(5)-B2	253	8.2	375	51.0	CFRP rupture
	BF-N0.50-F1(5)-B2	195	6.5	307	24.0	CFRP rupture
G3	BF-H0.33-F2(1)-B2	250	8.4	344	46.1	CFRP peeling
	BF-H0.33-F2(1)-B2w	260	8.6	347	48.7	CFRP peeling
G4	BF-H0.33-F1(1)-A1D1	240	7.3	323	43.9	CFRP rupture
	BF-H0.33-F1(1)-A2D1	246	7.8	320	44	Yield in ductile link followed by CFRP rupture
	BF-H0.33-F1(5)-A2D2	250	7.7	304	32	CFRP premature rupture

Conclusions:

- In terms of yielding and ultimate load. the improvement given by FRP retrofitted beams is not very remarkable. However, deflection at yield and failure was approximately 30% less.
- The new anchorage system was successful delaying debonding failure in beams retrofitted with FRP and decreasing deflections.

7. FRP Strengthening of Bridges:

T-girders Strengthened in Flexure Using New Mechanically Anchored System:

Objectives: Evaluate FRP reinforcing T-girders usually used in bridges, compare bonding system retrofitting with ductile anchors used instead of bonding.

Test Conditions: Four half-scale specimens of reinforced concrete T-beams supported by two-column slab were tested under increasing monotonic loads until failure. Table 20 is a summary of retrofit systems for each specimen:

Table 20. Specimens' properties. Source: Own.

Specimen	Retrofit Method	FRP layers Number
F-C-O (Control beam)	N/A	0
F-E-B	epoxy-bonded FRP	1
F-M-U	FRP sheet/ductile anchor system	1
F-M-B	FRP sheet/ductile anchor system - FRP bonded to the soffit	1

Results: Table 21 is a summary of test results:

Table 21. Table 21. Test results. Source: Own.

Specimen	Mode of Failure	Load capacity improvement	Deflection improvement	Ductility
F-C-O (Control beam)	Steel yielding	0	-	-
F-E-B	CFRP de-bonding	7%	54%	-
F-M-U	Yield in the anchors	21%	96%	9.09
F-M-B	CFRP Rupture	27%	19%	3.37

Conclusions:

- It's worth expressing that F-M-U had the best performance with the highest ductility and deflection improvement in general terms. Though beam F-M-B had more links to the concrete than F-M-U, which was reflected in higher load capacity, it was too stiff compared with F-M-U beam.
- All the specimens retrofitted with FRP had better performance than the control beam, which exhibited FRP success retrofitting bridge elements.

UHPFRC:

1. Experimental and Numerical Investigation on Shear Retrofitting of RC Beams by Prefabricated UHPFRC Sheets

Objectives: Investigate the applicability of shear and flexural retrofitting by UHPFRC prefabricated sheets in reinforced concrete beams.

Test Conditions: Two groups of beams (the first group was designed to have a shear failure, and the second one was designed to have a flexural failure) of reinforcing beams with 10x20x150 cm dimensions were made and were loaded at three points bending configuration. It's worth mentioning that two from the four specimens are control beams. It also is worth to note that the thickness of the prefabricated UHPFRC sheets was 30 mm for all beams. Table # exhibits specimen properties:

Table 22. Specimens' properties. By: Own.

Specimen	Type	Tensile reinforcement	Compression reinforcement	Shear reinforcement
B	Control beam	2Φ10	2Φ6	Φ6 @ 20cm
S	Control beam	2Φ12	2Φ6	Φ6 @ 20cm
B-re	Retrofitted	2Φ10	2Φ6	Φ6 @ 20cm
S-re	Retrofitted	2Φ12	2Φ6	Φ6 @ 20cm

Figure 30, shows schemes of the beams and the location of prefabricated UHPFRC sheets:

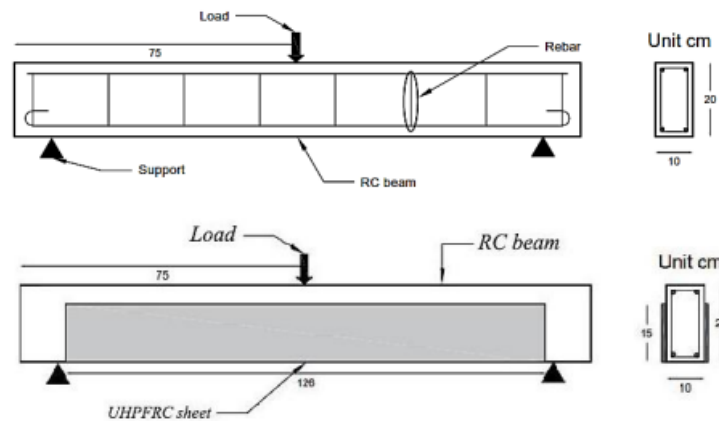


Figure 30. Reinforcement scheme & location of prefabricated UHPFRC sheets. By: Aghani.

Results:

Group 1: Table 23 & Figure 31 show group 1 results:

Table 23. Group 1 specimens results. By: Aghani.

Specimens	P_u (KN)	Failure mode
S1	58.1	Shear
S2	59.7	Shear
S3-re	73	Flexural
S4-re	72.3	Flexural

As show in the table 23, sheets were able to change the failure mode of the beams and even better increase the bearing capacity by 23%, respect to control beams, approximately.

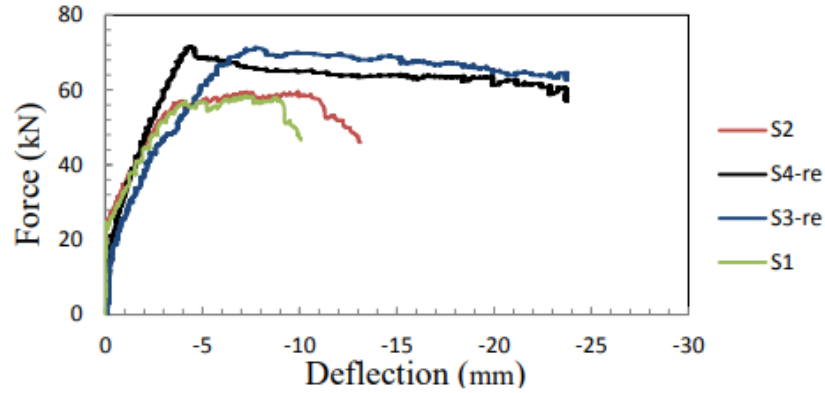


Figure 31. Load vs deflection relationship for group 1 specimens. By: Aghani.

It is easy to observe that reinforced beams showed pretty much higher (approximately 278%) energy absorption capacity and moreover higher ductility.

In that sense, the crack pattern is shown in figure 32:

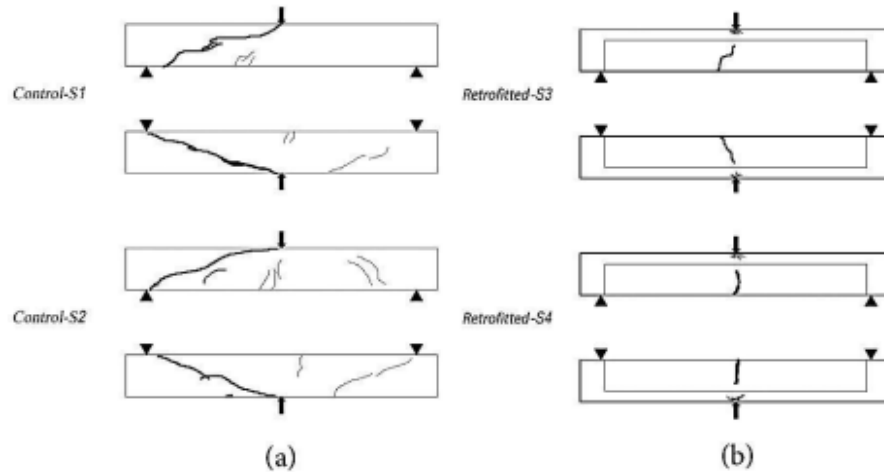


Figure 32. Crack pattern: (a) control series, (b) reinforced series. By: Aghani.

Group 2:

Table 24. Group 2. Specimens' results. By: Aghani.

Specimens	P_u (KN)	Failure mode
B1	36	Shear-flexural
B4	38.2	Shear-flexural
B3-re	47.5	Flexural
B2-re	46.8	Flexural

As shown in Table 24, UHPFRC sheets approximately improved loading capacity in 27%.

Therefore, Figure 33 shows that UHPFRC reinforces enhanced stiffness of the beams. However, in this case ductility was almost the same.

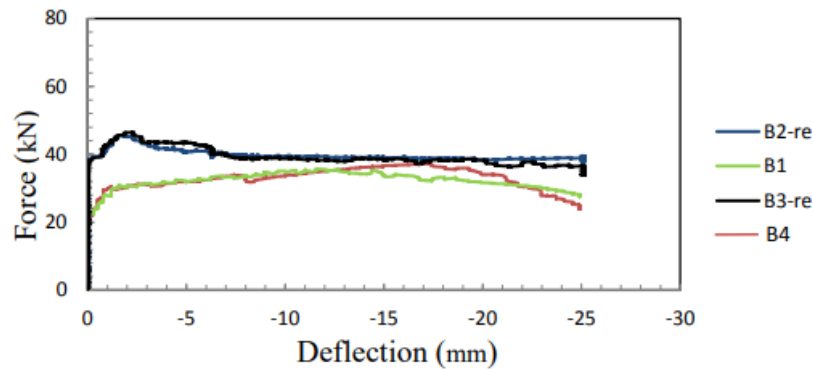


Figure 33. Load vs deflection relationship for group 1 specimens. By: Aghani.

Crack patterns for Group 2 beams are shown in next Figure:

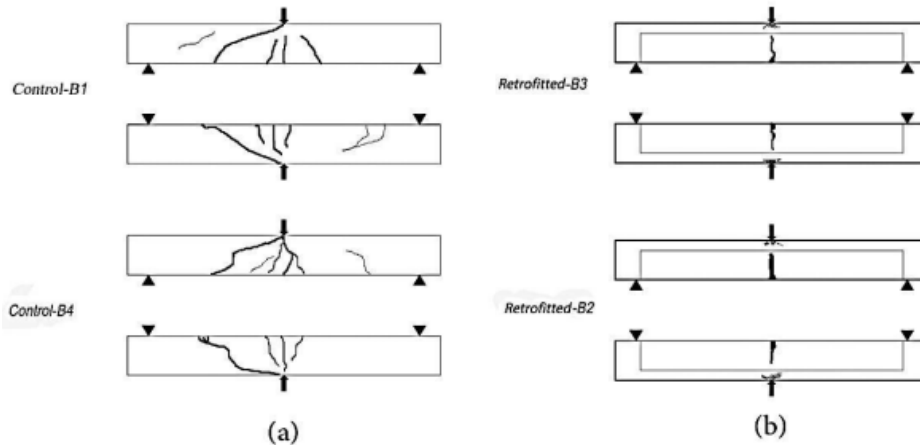


Figure 34. Crack pattern: (a) control series, (b) reinforced series. By: Aghani.

Conclusions:

- Loading capacity of the beams increased by 25% approximately with the use of UHPFRC prefabricated sheets. Therefore, this reinforcement was able to change the failure mode of the beam, showing an incredible performance. It is worth mentioning that in security terms is great to alter the failure mode from sudden failure to a pre-warning failure mechanism.
- UHPFRC showed an incredible improvement in beams ductility, reaching, and enhancement, with respect to control beams, up to 278%. Hence, steel fibers were able to absorb the loading energy.
- In worth mentioning that were no debonding between the beam's surface and UHPFRC prefabricated sheets, which were bonded with an adhesive epoxy.

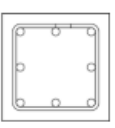
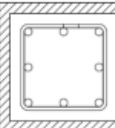
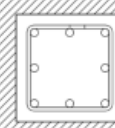
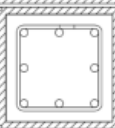
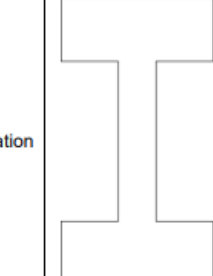
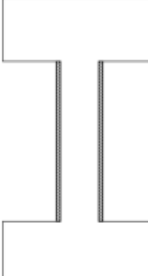
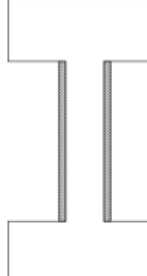
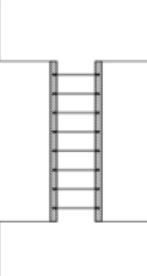
2. Strengthening RC Columns with Ultra-High-Performance Concrete

Objective: Study retrofitting of reinforced concrete columns with UHPFRC jackets.

Test Conditions: Four columns' specimens were constructed in half scale size and with a cross-section of 300x300mm. In the same way, one of the columns was the

control column, and the others were retrofitted with UHPFRC jackets varying thickness and stirrups. Table 25 is a summary of specimens' details:

Table 25. Specimens' details. By: Yeong Koo.

	R0	R3	R5	R5S
Retrofit method	unstrengthened	30mm jacket (10% thickness of column)	50mm jacket (16.7% thickness of column)	50mm jacket + stirrups (D10@150)
Section				
Elevation				

Is worth to mention that before casting UHPFRC, the column surface was roughened by sandblasting to achieve a unified behavior between the UHPFRC jacket and the column.

Results: Load-displacement curve is show in Figure 35:

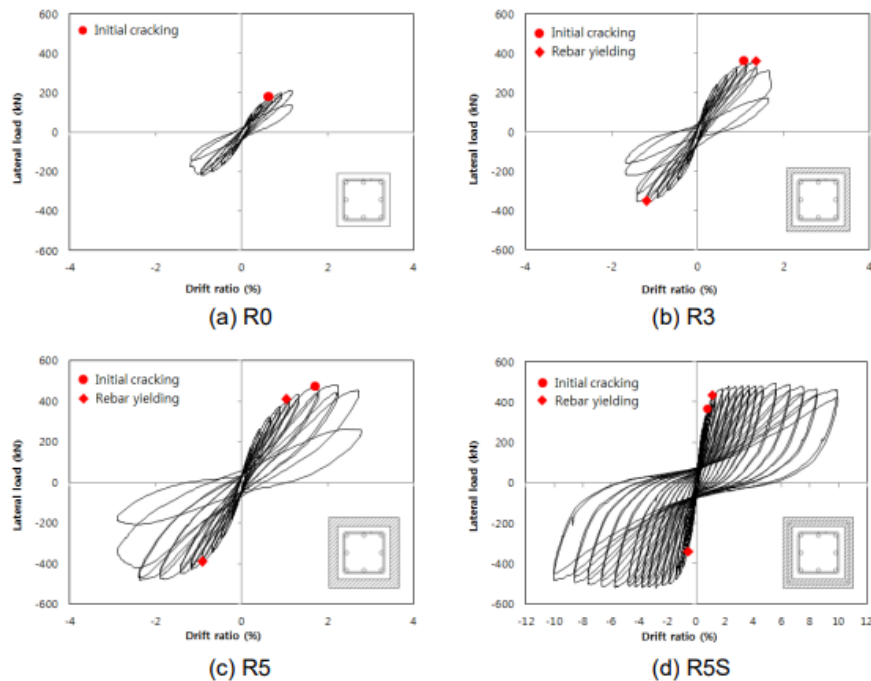


Figure 35. Load vs displacement curves. By: Yeong Koo.

In that sense, the load-displacement envelope of four specimens is shown in Figure 36:

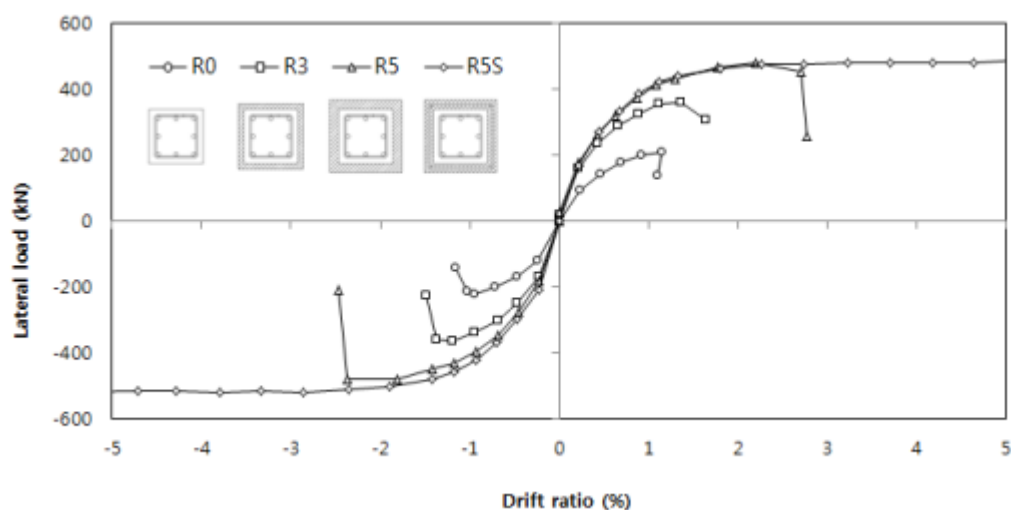


Figure 36. Load-displacement envelop. By: Yeong Koo.

Finally, Table 26, is a summary of the test's results:

Table 26. Test result. By: Yeong Koo.

	R0	R3	R5	R5S
Failure mode	bond	shear	Flexure-shear	-
Jacket thickness	-	10%	16.7%	16.7%
Area increase	-	44%	77%	77%
Max. strength	210.4 kN	359.8 kN	478.9 kN	491.8kN
Max. drift ratio	1.16 %	1.65 %	2.72 %	10%
Strength increase	-	149.4kN	268.9kN	281.4kN
	-	71.0%	127.8%	133.7%

Conclusions:

- Specimens with more thickness (R5, R5S) had the best performance with a bearing capacity of around 130% in both cases, exhibiting the success of this method and showing that, in this case, more thickness means more strength.
- This strengthening method contributes to altering the failure mode from brittle shear to flexural shear failure and consequently improve the ductile behavior of columns.


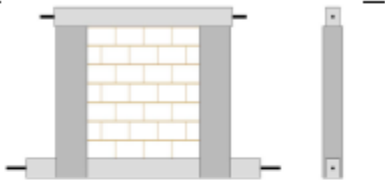
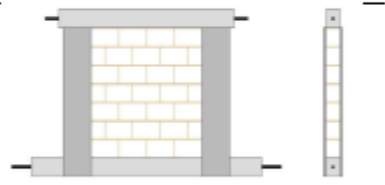

3. Seismic retrofitting of masonry walls with thin UHPFRC layers

Objectives: Evaluate an alternative technique for retrofit masonry walls, which are focused on improving strength and ductility by UHPFRC layers.

Test Conditions: Tests were carried out on four clay brick masonry specimens: one was unreinforced as a reference wall, and three were reinforced with UHPFRC layers. Specimens were subjected to a constant normal force with varying horizontal cyclic forces, based on the assumption that a simple cantilever subjected to such a loading pattern can represent the behavior of a real shear wall under earthquake action. In that sense, Test walls are composed of 7 brick (type ME15) courses, each being 19 cm high

and 15 cm thick. Walls were thus 1.8 m long, 1.4 m high and 15 cm thick, which are representative dimensions (H/L ratio) for traditional load-bearing masonry walls. Next table is a summary of the specimens' specifications:

Table 27. Description of specimens. By: Devaux.

Specimen	Description (UHPFRC arrangement)	Layout (front and side views)
1. WUR	Unreinforced wall	
2. WRU	Wall reinforced with two U-shaped UHPFRC layers with following dimensions: length: 330 mm; thickness: 30 mm.	
3. WRL	Wall reinforced with 2x2 UHPFRC vertical strips with following dimensions: length: 300 mm; thickness: 30 mm.	
4. WRS	Wall with fully reinforced lateral surfaces with a thickness of 30 mm.	

Results: Test results are shown below for every specimen separately. In the left part is the hysteresis loop, and in the right are presented schemes of the cracking pattern:

Specimen WUR:

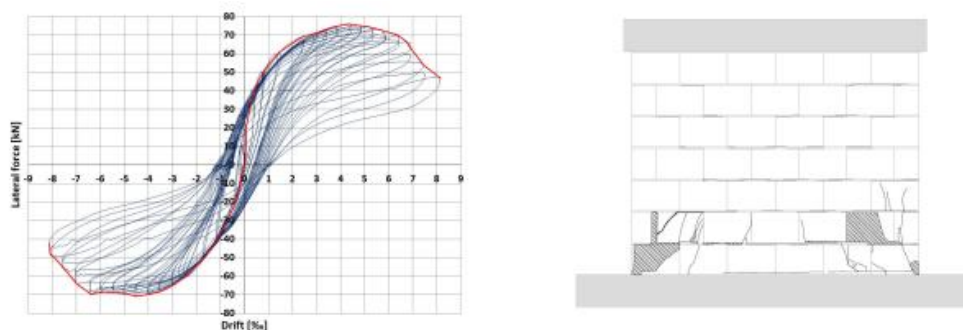


Figure 37. hysteresis loop (left) and cracking pattern at the end of the test (right) for WUR wall. By: Devaux.

Specimen WRU:

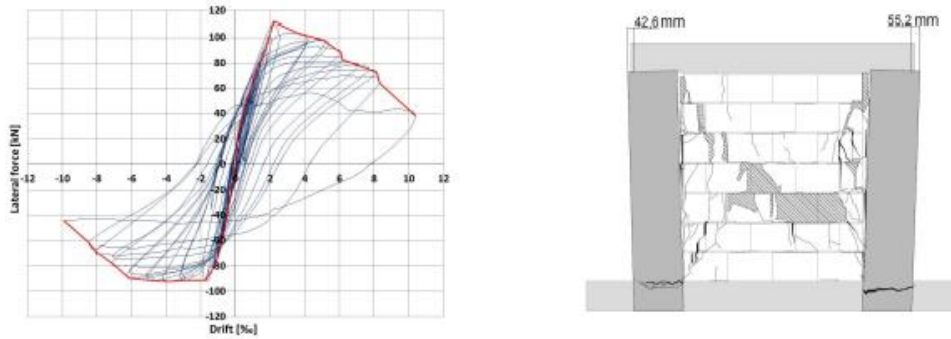


Figure 38. Hysteresis loop recorded during testing the WRU specimen (left); cracking pattern at the end of the WRU specimen testing (right). Legend: hatched areas show falling parts of masonry and cracks are reported with dashes whose thickness represents the cracks opening. By: Devaux.

Specimen WRL:

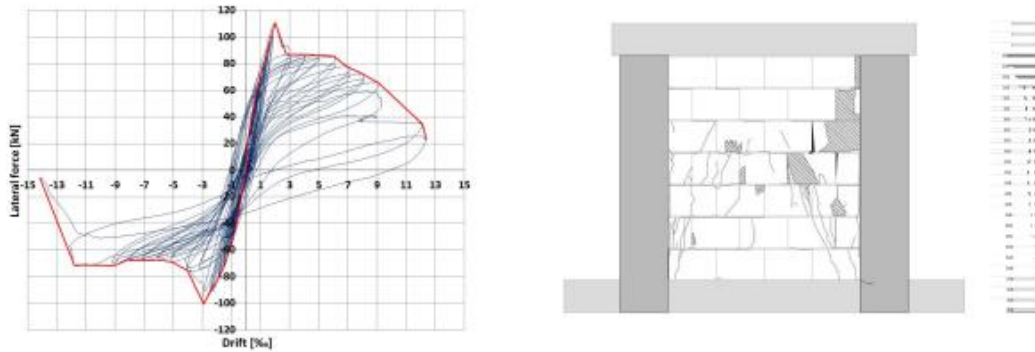


Figure 39. Hysteresis loop recorded during testing the WRL specimen (left); cracking pattern at the end of the WRL specimen testing (right). Legend: see Figure 38. By: Devaux.

Specimen WRS:

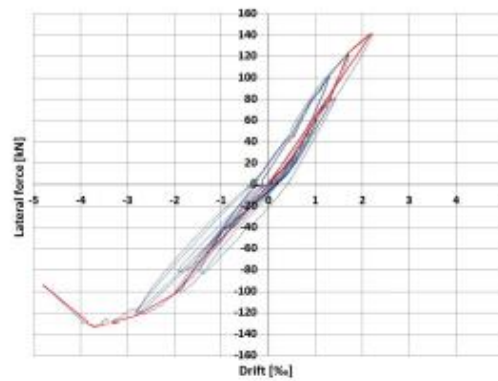


Figure 40. hysteresis loop recorded during testing the WRS specimen. By: Devaux.

Specimens Envelop: Figure 41 is the envelope of all the study cases, this is a good way to observe and analyze all the results in one graphic:

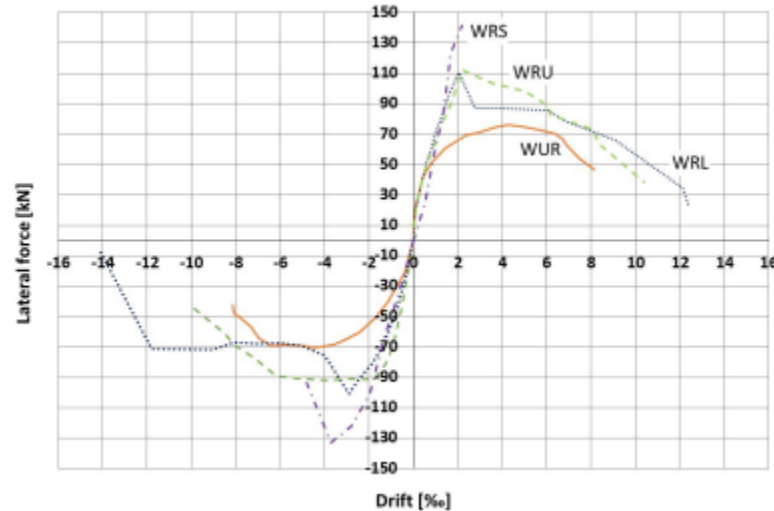


Figure 41. Specimens envelop curve. By: Devaux.

Conclusions:

- UHPFRC 30 mm layers were used for reinforcing brick walls, and this layer improved the shear strength of the masonry walls. However, the specimen's ductility was not as good as expected. Hence in the case of specimens, WRU & WRL ductility was a little higher than the ductility of the control wall. In the same way, in the wall, fully reinforced ductility was lower than in the reference wall.
- Therefore, because of the brittle behavior of bricks, the possibility to transfer the load to the UHPFRC layers reinforcements was limited. In that sense, full contribution of reinforcement was not achieved.
- U-shaped reinforcement (specimen WRU) showed the best performance thanks to stress transfer provided by the abutment effect.
- Finally, it is worth mentioning that more investigations are required to continue studying walls reinforcement through UHPFRC and looking to develop other reinforcing methods with this material.

4. Accelerated retrofit of bridge columns using UHPC shell – Phase I: Feasibility Study

Objectives: Study the performance of UHPFRC for retrofitting damaged bridge columns.

Test Conditions: Three RC columns (one of these is the control columns, which is damaged but is not retrofitted) specimens were damaged with spalling cover and will be tested under a cyclic lateral load and a static axial load. In that sense, test specimen dimensions are presented in Figure 42:

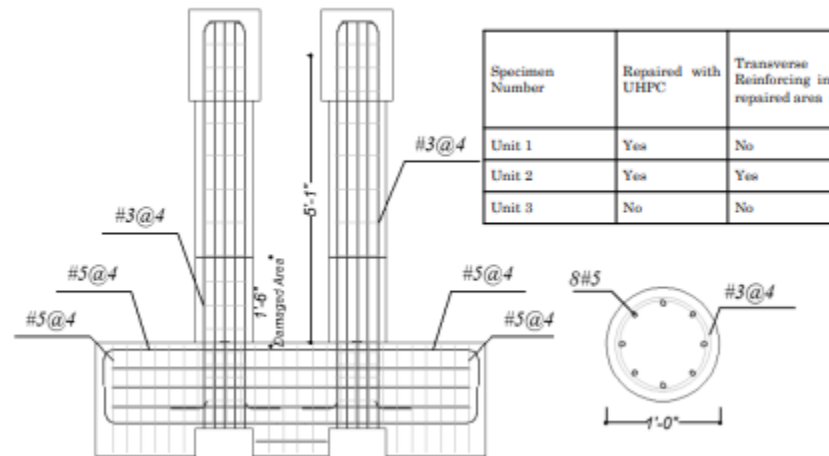


Figure 42. Specimens Dimensions. By: Azizinamini.

Note: The figure includes some specifications of the specimen’s conditions for the test

Furthermore, Figure 43 exhibits multiple schemes which illustrate the damaged zone and the reinforced zone reinforced by cleaning the surface followed for the casting UHPFRC (for specimens 1 & 2) and the damaged pier without reinforcement (specimen 3, which is the test baseline):

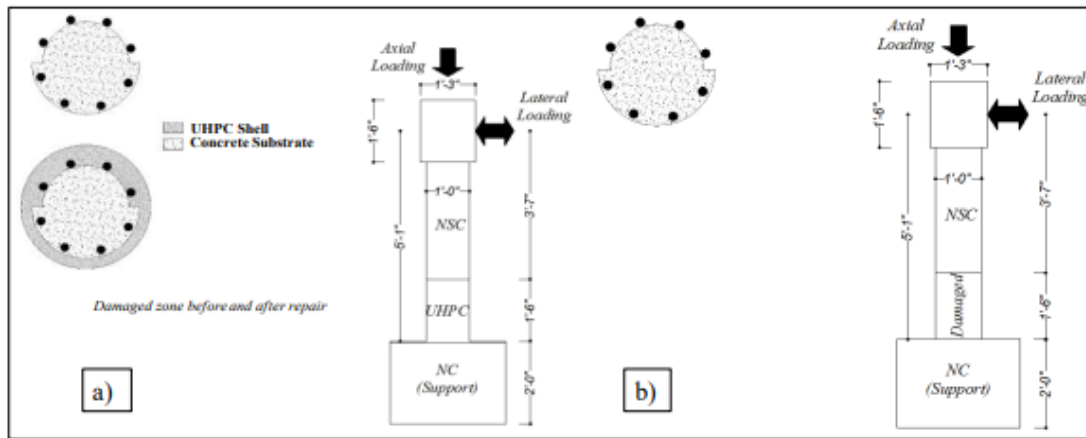


Figure 43. a) Damaged part before and after repair using UHPFRC shell (Unit 1 and 2), b) Damaged part with no repair (Unit 3).

Results: All the samples failed by fracture and buckling of longitudinal steels. Furthermore, the failure surface is ubicated only in the normal strength concrete (NSC), which means a good bonding between both UHPFRC and NSC concrete layers.

Then, force and moment hysteretic responses are presented in Figure 44:

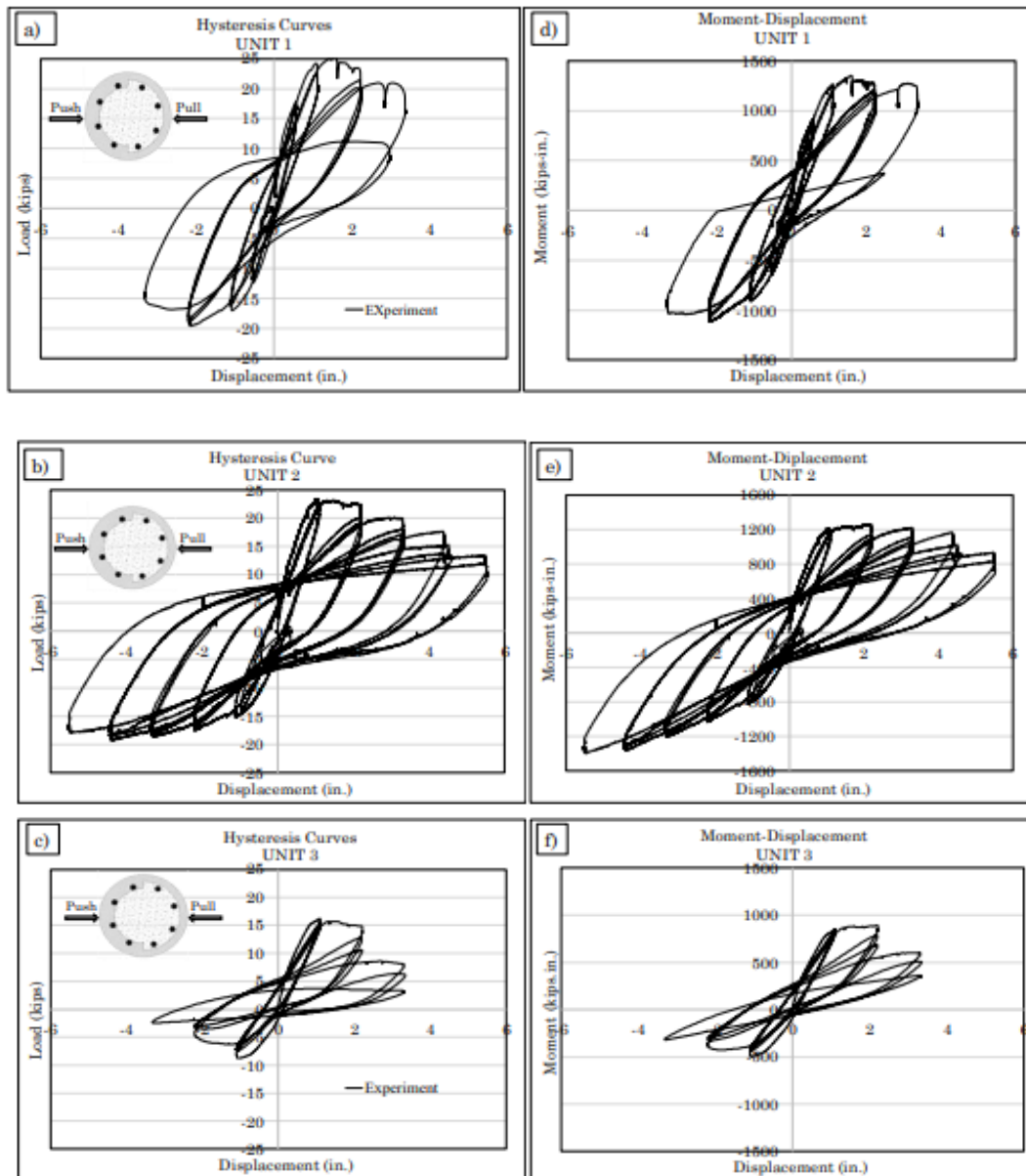


Figure 44. Force vs displacement hysteresis responses of a) Unit 1, b) Unit 2, c) Unit 3; Moment vs displacement hysteresis responses of d) Unit 1, e) Unit 2, f) Unit 3.

Now, the specimen's stiffness can be investigated with the graphics presented in Figure 45:

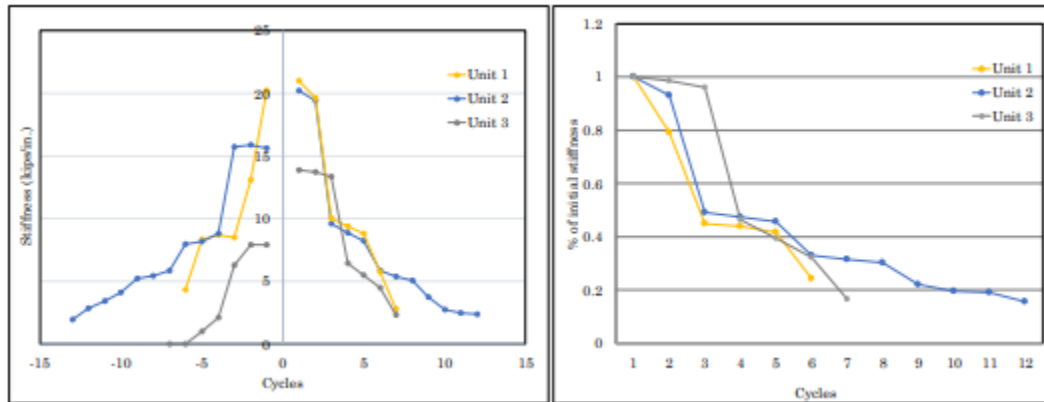


Figure 45. Stiffness curves (left), Stiffness degradation curves (right).

Finally, energy dissipation of each specimen is studied in the next graphics (Figure 46):

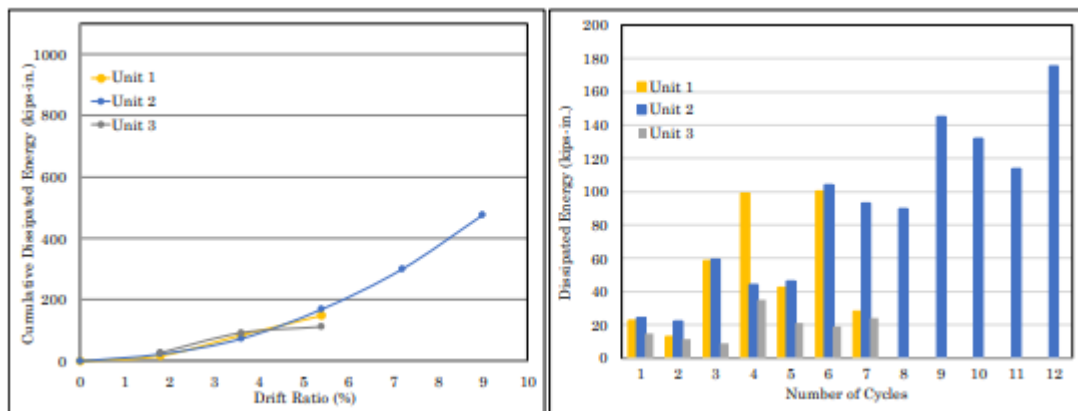


Figure 46. The energy dissipated vs. drift ratio (left). Energy dissipated energy vs. number of cycles (right).

Conclusions:

- In all the cases of study (load & moment bearing capacity, stiffness, and energy dissipation capacity) the specimen number 2 (unit 2) showed the best performance, which means that the longitudinal steel reinforces adequately the UHPFRC reinforce, to enhance the structures retrofitting especially in bridge columns.
 - The UHPFRC reinforcement improved the strength of the damaged elements without a growth in the element's size.
 - Fibers on UHPFRC lead to limit the cracks progression in the concrete sample, which let the material to enhance its performance at large strains.
 - The unit 1 showed that UHPFRC improved the load-carrying capacity and stiffness of the columns. However, didn't significantly improve the ductility of this.
5. Seismic Retrofitting of a Bridge Pier with Ultra High Performance Fiber Reinforced Concrete

Objectives: Investigate the performance of reinforce a bridge pier with thin layers of UHPFRC.

Test Conditions: A 1:4 scale bridge pier specimen retrofitted with a 30mm UHPFRC layer was tested under a static, unidirectional, cyclic loading along the minor axis of inertia. Table 28 exhibits specimen's design characteristics:

Table 28. Specimens details.

	Real scale (1:1)	Reduced scale (1:4)
A_c	9.386 m ²	0.596 m ²
A_s	164,588 mm ²	10,160 mm ²
t_{UHPFRC}	120 mm	30 mm
ρ_s	1.75%	1.70%
$\rho_{s,added}$	0.65%	0.65%

By the same way, Figure 47 presents a scheme of the test:

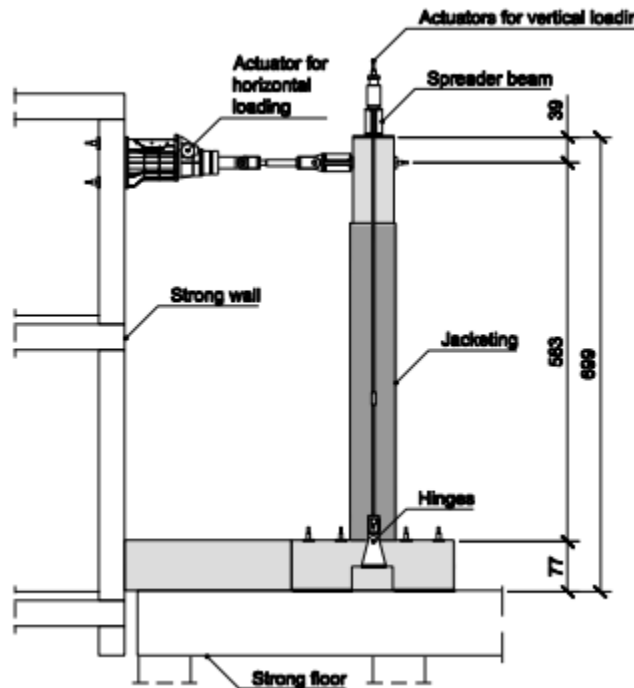


Figure 47. Test Scheme.

It is worth mentioning that this test has two stages. The first one was carried out until the first cracking of the reinforced concrete element (not UHPFRC retrofitting yet).

And the second one was carried out until the failure of the element retrofitted with the UHPFRC jacketing. In that sense, table 29 presents the test program:

Table 29. Program test.

Test 1	d [mm]	θ [%]	Cycles
Step 1	2.5	0.05	3
Step 2	5	0.1	3
Step 3	12.5	0.25	3
Test 2	d [mm]	θ [%]	Cycles
Step 1	2.5	0.05	3
Step 2	5	0.1	3
Step 3	10	0.2	3
Step 4	15	0.25	3
Step 5	20	0.35	3
Step 6	25	0.4	3
Step 7	50	1.0	3
Step 8	75	1.3	3
Step 9	100	1.7	3
Step 10	125	2.1	3
Step 11	150	2.6	3
Step 12	200	3.4	3

Results: In the northward direction, the retrofitted sample achieved a maximum load of 451 kN during cycle with $\theta = 3.4\%$ ($d = 200$ mm). In the southward direction, load-carrying capacity achieved a maximum value of 407 kN during cycle with $\theta = 1.7\%$ ($d = 100$ mm) followed by a reduction (-12%) to 360 kN (80.940) with $\theta = 3.4\%$ ($d = 200$ mm). Therefore, buckling of the jacketing was observed at the base of the south face (front) after reaching the maximum drift ($\theta = 3.4\%$; $d = 200$ mm). Finally, a reduction of the stiffness of the sample was observed after the local delamination of the UHPFRC jacketing. Thus, the test was interrupted to avoid any dangerous collapse.

In that sense, Figure 48 presents the Load vs Horizontal displacement response:

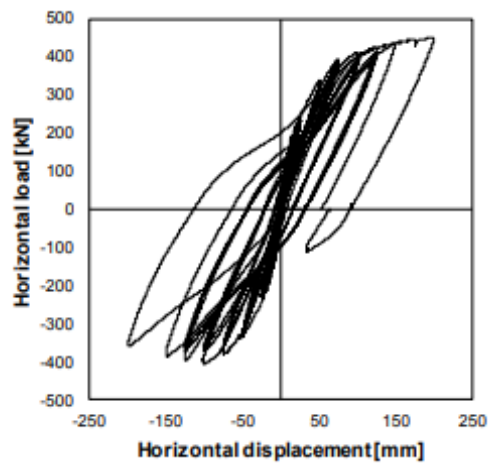


Figure 48. Horizontal load vs horizontal displacement response.

By the same way, Figure 49 exhibits the crack pattern of the specimen, before the strengthening (left) and after the strengthening (right)

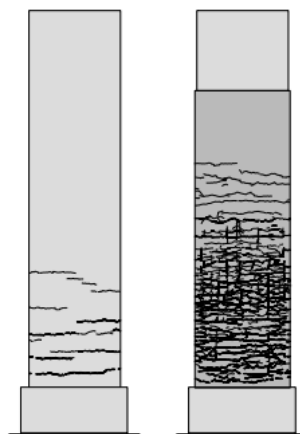


Figure 49. crack pattern of the specimen, before the strengthening (left) and after the strengthening (right)

Figure 50 & 51 shows the crack spacing and width development respectively, of the retrofitted specimen at the base in the test cycles:

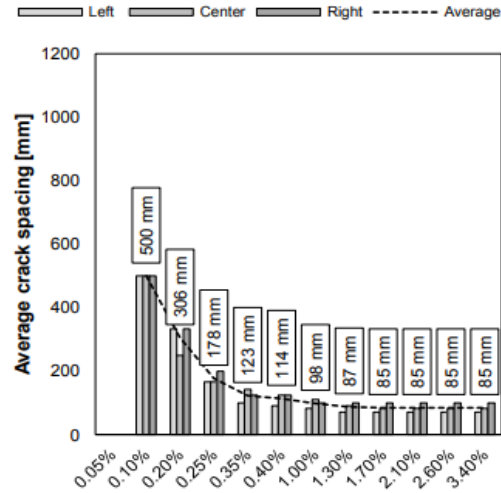


Figure 50. Average crack spacing.

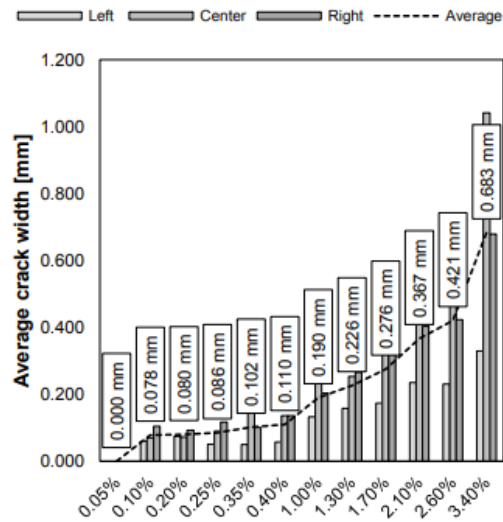


Figure 51. Average crack width.

Table 30, summarizes some of the most important results gotten on this test:

Table 30. Test results.

First cracking	H [kN]	d [mm]	θ [%]
Un-strengthened	70	5.8	0.1
Strengthened	100 (+42%)	5 (-14%)	0.1 (-14%)
First yielding	H [kN]	d [mm]	θ [%]
Un-strengthened	208*	49*	0.8*
Strengthened	395 (+90%)	75 (+53%)	1.3 (+53%)
Failure	H [kN]	d [mm]	θ [%]
Un-strengthened	259*	127*	2.2*
Strengthened	451 (+74%)	200 (+57%)	3.4 (+57%)

*Calculated values with $f_y = 450$ MPa.

Finally, Figure 52 compares the performance of the un-strengthened element and the strengthened element. It is worth to mention that the prediction of the un-strengthened specimen was made with an analytical model.

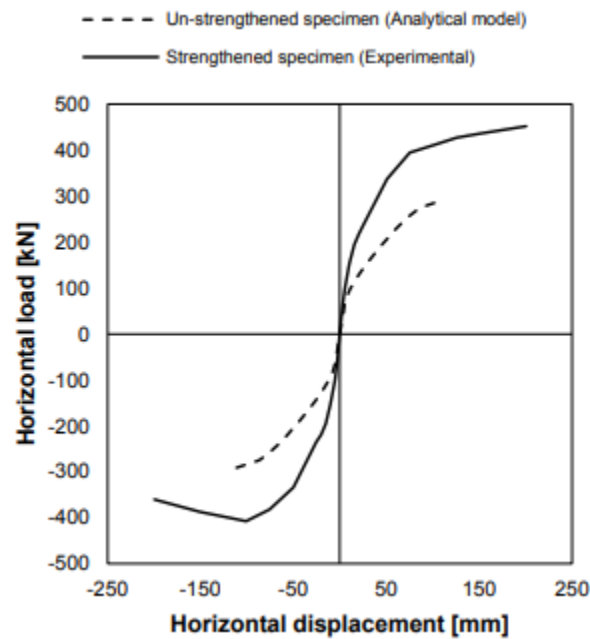


Figure 52. Horizontal load vs Horizontal displacement.

Conclusions:

- Thought, the reinforced jacket was relatively thin (30 mm), the load-carrying capacity improved in 74% in failure conditions (ultimate state) and in 43% for first cracking phase. Therefore, the ultimate displacement reached an improvement of 57%.
- When is required that an element size have not be significantly increased to be retrofitted, UHPFRC is a successful solution.
- UHPFRC jacketing system improved considerably the structural behavior of the pier, leading to remain the crack spacing for multiple cycles.

To summarize all the investigations, there will be presented a comparative table:

Beams

Table 31. Beams Comparison. Source: Own.

FRP	UHPFRC
<ul style="list-style-type: none"> • More thickness sheets do not improve the performance of the retrofitted elements. • Bearing capacity improvement from 46 to 70%. • Debonding is the most common type of failure. • Ductility improves the most when the specimens are full wrapped with FRP layers. • Can be implemented to retrofit steel beams, improving its bearing capacity. And anchorage can be used to change the mode of failure. 	<ul style="list-style-type: none"> • More thickness layers are related with better performance of the mechanical properties of the element retrofitted. • Load carrying capacity between 20 and 30%. • Fiber can absorb the loading energy. Hence, ductility improved around 250%. • Reinforcement, capable of change the failure mode from shear to flexural.

Columns

Table 32. Columns Comparison. Source: Own.

FRP	UHPFRC
<ul style="list-style-type: none"> • In circular areas the effective confinement area is better. In that sense in circular areas or rounded edged the performance is better than in sharp edged columns. • Carrying-load capacity improvement between 40 and 70%. 	<ul style="list-style-type: none"> • Whatever be the shape of the column, UHPFRC layers have a successful retrofitting performance. • Specimens with more thickness had the best performance in bearing capacity aspect. • Carrying-load capacity between 70 and 140%. • Good ductile behavior.

Masonry Walls

Table 33. Masonry walls comparison. Source: Own.

FRP	UHPFRC
<ul style="list-style-type: none"> • Bearing capacity improvement from 110 to 240%. Displacement deformation improvement around 60%. 	<ul style="list-style-type: none"> • Shear strength improves. However, ductility doesn't improve too much. In the case of full the wall fully

<ul style="list-style-type: none"> • Anchorage delay the failure and help to prevent sudden failures. • Distribute the FRP reinforce more evenly is better than less sheets more width. In that sense, for efficient use FRP, is recommended that optimal strip spacing be used rather than increasing the reinforcing ratio to get better results in the overall behavior of the wall. 	<p>reinforced ductility was less than in the un-reinforced wall.</p> <ul style="list-style-type: none"> • Is not achieved a full contribution of UHPFRC reinforce. • More investigations are required in this area.
---	---

Bridges

Table 34. Bridges Comparison. Source: Own.

FRP	UHPFRC
<ul style="list-style-type: none"> • Loading capacity improvement from 5 to 30%. • Deflection enhancement between 20 and 100%. • Improvement in stiffness and ductility. • Anchorage systems can be implemented. 	<ul style="list-style-type: none"> • UHPFRC improve bearing capacity (around 70%), stiffness and energy dissipation capacity. • Improvement in displacement around 60%. • UHPFRC complemented with longitudinal steel reinforce exhibited a better performance in carrying-load capacity and ductility. • UHPFRC thin layers are effective for reinforce bridge piers. In that sense, UHPFRC are success way of retrofit when is necessary to not increase the size of the element in retrofitting. • Fibers lead to limit cracks progression, which improve the material performance at large strains.

EVALUATION OF FRP AND UHPFRC WORKING TOGETHER

There are not many researches about use FRP and UHPFRC together for retrofit structures. However, there are two studies, the first one study the strengthening of corroded beams with a UHPC-FRP composite and the other ones studies the behavior of UHPFRC specimens confined with FRP sheets:

Compressive behavior of ultra-high-performance fiber-reinforced concrete (UHPFRC) confined with FRP:

Objectives: study the compressive performance of fiber reinforced polymers (FRP) confined ultra-high-performance fiber reinforce concrete (UHPFRC) and compare it with FRP confined ultra-high-performance concrete, high strength concrete (HSC) and normal strength concrete (NSC).

Test Conditions: 38 cylinders of 150mm diameter and 300mm in height of FRP confined different types of concrete specimens were tested under axial compression, Table 35 summarizes test specimens' characteristics:

Table 35. Test specimens' characteristics. By: Wang.

Concrete type	Specimen	FRP layers	FRP Type	Steel fiber addition
UHPFRC	UHPFRC-C1-I, II	1	CFRP	Yes
	UHPFRC-C2-I, II	2	CFRP	Yes
	UHPFRC-C3-I, II	3	CFRP	Yes
	UHPFRC-C5-I, II	5	CFRP	Yes
	UHPFRC-G3-I, II	3	GFRP	Yes
	UHPFRC-G5-I, II	5	GFRP	Yes
	UHPFRC-G9-I, II	9	GFRP	Yes
UHPC	UHPC-C1-I, II	1	CFRP	-
	UHPC-C3-I, II	3	CFRP	-
	UHPC-C5-I, II	5	CFRP	-
	UHPC-G5-I, II	5	GFRP	-
HSC	HSC-C1-I, II	1	CFRP	-
	HSC-C3-I, II	3	CFRP	-
	HSC-C5-I, II	5	CFRP	-
	HSC-G5-I, II	5	GFRP	-
NSC	NSC-C1-I, II	1	CFRP	-
	NSC-C3-I, II	3	CFRP	-
	NSC-G3-I, II	3	GFRP	-
	NSC-G5-I, II	5	GFRP	-

Results: Tables 36 & 37 show strength and deformation results respectively:

Individual Comparison and Joint Evaluation of FRP and UHPFRC Used to Retrofit Structures

Table 36. Strength specimens' results. By: Wang.

Specimens	f_{c1} (MPa)	$f_{c1,Ave}$ (MPa)	f_{c2} (MPa)	$f_{c2,Ave}$ (MPa)	f_{c3} (MPa)	$f_{c3,Ave}$ (MPa)	$f_{c3,Ave}/f_{c0}$	f_{la} (MPa)	$f_{la,Ave}$ (MPa)	f_{la}/f_{c0}	$f_{la,Ave}/f_{c0}$
UHPFRC-C1-I	180.8	174.9	-	-	125.3	105.3	0.77	2.61	2.79	0.019	0.021
UHPFRC-C1-II	169.0	-	-	-	85.2	-	-	2.97	-	0.022	-
UHPFRC-C2-I	192.8	181.4	-	-	158.2	132.6	0.98	6.86	8.19	0.050	0.060
UHPFRC-C2-II	170.0	-	-	-	107.0	-	-	9.53	-	0.070	-
UHPFRC-C3-I	183.8	190.1	179.0	179.9	173.4	168.6	1.24	14.75	17.05	0.108	0.125
UHPFRC-C3-II	196.3	-	180.8	-	163.8	-	-	19.36	-	0.142	-
UHPFRC-C5-I	205.9	210.3	179.3	193.8	250.7	247.4	1.82	35.08	35.47	0.258	0.261
UHPFRC-C5-II	214.7	-	208.3	-	244.0	-	-	35.85	-	0.264	-
UHPFRC-G3-I	180.2	175.6	148.8	137.6	159.0	147.7	1.09	12.30	12.13	0.090	0.089
UHPFRC-G3-II	170.9	-	126.3	-	136.3	-	-	11.97	-	0.088	-
UHPFRC-G5-I	185.6	183.8	151.9	151.5	182.5	176.9	1.30	20.28	20.05	0.149	0.147
UHPFRC-G5-II	181.9	-	151.0	-	171.2	-	-	19.83	-	0.146	-
UHPFRC-G9-I	208.7	196.8	187.8	180.7	269.1	259.7	1.91	37.52	37.32	0.276	0.274
UHPFRC-G9-II	184.9	-	173.6	-	250.3	-	-	37.11	-	0.273	-
UHPC-C1-I	116.8	118.8	-	-	100.7	98.5	1.12	3.53	3.46	0.040	0.039
UHPC-C1-II	120.8	-	-	-	96.3	-	-	3.38	-	0.038	-
UHPC-C3-I	137.0	133.8	136.3	131.0	178.7	167.9	1.91	16.44	15.59	0.187	0.177
UHPC-C3-II	130.6	-	125.7	-	157.0	-	-	14.75	-	0.168	-
UHPC-C5-I	145.3	148.2	-	148.0	240.0	232.7	2.64	36.87	36.49	0.419	0.415
UHPC-C5-II	151.1	-	148.0	-	225.4	-	-	36.11	-	0.410	-
UHPC-G5-I	152.5	144.4	140.3	136.9	168.3	168.0	1.91	19.60	18.53	0.223	0.211
UHPC-G5-II	136.3	-	133.5	-	167.6	-	-	17.46	-	0.198	-
HSC-C1-I	94.7	95.1	-	-	77.7	75.1	0.98	5.84	4.35	0.076	0.057
HSC-C1-II	95.4	-	-	-	72.5	-	-	2.87	-	0.037	-
HSC-C3-I	107.9	112.5	94.0	98.8	138.6	142.1	1.85	11.22	15.59	0.146	0.203
HSC-C3-II	117.0	-	102.9	-	145.6	-	-	19.97	-	0.259	-
HSC-C5-I	126.8	123.6	121.9	116.2	192.2	191.7	2.49	37.64	37.77	0.489	0.491
HSC-C5-II	120.4	-	110.4	-	191.2	-	-	37.90	-	0.492	-
HSC-G5-I	98.1	96.4	90.0	90.0	151.6	154.5	2.01	21.07	21.18	0.274	0.275
HSC-G5-II	94.7	-	-	-	157.3	-	-	21.29	-	0.277	-
NSC-C1-I	-	-	-	-	61.3	59.4	1.32	5.99	6.09	0.150	0.152
NSC-C1-II	-	-	-	-	57.4	-	-	6.20	-	0.155	-
NSC-C3-I	-	-	-	-	-	-	-	-	-	-	-
NSC-C3-II	-	-	117.7	116.7	2.59	22.28	21.97	0.557	0.549	-	-
NSC-G3-I	-	-	-	-	115.7	-	-	21.66	-	0.542	-
NSC-G3-II	-	-	-	-	85.1	83.6	1.86	10.61	11.26	0.265	0.281
NSC-G5-I	-	-	-	-	82.0	-	-	11.90	-	0.297	-
NSC-G5-II	-	-	-	-	105.4	108.1	2.40	20.51	19.21	0.513	0.480
NSC-G5-II	-	-	-	-	110.7	-	-	17.91	-	0.448	-

Table 37. Deformation specimens' results. By: Wang.

Specimens	ϵ_{c1} (%)	$\epsilon_{c1,Ave}$ (%)	ϵ_{c2} (%)	$\epsilon_{c2,Ave}$ (%)	ϵ_{c3} (%)	$\epsilon_{c3,Ave}$ (%)	$\epsilon_{c3,Ave}/\epsilon_{c0}$	$\epsilon_{l,rup}$ (%)	$\epsilon_{l,rup,Ave}$ (%)	k_{ϵ}
UHPFRC-C1-I	0.55	0.53	-	-	0.79	0.86	1.62	0.51	0.55	0.32
UHPFRC-C1-II	0.50	-	-	-	0.92	-	-	0.58	-	-
UHPFRC-C2-I	0.58	0.55	-	-	1.06	1.15	2.09	0.67	0.80	0.47
UHPFRC-C2-II	0.52	-	-	-	1.24	-	-	0.93	-	-
UHPFRC-C3-I	0.56	0.57	0.60	0.61	1.77	1.76	3.09	0.96	1.11	0.65
UHPFRC-C3-II	0.58	-	0.61	-	1.75	-	-	1.26	-	-
UHPFRC-C5-I	0.62	0.66	0.64	0.68	1.99	2.05	3.11	1.37	1.39	0.81
UHPFRC-C5-II	0.69	-	0.72	-	2.11	-	-	1.40	-	-
UHPFRC-G3-I	0.55	0.55	0.72	0.78	1.96	1.98	3.60	1.82	1.80	0.89
UHPFRC-G3-II	0.55	-	0.83	-	1.99	-	-	1.77	-	-
UHPFRC-G5-I	0.57	0.56	0.76	0.72	2.73	2.4	4.29	1.80	1.78	0.88
UHPFRC-G5-II	0.54	-	0.68	-	2.07	-	-	1.76	-	-
UHPFRC-G9-I	0.71	0.66	0.78	0.72	3.22	3.07	4.65	1.85	1.84	0.91
UHPFRC-G9-II	0.61	-	0.66	-	2.92	-	-	1.83	-	-
UHPC-C1-I	0.39	0.40	-	-	1.04	1.01	2.525	0.69	0.68	0.40
UHPC-C1-II	0.41	-	-	-	0.97	-	-	0.66	-	-
UHPC-C3-I	0.46	0.48	0.59	0.58	1.95	1.94	4.04	1.07	1.02	0.59
UHPC-C3-II	0.49	-	0.56	-	1.92	-	-	0.96	-	-
UHPC-C5-I	0.51	0.52	-	0.54	2.62	2.57	4.94	1.44	1.43	0.83
UHPC-C5-II	0.53	-	0.54	-	2.52	-	-	1.41	-	-
UHPC-G5-I	0.55	0.53	0.64	0.69	2.61	2.84	5.36	1.74	1.65	0.81
UHPC-G5-II	0.50	-	0.73	-	3.06	-	-	1.55	-	-
HSC-C1-I	0.42	0.43	-	-	0.98	0.88	2.04	1.14	0.85	0.49
HSC-C1-II	0.43	-	-	-	0.77	-	-	0.56	-	-
HSC-C3-I	0.51	0.53	0.53	0.56	1.76	1.91	3.60	0.73	1.02	0.59
HSC-C3-II	0.54	-	0.58	-	2.05	-	-	1.30	-	-
HSC-C5-I	0.58	0.58	0.68	0.65	3.06	3.01	5.19	1.47	1.48	0.86
HSC-C5-II	0.57	-	0.61	-	2.95	-	-	1.48	-	-
HSC-G5-I	0.54	0.48	0.66	0.66	4.14	3.91	8.15	1.87	1.88	0.93
HSC-G5-II	0.41	-	-	-	3.67	-	-	1.89	-	-
NSC-C1-I	0.31	0.33	-	-	1.80	1.71	5.18	1.17	1.19	0.69
NSC-C1-II	0.35	-	-	-	1.61	-	-	1.21	-	-
NSC-C3-I	0.32	0.37	-	-	4.69	4.74	12.81	1.45	1.43	0.83
NSC-C3-II	0.41	-	-	-	4.78	-	-	1.41	-	-
NSC-G3-I	0.39	0.40	-	-	4.48	4.23	10.58	1.57	1.67	0.82
NSC-G3-II	0.41	-	-	-	3.98	-	-	1.76	-	-
NSC-G5-I	0.42	0.42	-	-	5.18	5.13	12.21	1.82	1.71	0.84
NSC-G5-II	0.41	-	-	-	5.07	-	-	1.59	-	-

In addition, stress-strain curves, for different types of concrete confined in FRP sheets, are exhibited in next graphics:

CFRP Confined UHPFRC:

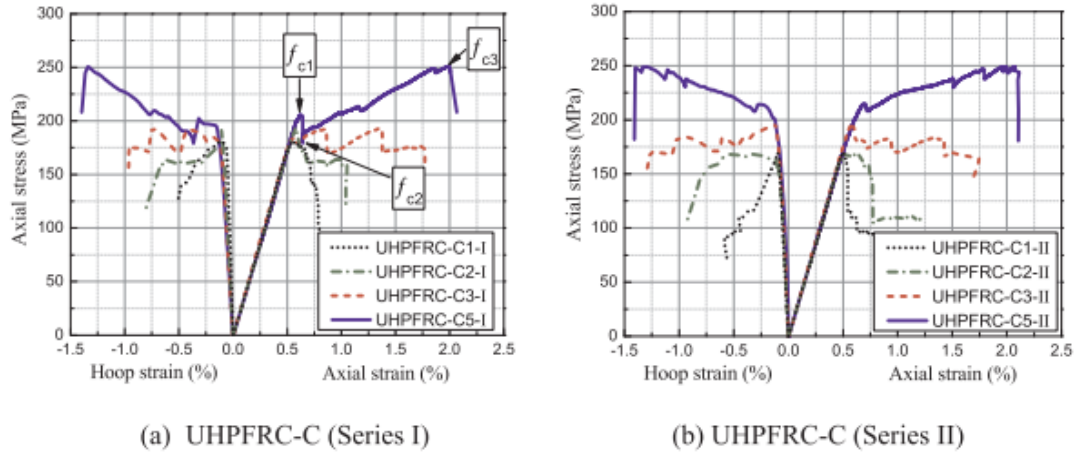


Figure 53. Axial stress-strain behaviors of specimens. By: Wang.

GFRP Confined UHPFRC:

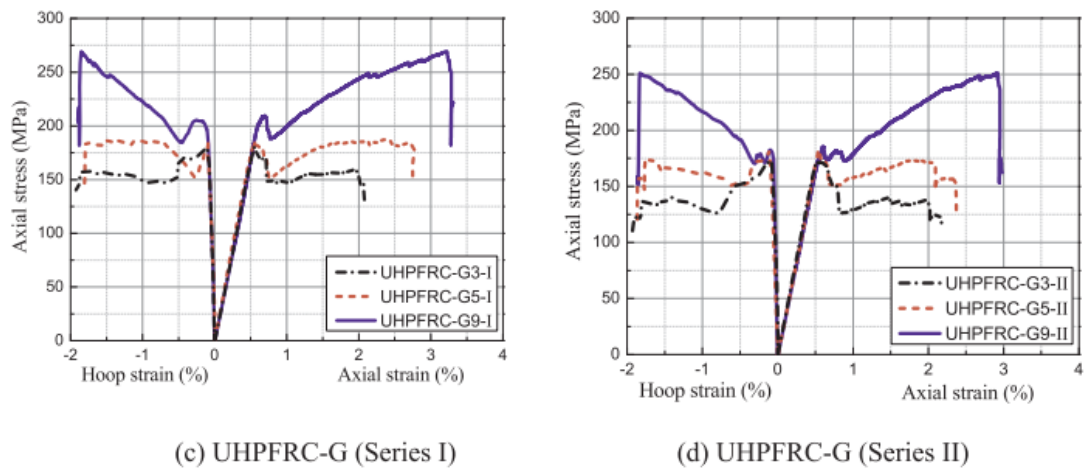
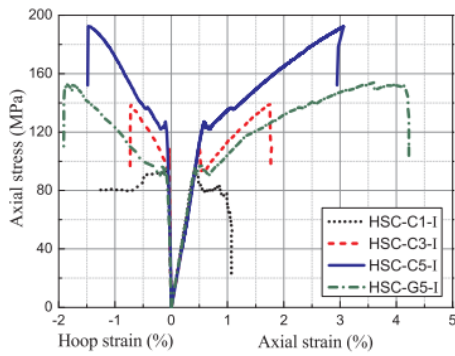
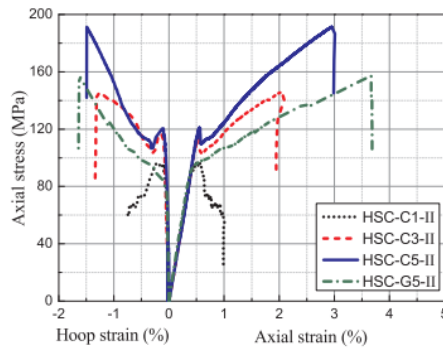


Figure 54. Axial stress-strain behaviors of specimens. By: Wang.

CFRP & GFRP Confined UHPC:



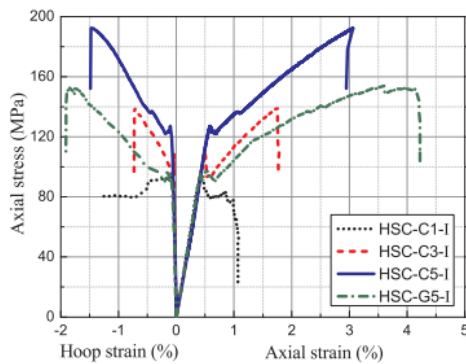
(g) HSC (Series I)



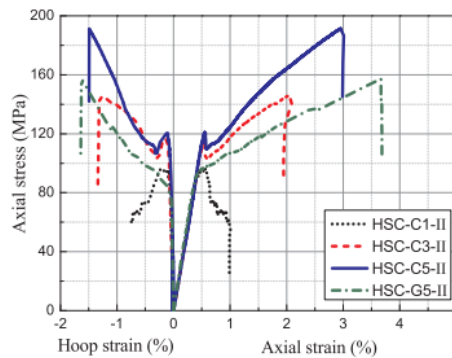
(h) HSC (Series II)

Figure 55. Axial stress-strain behaviors of specimens. By: Wang.

CFRP & GFRP Confined HSC:



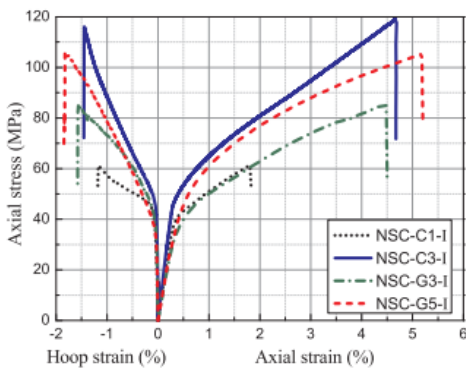
(g) HSC (Series I)



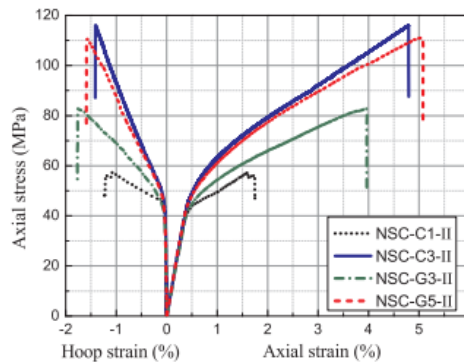
(h) HSC (Series II)

Figure 56. Axial stress-strain behaviors of specimens. By: Wang.

CFRP & GFRP Confined NSC:



(i) NSC (Series I)



(j) NSC (Series II)

Figure 57. Axial stress-strain behaviors of specimens. By: Wang.

Finally, modes of failure for different specimens are presented in Figure 58:



Figure 58. Specimens' mode of failure. By: Wang.

Conclusions:

- This investigation showed that confine concrete with five layers of CFRP or with nine layers of GFRP exhibited the best performance, little bit more bearing capacity was gotten by GFRP-9, though strain was around 3% and in CFRP-5 was around 2%. In that sense, CFRP can be the best alternative in performance aspects. However, it would be necessary to do a cost analysis.
- Is necessary to provide enough FRP confinement to UHPFRC specimens can exhibit ductile behavior.
- FRP confined UHPFRC show more brittle behavior than FRP confined NSC and HSC. In that sense, if not enough FRP reinforcement is provided, the axial stress can experience a decrease. Though, enough reinforcement is provided the axial stress can improve.
- The failure mode of FRP confined UHPC was explosive with loss of concrete segments. However, in UHPFRC thanks to fibers presence the explosion can be avoided because the fibers mitigate the cracks propagation and the spalling of concrete.
- The efficiency is higher for FRP confined NSC in comparison with FRP confined UHPFRC and the compressive strength enhance with the increase of FRP layers. Furthermore, to ensure a strain hardening behavior more FRP layers are required.

Shear Strengthening of Corroded RC Beams Using UHPC–FRP Composites

Objectives: Study the behavior of UHPC-FRP composites used for retrofitting a corroded RC beam.

Test Conditions: Nine RC beams specimens (three were the control beams) were tested. Then, each rectangular RC beam specimen was designed to be 200-mm wide, 300-mm deep, and 2,800-mm long. In addition, to further minimize the shear–flexure interaction within the test span, the load was applied at the midspan such that the test span was subjected to a low bending moment but a high shear force. Is worth to mention that to simulate corrosion and damaged, the stirrups were corroded using electrochemical corrosion in different levels. Table 38 summarizes test specimens’ conditions:

Table 38. Specimens’ conditions. By: Cheng. Source: ASCE.

Group	Specimen	Corrosion level (%)	UHPC–FPR	
			Thickness (mm)	Layers of CFRP mesh
US	US-0-0	0	NA ^a	NA
	US-8.1-0	8.1		
	US-15.4-0	15.4		
S	S-0-6	0	30	6
	S-11.6-6	11.6		6
	S-15.1-6	15.1		6
	S-15-0	15		0
	S-15-3	15		3
	S-18.5-6	18.5		6
	S-24.6-6	24.6		6

^aNA = not applicable.

Results: Results of this test are presented in Table 39:

Table 39. Specimens test results. By: Cheng. Source: ASCE.

Group	Specimen	Yielding level ^a		Ultimate level		Failure mode
		Load (kN)	Deflection ^b (mm)	Load (kN)	Deflection ^b (mm)	
US	US-0-0	173.1	7.1	181.3	7.8	Shear
	US-8.1-0	— ^c	— ^c	132.7	5.8	
	US-15.4-0	— ^c	— ^c	105.9	3.9	
S	S-0-6	340.4	10.8	384.2	12.8	Flexure
	S-11.6-6	340.1	11.1	369.2	12.7	
	S-15.1-6	— ^c	— ^c	365.4	13.3	Flexure-shear
	S-15-0	325.2	14.2	333.3	15.1	
	S-15-3	— ^c	— ^c	393.4	14.2	Shear
	S-18.5-6	— ^c	— ^c	339.1	10.7	
	S-24.6-6	— ^c	— ^c	342.7	11.9	

^aDetermined when the tensile strain of steel rebar exceeds its yielding strain.

^bMidspan deflection.

^cYielding did not occur.

Therefore, Load-deflection curves for different corrosion levels and layer are presented in Figure #:

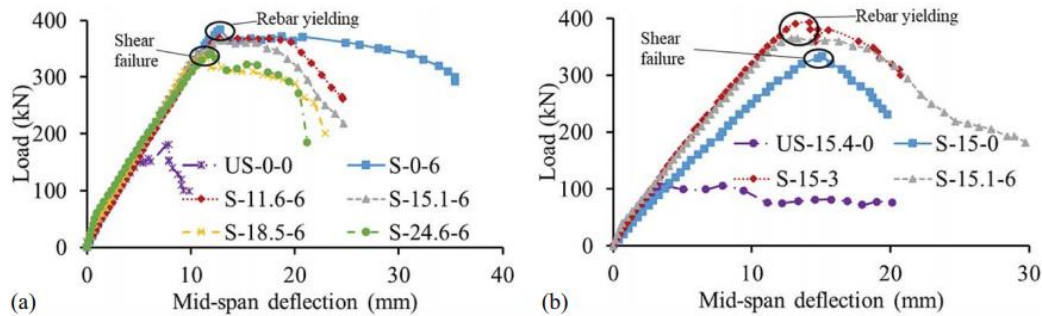


Figure 59. Load-deflection curves. By: Cheng. Source: ASCE.

Conclusions:

- In comparison with control beams, used FRP-UHPC composites increase the shear capacity of the beams. Moreover, this retrofitting system enhances the crack control behavior.
- Adding CGRP to the retrofit system enhances the crack control behavior which benefits the long-term strength of the structural element. However, the contribution of CFRP in shear strengthening is much less significant in comparison with UHPC alone.
- Crack pattern behavior was affected by the corrosion level in the stirrups. In that sense, the cracks lead to change form flexural to flexural-shear failure when the stirrups had a higher corrosion level.
- In specimens retrofitted by UHPC-FRO system the load-carrying capacity and the mid-span deflection at the ultimate stage was not significant in comparison with the un-strengthened beam.
- Thanks to the composite action, large tensile strain is developed and no debonding is observed between CFRP layers and UHPC. Hence, the addition of the CFRP meshes in UHPC shear strengthening enhances the flexural stiffness of the beams prior to rebar yielding and decreases the principal strain experienced in UHPC. However, the shear contribution enhances because of the addition of CFRP mesh layers is limited, indicating potential for future improvement

CONCLUSIONS

1. FRP & UHPFRC Performance for retrofitting structures is similar. In that sense, carrying load capacity can improve around 28% in both cases. Also, in a study case FRP got an improvement between 46-70%. However, along the investigations UHPFRC retrofitting exhibited better energy capacity absorption (ductility) with enhancement values around 278%. In addition, the failure mode change from a shear mode to a flexural mode due to the reinforce. Then, UHPFRC shows more efficient than FRP in general performance facts. Thought, FRP versatility and its application speed put this material as a principal option for retrofitting structures in emergency cases which is important to act quickly.
2. In columns retrofitting, UHPFRC for retrofitting columns showed an increase of bearing capacity around 133% and a high improvement in ductility. Furthermore, as showed in columns the mode of failure changed from shear to flexural. In FRP case carrying-load capacity enhanced in 67%. However, in this case ductility did not improve significantly. Hence, in general terms UHPFRC has a better behavior for retrofitting columns in comparison with FRP.
3. FRP for retrofitting masonry walls has shown good performance results, with a compressive strength enhancement and ductility. In that sense, is worth to mention that distribute the more FRP sheets reinforce more evenly is better than less sheets with more width. In that sense, for efficient use FRP, is recommended that optimal strip spacing be used rather than increasing the reinforcing ratio to get better results in the overall behavior of the wall. In the case of UHPFRC reinforcing masonry walls, the UHPFRC reinforcement cannot develop its qualities due to bricks have a premature failure when are wrapped with this concrete layers. Hence, in this case more investigations to develop a better UHPFRC retrofitting system.
4. In FRP retrofitting bridges the bearing capacity, deflection, stiffness, and ductility improved significantly and anchorage systems are developed to be implemented and change the debonding failure. In the case of UHPFRC energy dissipation capacity improved, bearing capacity and stiffness too. Finally, is worth to mention that UHPFRC thin layers are effective for reinforce bridge piers. In that sense, UHPFRC are success way of retrofit when is necessary to not increase the size of the element in retrofitting.
5. Finally, evaluating the use of this material together for retrofitting, it was found that in the case of FRP confined UHPFRC the efficiency and ductility was not as good as FRP confined NSC, which means that this retrofitting idea is not very successful yet. Other fact studied was the layers number effect. In that sense, with more layers the bearing capacity, ductility & strain-hardening behavior enhanced compared with less layers. Other researches, which evaluate this both materials retrofitting together showed an improvement in shear strength & the development of large tensile strain. Is worth to mention that no debonding was observed between CFRP layers and

UHPC. More researches are needed in this area because there are some facts that make this system not much successful and perhaps unnecessary to use them together.

REFERENCES

- [1] Wille, K., El-tawil, S., Naaman, A.E., Properties of strain hardening ultra high performance fiber reinforced concrete (UHP-FRC) under direct tensile loading, *Cem. Concr. Compos.* 48 (2014) 53–66. doi:10.1016/j.cemconcomp.2013.12.015.
- [2] Abellán-García, J., Four-layer perceptron approach for strength prediction of UHPC, *Constr. Build. Mater.* 256 (2020). doi:10.1016/j.conbuildmat.2020.119465.
- [3] Naderpour, H., Kheyroddin, A., Amiri, G.G., Prediction of FRP-confined compressive strength of concrete using artificial neural networks, *Compos. Struct.* 92 (2010) 2817–2829. doi:10.1016/j.compstruct.2010.04.008.
- [4] Byars, E.A., Waldron, P., Dejke, V., Demis, S., *Durability of FRP in Concrete Current Specifications and a New Approach*, FRP Compos, Hong Kong, 2001.
- [5] Li, Z., Rangaraju, P.R., Development of UHPC Using a Ternary Blend of Ultra-Fine Class F Fly Ash, Meta-kaolin and Portland Cement, in: *First Int. Interact. Symp. UHPC*, 2016: pp. 1–12. doi:10.21838/uhpc.2016.64.
- [6] Lavorato, D., Bergami, A. V., Nuti, C., Briseghella, B., Xue, J., Tarantino, A.M., Marano, G.C., Santini, S., Ultra-high-performance fibre-reinforced concrete jacket for the repair and the seismic retrofitting of Italian and Chinese RC bridges, *COMPdyn 2017 - Proc. 6th Int. Conf. Comput. Methods Struct. Dyn. Earthq. Eng.* 1 (2017) 2149–2160. doi:10.7712/120117.5556.18147.
- [7] Soudki, K., Alkhrdaji, T., *Guide for the Design and Construction of Externally Bonded FRP Systems for Strengthening Concrete Structures (ACI 440.2R-02)*, 2005. doi:10.1061/40753(171)159.
- [8] Abellán-García, J., *Dosage optimization and seismic retrofitting applications of Ultra-HighPerformance Fiber Reinforced Concrete (UHPFRC)*, Universidad Politécnica de Madrid, 2020.
- [9] Aghdasi, P., Heid, A.E., Chao, S.H., Developing ultra-high-performance fiber-reinforced concrete for large-scale structural applications, *ACI Mater. J.* 113 (2016) 559–569. doi:10.14359/51689103.
- [10] Abellán-García, J., Núñez-López, A., Torres-Castellanos, N., Fernández-Gómez, J., Effect of FC3R on the properties of ultra-high-performance concrete with recycled glass, *Dyna.* 86 (2019) 84–92. doi:10.15446/dyna.v86n211.79596.
- [11] Abellán, J., Fernández, J., Torres, N., Núñez, A., Statistical Optimization of ultra-high-performance glass concrete, *ACI Mater J.* (2020). doi:10.14359/51720292.
- [12] Wille, K., Naaman, A.E., Ultra-high performance concrete and fiber reinforced concrete : achieving strength and ductility without heat curing, (2012) 309–324. doi:10.1617/s11527-011-9767-0.
- [13] Shi, C., Wu, Z., Xiao, J., Wang, D., Huang, Z., Fang, Z., A review on ultra high

- performance concrete: Part I. Raw materials and mixture design, *Constr. Build. Mater.* 101 (2015) 741–751. doi:10.1016/j.conbuildmat.2015.10.088.
- [14] Ahmed, T., Elchalakani, M., Karrech, A., Dong, M., Mohamed Ali, M.S., Yang, H., ECO-UHPC with High-Volume Class-F Fly Ash: New Insight into Mechanical and Durability Properties, *J. Mater. Civ. Eng.* 33 (2021) 1–20. doi:10.1061/(asce)mt.1943-5533.0003726.
- [15] Li, W., Huang, Z., Zu, T., Shi, C., Duan, W.H., Shah, S.P., Influence of Nanolimestone on the Hydration, Mechanical Strength, and Autogenous Shrinkage of Ultrahigh-Performance Concrete, *J. Mater. Civ. Eng.* 28 (2016) 1–9. doi:10.1061/(ASCE)MT.1943-5533.0001327.
- [16] Shi, C., Wu, Z., Xiao, J., Wang, D., Huang, Z., Fang, Z., A review on ultra high performance concrete: Part II. Hydration, microstructure and properties, *Constr. Build. Mater.* 96 (2015) 368–377. doi:10.1016/j.conbuildmat.2015.10.088.
- [17] Li, J., Wu, Z., Shi, C., Yuan, Q., Zhang, Z., Durability of ultra-high performance concrete – A review, *Constr. Build. Mater.* 255 (2020) 119296. doi:10.1016/j.conbuildmat.2020.119296.
- [18] Abellán-García, J., Fernández-Gómez, J., Torres-Castellanos, N., Properties prediction of environmentally friendly ultra-high-performance concrete using artificial neural networks, *Eur. J. Environ. Civ. Eng.* 0 (2020) 1–25. doi:10.1080/19648189.2020.1762749.
- [19] Abellán-García, J., Artificial Neural Network Model for Strength Prediction of Ultra-High-Performance Concrete, *ACI Mater. J.* 118 (2021) 3–14. doi:10.14359/51732710.
- [20] Abellán, J., Fernández, J., Torres, N., Núñez, A., Development of cost-efficient UHPC with local materials in Colombia, in: B. Middendorf, E. Fehling, A. Wetzel (Eds.), *Proc. Hipermat 2020 - 5th Int. Symp. UHPC Nanotechnol. Constr. Mater.*, University of Kassel, Kassel, Germany, 2020: pp. 97–98.
- [21] Abellán-García, J., Fernández-Gómez, J., Torres-Castellanos, N., Núñez-López, A., Tensile behavior of normal strength steel fiber green UHPFRC, *ACI Mater. J.* 118 (2021) 127–138. doi:10.14359/51725992.
- [22] Abellán-García, J., Guzmán-Guzmán, J.S., Random forest-based optimization of UHPFRC under ductility requirements for seismic retrofitting applications, *Constr. Build. Mater.* 285 (2021). doi:10.1016/j.conbuildmat.2021.122869.
- [23] Abellán-García, J., Sánchez-Díaz, J., Ospina-Becerra, V., Neural network-based optimization of fibers for seismic retrofitting applications of UHPFRC, *Eur. J. Environ. Civ. Eng.* June (2021). doi:10.1080/19648189.2021.1938687.
- [24] Alsalman, A., Dang, C.N., Micah Hale, W., Development of ultra-high performance concrete with locally available materials, *Constr. Build. Mater.* 133 (2017) 135–145. doi:10.1016/j.conbuildmat.2016.12.040.

- [25] Abellán-García, J., K -fold Validation Neural Network Approach for Predicting the One-Day Compressive Strength of UHPC, *Adv. Civ. Eng. Mater.* Doi10.1520/ACEM20200055. 10 (2021) 223–243. doi:10.1520/ACEM20200055.
- [26] Abellán-García, J., Torres-Castellanos, N., Fernández-Gómez, J.A., Núñez-López, A.M., Ultra-high-performance concrete with local high unburned carbon fly ash, *Dyna.* 88 (2021) 38–47. doi:http://doi.org/10.15446/dyna.v88n216.89234.
- [27] Abellan-Garcia, J., Santofimo-Vargas, M.A., Torres-Castellanos, N., Analysis of metakaolin as partial substitution of ordinary Portland cement in Reactive Powder Concrete, *Adv. Civ. Eng. Mater.* 9 (2020) 368–386. doi:10.1520/ACEM20190224.
- [28] Park, S., Wu, S., Liu, Z., Pyo, S., The role of supplementary cementitious materials (Scms) in ultra high performance concrete (uhpc): A review, *Materials (Basel).* 14 (2021) 1–24. doi:10.3390/ma14061472.
- [29] Yazici, H., The effect of curing conditions on compressive strength of ultra high strength concrete with high volume mineral admixtures, *Build. Environ.* 42 (2007) 2083–2089. doi:10.1016/j.buildenv.2006.03.013.
- [30] Naderpour, H., Hossein, A., Fakharian, P., Compressive strength prediction of environmentally friendly concrete using artificial neural networks, *J. Build. Eng.* 16 (2018) 213–219. doi:10.1016/j.jobe.2018.01.007.
- [31] Dagenais, M.A., Massicotte, B., Boucher-Proulx, G., Seismic Retrofitting of Rectangular Bridge Piers with Deficient Lap Splices Using Ultrahigh-Performance Fiber-Reinforced Concrete, *J. Bridg. Eng.* 23 (2018) 1–13. doi:10.1061/(ASCE)BE.1943-5592.0001173.
- [32] Wang, W., Wu, C., Liu, Z., Si, H., Compressive behavior of ultra-high performance fiber-reinforced concrete (UHPFRC) confined with FRP, *Compos. Struct.* 204 (2018) 419–437. doi:10.1016/j.compstruct.2018.07.102.
- [33] Masuelli, M.A., Introduction of Fiber-Reinforced Polymers – Polymers and Composites: Concepts, Properties and Processes, *Fiber Reinforced Polymers*, in: InTech DTP team (Ed.), *Technol. Appl. Concr. Repair*, 2013: p. 240.
- [34] Ilki, A., Ispir, M., As, F., Demir, C., Kumbasar, N., Frp Retrofit of Walls Constructed With Historical Bricks, *Challenges Civ. Constr.* (2008).
- [35] Dinesh Kumar, J., Sattainathan Sharma, A., Suganya Devi, K., Study on flexural behaviour of RC beam strengthened with FRP, *J. Phys. Conf. Ser.* 2040 (2021). doi:10.1088/1742-6596/2040/1/012019.
- [36] Devaux, M., Redaelli, D., Moix, J., Seismic Retrofitting of Masonry Walls with thin UHPFRC Layers, *Proc. Hipermat 2016 - 4th Int. Symp. Ultra-High Perform. Concr. High Perform. Constr. Mater. Kassel.* (2016) 1–9.
- [37] Renić, T., Kišiček, T., Ductility of concrete beams reinforced with frp rebars, *Buildings.* 11 (2021). doi:10.3390/buildings11090424.
- [38] Visser, G., Van Ijsele, K., Klamer, E., Van Zijl, G., Retrofit and Renovation

- of Concrete Bridges with Fibre Reinforced Polymer (FRP): The Third Alternative, MATEC Web Conf. 199 (2018). doi:10.1051/mateconf/201819909010.
- [39] Banthia, N., Abdolrahimzadeh, A., Demers, M., Mufti, A., Sheikh, S., Durability of FRP-concrete bond in FRP-strengthened bridges, *Concr. Int.* 32 (2010) 45–51.
- [40] Zheng, R., Zohrevand, P., Erdogan, H., Mirmiran, A., Performance of FRP-retrofitted concrete bridge columns under blast loading, *Int. J. Comput. Methods Exp. Meas.* 2 (2014) 346–361. doi:10.2495/CMEM-V2-N4-346-361.
- [41] Pavese, A., Bolognini, D., Peloso, S., FRP seismic retrofit of rc square hollow section bridge piers, *J. Earthq. Eng.* 8 (2004) 225–250. doi:10.1080/13632460409350526.
- [42] Committee, A.C.I., ACI 318-14, n.d.
- [43] Higazy, E.M., El-kateb, M., Strengthening of Reinforced Concrete, (2011). doi:10.7665/182.
- [44] Yoo, D.Y., Sohn, H.K., Borges, P.H.R., Fediuk, R., Kim, S., Enhancing the tensile performance of ultra-high-performance concrete through strategic use of novel half-hooked steel fibers, *J. Mater. Res. Technol.* 9 (2020) 2914–2925. doi:10.1016/j.jmrt.2020.01.042.
- [45] Malatesta, S.C., Contreras, M.C., Comportamiento al corte de hormigones reforzado con fibras de acero, *Rev. Ing. Constr.* 24 (2009) 79–94.
- [46] Sun, Y., Li, G., Zhang, J., Qian, D., Prediction of the Strength of Rubberized Concrete by an Evolved Random Forest Model, *Adv. Civ. Eng.* 2019 (2019). doi:10.1155/2019/5198583.
- [47] Liu, Z., Hansen, W., Aggregate and slag cement effects on autogenous shrinkage in cementitious materials, *Constr. Build. Mater.* 121 (2016) 429–436. doi:10.1016/j.conbuildmat.2016.06.012.
- [48] Zych, T., New Generation Cementitious Composites With Fibres – Properties and Application Fibrokompozyty Cementowe Nowej Generacji – Właściwości I Zastosowania, (2014) 18.
- [49] Abellán-García, J., Guzmán-Guzmán, J.S., Sánchez-Díaz, J.A., Rojas-Grillo, J., Experimental validation of Artificial Intelligence model for the energy absorption capacity of UHPFRC, *Dyna.* 88 (2021) 150–159. doi:https://doi.org/10.15446/dyna.v88n217.
- [50] Abellán-García, J., Comparison of artificial intelligence and multivariate regression in modeling the flexural behavior of UHPFRC, *Dyna.* 87 (2020) 239–248. doi:http://doi.org/10.15446/dyna.v87n214.86172.
- [51] Neira-Medina, A., Abellan-Garcia, J., Torres-Castellanos, N., Flexural behavior of environmentally friendly ultra-high-performance concrete with locally available low-cost synthetic fibers, *Eur. J. Environ. Civ. Eng.* June (2021) 1–20. doi:10.1080/19648189.2021.1938686.

- [52] Park, S.H., Kim, D.J., Ryu, G.S., Koh, K.T., Tensile behavior of Ultra High Performance Hybrid Fiber Reinforced Concrete, *Cem. Concr. Compos.* 34 (2012) 172–184. doi:10.1016/j.cemconcomp.2011.09.009.
- [53] Pyo, S., Wille, K., El-Tawil, S., Naaman, A.E., Strain rate dependent properties of ultra high performance fiber reinforced concrete (UHP-FRC) under tension, *Cem. Concr. Compos.* 56 (2015) 15–24. doi:10.1016/j.cemconcomp.2014.10.002.
- [54] Wille, K., Kim, D., Naaman, A.E., Strain hardening UHP-FRC with low fiber contents., in: *Mater. Struct.*, 2011: pp. 538–598.
- [55] Abellán-García, J., Fernández-Gómez, J.A., Torres-Castellanos, N., Núñez-López, A.M., Machine Learning Prediction of Flexural Behavior of UHPFRC, in: P. Serna, A. Llano-Torre, J.R. Martí-Vargas, J. Navarro-Gregori (Eds.), *Fibre Reinf. Concr. Improv. Innov. BEFIB 2020.*, RILEM Bookseries, Valencia, Spain, 2020: pp. 570–583. doi:10.1007/978-3-030-58482-5_52.
- [56] Abellán-García, J., Núñez-López, A., Torres-Castellanos, N., Fernández-Gómez, J., Factorial design of reactive powder concrete containing electric arc slag furnace and recycled glass powder, *Dyna.* 87 (2020) 42–51. doi:http://doi.org/10.15446/dyna.v87n213.82655.
- [57] Abellán-García, J., Nuñez-Lopez, A., Arango-Campo, S., Pedestrian Bridge over Las Vegas Avenue in Medellín. First Latin American Infrastructure in UHPFRC, in: P. Serna, A. Llano-Torre, J.R. Martí-Vargas, J. Navarro-Gregori (Eds.), *BEFIB 2020*, RILEM Bookseries, Valencia (Spain), 2020: pp. 864–872. doi:https://doi.org/10.1007/978-3-030-58482-5_76.
- [58] Abellán, J., Núñez, A., Arango, S., Pedestrian bridge of UNAL in Manizales : A new UHPFRC application in the Colombian building market, in: *Proc. Hipermat 2020 - 5th Int. Symp. UHPC Nanotechnol. Constr. Mater.*, Kassel, Germany, 2020: pp. 43–44.
- [59] Ahmed, T., Elchalakani, M., Karrech, A., Mohamed Ali, M.S., Guo, L., Development of ECO-UHPC with very-low-C3A cement and ground granulated blast-furnace slag, *Constr. Build. Mater.* 284 (2021) 122787. doi:10.1016/j.conbuildmat.2021.122787.
- [60] AlHallaq, A.F., Tayeh, B.A., Shihada, S., Investigation of the Bond Strength Between Existing Concrete Substrate and UHPC as a Repair Material, *Int. J. Eng. Adv. Technol.* 6 (2017) 210–217.
- [61] Markovic, I., *High-performance Hybrid-fibre Concrete: Development and Utilisation*, DUP Science, 2006.
- [62] Abellán-García, J., Guzmán-Guzmán, J.S., Random forest-based optimization of UHPFRC under ductility requirements for seismic retrofitting applications, *Constr. Build. Mater.* 285 (2021). doi:10.1016/j.conbuildmat.2021.122869.
- [63] Tran, N.T., Kim, D.J., Synergistic response of blending fibers in ultra-high-performance concrete under high rate tensile loads, *Cem. Concr. Compos.* 78 (2017)

- 132–145. doi:10.1016/j.cemconcomp.2017.01.008.
- [64] Konvalinka, P., Mixture Design and Testing of Ultra High Performance Fiber Reinforced Concrete, *Malaysian J. Civ. Eng.* 25 (2013) 74–87. doi:10.11113/mjce.v25n0.315.
- [65] Wang, R., Gao, X., Zhang, J., Han, G., Spatial distribution of steel fibers and air bubbles in UHPC cylinder determined by X-ray CT method, *Constr. Build. Mater.* 160 (2018) 39–47. doi:10.1016/j.conbuildmat.2017.11.030.
- [66] Meng, W., Samaranayake, V.A., Khayat, K.H., Factorial design and optimization of ultra-high-performance concrete with lightweight sand, *ACI Mater. J.* 115 (2018) 129–138. doi:10.14359/51700995.
- [67] Ghezal, A., Khayat, K.H., Optimization of cost-effective self-consolidating concrete Optimizing Self-Consolidating Concrete with Limestone Filler by using Statistical Factorial Design Methods, (2016).
- [68] Šerelis, E., Vaitkevičius, V., Kerševičius, V., Mechanical Properties and Microstructural Investigation of Ultra-High Performance Glass Powder Concrete, *J. Sustain. Archit. Civ. Eng.* 1 (2016) 5–11. doi:10.5755/j01.sace.14.1.14478.
- [69] De Larrard, F., Sedran, T., “Mixture-proportioning of high-performance concrete,” *Cem. Concr. Res.* 32 (2002) 1699–1704. doi:10.1016/S0008-8846(02)00861-X.
- [70] Maya Duque, L.F., Graybeal, B., Fiber orientation distribution and tensile mechanical response in UHPFRC, *Mater. Struct. Constr.* 50 (2017). doi:10.1617/s11527-016-0914-5.
- [71] Ahmad, S., Hakeem, I., Maslehuddin, M., Development of UHPC Mixtures Utilizing Natural and Industrial Waste Materials as Partial Replacements of Silica Fume and Sand, *Eur. J. Environ. Civ. Eng.* 2014 (2014) 1106–1126. doi:10.1155/2014/713531.
- [72] hai He, Z., gui Du, S., Chen, D., Microstructure of ultra high performance concrete containing lithium slag, *J. Hazard. Mater.* 353 (2018) 35–43. doi:10.1016/j.jhazmat.2018.03.063.
- [73] Haber, Z.B., la Varga, I. De, Graybeal, B.A., Nakashoji, B., El-Helou, R., Properties and Behavior of UHPC-Class Materials, 2018.
- [74] Wille, K., Kim, D.J., Naaman, A.E., Strain-hardening UHP-FRC with low fiber contents, *Mater. Struct. Constr.* 44 (2011) 583–598. doi:10.1617/s11527-010-9650-4.
- [75] He, S., Qiu, J., Li, J., Yang, E.H., Strain hardening ultra-high performance concrete (SHUHPC) incorporating CNF-coated polyethylene fibers, *Cem. Concr. Res.* 98 (2017) 50–60. doi:10.1016/j.cemconres.2017.04.003.
- [76] ACI Committe 239R, Ultra-high-performance concrete: An emerging technology report, 2018.
- [77] Denarié, E., Habel, K., Brühwiler, E., Structural behavior of hybrid elements with

Advanced Cementitious Materials (HPCRCC), in: 4th Int. Work. High Perform.
Fiber Reinf. Cem. Compos., 2003: pp. 1–12.